Analyses of alpha-dystrobrevin-null mice implicate Niemann-Pick C1 in muscular dystrophy

Michelle Sabrina Steen

A dissertation submitted in partial fulfillment
of the requirements for the degree of

Doctor of Philosophy

University of Washington

2008

Program Authorized to Offer Degree:
Physiology and Biophysics

INFORMATION TO USERS

The quality of this reproduction is dependent upon the quality of the copy submitted. Broken or indistinct print, colored or poor quality illustrations and photographs, print bleed-through, substandard margins, and improper alignment can adversely affect reproduction.

In the unlikely event that the author did not send a complete manuscript and there are missing pages, these will be noted. Also, if unauthorized copyright material had to be removed, a note will indicate the deletion.

ProQuest LLC
789 E. Eisenhower Parkway
PO Box 1346
Ann Arbor, MI 48106-1346

University of Washington
Graduate School

This is to certify that I have examined this copy of a doctoral dissertation by

Michelle Sabrina Steen

and have found that it is complete and satisfactory in all respects,
and that any and all revisions required by the final
examining committee have been made.

Chair of the Supervisory Committee:

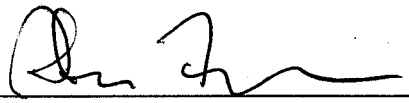

Stanley C. Froehner

Reading Committee:

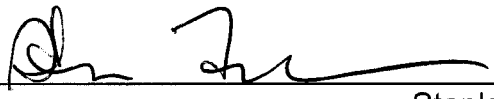

Stanley C. Froehner

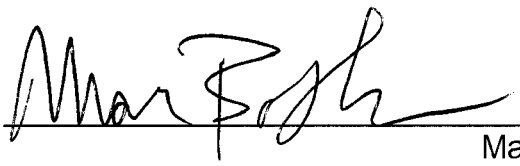

Mark Bothwell

Linda Wordeman

Date: 2/1/08

In presenting this dissertation in partial fulfillment of the requirements for the doctoral degree at the University of Washington, I agree that the Library shall make its copies freely available for inspection. I further agree that extensive copying of the dissertation is allowable only for scholarly purposes, consistent with "fair use" as prescribed in the U.S. Copyright Law. Requests for copying or reproduction of this dissertation may be referred to ProQuest Information and Learning, 300 North Zeeb Road, Ann Arbor, MI 48106-1346, 1-800-521-0600, to whom the author has granted "the right to reproduce and sell (a) copies of the manuscript in microform and/or (b) printed copies of the manuscript made from microform."

Signature Michelle S. Steen

Date 2/1/08

University of Washington

Abstract

Analyses of alpha-dystrobrevin-null mice implicate Niemann-Pick C1 in muscular dystrophy

Michelle Sabrina Steen

Chair of the Supervisory Committee:
Professor and Chair Stanley C. Froehner
Department of Physiology and Biophysics

In skeletal muscle, the dystrophin-associated protein complex (DPC) links the intracellular actin cytoskeleton to the extracellular matrix. Duchenne muscular dystrophy (DMD) and various other muscular dystrophies are caused by the loss or alteration of certain proteins of the DPC. Abnormalities of the neuromuscular junction (NMJ) are also caused by the loss of various DPC proteins. We performed gene expression analyses on skeletal muscles from mice lacking the DPC members α-dystrobrevin (*Dtna*) or α-syntrophin (*Snta*) in order to identify molecular alterations that result in muscular dystrophy and/or NMJ abnormalities. We identified a highly significant reduction in Niemann-Pick C1 (*Npc1*) transcript levels in *Dtna*$^{-/-}$ compared to wild-type mice. Mutations in *Npc1*, a cholesterol- and sphingolipid-trafficking protein, cause a progressive, neurodegenerative lysosomal storage disorder (NPC disease). We generated transgenic mice expressing NPC1 exclusively in skeletal muscles of *Dtna*$^{-/-}$ and

mdx (dystrophin-null) mice and found a significant attenuation of the dystrophic phenotype in both the *Dtna*$^{-/-}$ and *mdx* mice. We also observed a significant improvement of the NPC phenotype in a line of NPC1-null mice possessing the *Npc1* transgene. The expression of transgenic NPC1 in skeletal muscle does not appear to explain the phenotypic improvement of the NPC1-null mice, but the insertion of the transgene into the chromosome may have physically affected a gene encoding a protein capable of modulating the phenotype of the disease. In conclusion, this research suggests a connection between altered NPC1 levels and muscular dystrophy, a connection that could lead to novel therapies for this grievous illness with few treatment options.

TABLE OF CONTENTS

LIST OF ABBREVIATIONS

AAV ..... adeno-associated virus
AB ..... actin-binding
ABCA1 ..... ATP-binding cassette A1
AChR ..... acetylcholine receptor
AO ..... antisense oligonucleotide
BMD ..... Becker muscular dystrophy
bp ..... base pairs
CK ..... creatine kinase
CNS ..... central nervous system
CR ..... cysteine-rich
CT ..... carboxy-terminal
DGC ..... dystrophin-glycoprotein complex
DMD ..... Duchenne muscular dystrophy
DPC ..... dystrophin-associated protein complex
Dtna ..... α-dystrobrevin
Dtna$^{-/-}$ ..... α-dystrobrevin-null mice
EBD ..... Evans blue dye
ER ..... endoplasmic reticulum
GEO ..... gene expression omnibus database
HSA ..... human skeletal α-actin
LDL ..... low-density lipoprotein
LGMD ..... limb-girdle muscular dystrophy
mdx ..... dystrophin-null mice
NMJ ..... neuromuscular junction
nNOS ..... neuronal nitric oxide synthase
NO ..... nitric oxide
NPC1 ..... Niemann-Pick C1
Npc$^{+/-}$ ..... Niemann-Pick C1-heterozygous mice
Npc$^{-/-}$ ..... Niemann-Pick C1-null mice
s.d. ..... standard deviation
Snta ..... α-syntrophin
Snta$^{-/-}$ ..... α-syntrophin-null mice
TA ..... tibialis anterior
Tg(*Npc1*) ..... mice expressing transgenic *Npc1*
WGA ..... wheat germ agglutinin
WT ..... wild-type

LIST OF FIGURES

LIST OF TABLES

ACKNOWLEDGEMENTS

I would first like to thank members of the Froehner lab, past and present, for your friendship and advice over the years. A special thanks to my advisor, Stan Froehner, for your advice and guidance and for giving me the freedom of scientific exploration; to Marv Adams for teaching me biochemistry and molecular biology; and to Yan Tesch and Kendra Anderson for excellently and tirelessly maintaining all my mouse strains.

Thanks to my committee members: Mark Bothwell, Neil Nathanson, Jashvant Unadkat, and Linda Wordeman for your feedback, suggestions, and guidance.

Thanks to Greg Martin at the Keck Imaging Center for your assistance with microscopy.

Thanks to Josh Sanes (Harvard University) and Mark Grady (Washington University) for providing the alpha-dystrobrevin-null mice and to Jeff Chamberlain (University of Washington) for the HSA promoter construct.

Thanks to the entire staff of the Physiology and Biophysics department. Your help and kindness are unmatched and very much appreciated.

Thanks to all the friends I've made since moving to Seattle. A special thanks to Kathleen Rankin for your support through the good times and the bad.

Finally, thanks to my family. I cannot describe how important your love and support have been to me during this journey. Thanks to my parents for encouraging me always to strive for the best. You have taught me strength, courage, and perseverance. Thank you for always being there for me. Thanks to my sister, Renée, for inspiring me with your own hard work and tenacity. Lastly, thanks to my partner, Sue Cottrell, for being my pillar and for showing never-ending patience and understanding. Thank you not only for believing in me but for teaching me to believe in myself. Now, onto our next little adventure.

DEDICATION

To my parents, Ronald and Regula Steen.

CHAPTER 1:

Introduction

Duchenne Muscular Dystrophy (DMD)

DMD is an X-linked recessive, muscle wasting disorder affecting nearly 1:3,500 males. The disorder is caused by mutations in the dystrophin gene, which result in the complete loss of the dystrophin protein (Hoffman et al., 1987). Although symptoms may appear as early as infancy, patients generally become symptomatic between the ages of two and five, exhibiting difficulty with motor skills such as walking and stair climbing, as a result of weakness of the leg and pelvic muscles. In addition to skeletal muscle weakness, patients also exhibit pseudohypertrophy of the calf muscles (enlarged calf due to replacement of muscle by fat and connective tissue) and may have cardiomyopathy and mental retardation. Muscle wasting of the leg and pelvic muscles worsens, followed by weakening of the upper body muscles, including respiratory muscles. By the age of twelve, children become confined to a wheelchair, followed by death in the early twenties, typically due to respiratory failure as a result of excessive weakening of the respiratory muscles, or more rarely, due to cardiac failure.

Diagnosis of DMD may involve a serum creatine kinase (CK) test, genetic testing, and/or a muscle biopsy. In healthy, non-exercised, intact muscle, creatine kinase is contained within the muscle fibers. However, when

muscle fibers are damaged or deteriorating, creatine kinase escapes from the fibers and enters the bloodstream. Elevated serum CK levels therefore may indicate damaged or diseased muscle, and are in fact, grossly elevated in DMD patients. Genetic testing may be performed to identify whether or not the dystrophin gene contains large deletions or duplications of the dystrophin gene. Unfortunately, only about two-thirds of DMD patients carry these large, common deletions/duplications that can be identified by the current, commonly-used PCR-based screening assays (Beggs et al., 1990; Chamberlain et al., 1988). Lastly, muscle biopsies are performed to determine if muscle fibers contain the dystrophin protein and to examine the fibers for signs of degeneration and regeneration. Normal, healthy muscle has uniformly sized fibers and nuclei located peripherally on the fibers. In contrast, DMD muscles characteristically have variably-sized fibers, fibers with central nuclei, which are regenerating fibers derived from satellite cells, and regions of necrotic or degenerating fibers surrounded by macrophages and CD4+ lymphocytes (McDouall et al., 1990). As the disease progresses, muscles lose their regenerative capacity and the fibers are replaced with connective and adipose tissues. Currently DMD cannot be cured. Treatments instead are aimed at improving the quality of life.

Dystrophin

Dystrophin is localized to Xp21 and consists of 2.5 million base pairs (Coffey et al., 1992; Hoffman et al., 1987; Monaco et al., 1992; Roberts et al.,

1993). The largest known gene at this time, dystrophin contains 79 exons and encodes a 427 kDa protein (Hoffman et al., 1987; Koenig et al., 1988; Roberts et al., 1993). In addition to causing DMD, mutations in the dystrophin gene also cause Becker muscular dystrophy (BMD), a less severe disease than DMD (Kingston et al., 1983). Whereas DMD patients essentially fail to produce the dystrophin protein, BMD patients can make a shortened, albeit functional dystrophin, at reduced levels.

Expression of full-length dystrophin (Dp427) is driven by three different tissue-specific promoters: brain, muscle, and Purkinje promoters (Blake et al., 2002). The protein products of the different promoters differ only in the first exon. In addition, alternate promoters located within the dystrophin gene drive expression of four short versions of dystrophin with unique amino-terminals: Dp260 (260 kDa), Dp140 (140 kDa), Dp116 (116 kDa), and Dp71 (71 kDa). Dp260 is expressed in the retina (D'Souza et al., 1995); Dp140 is expressed in the brain and kidney (Durbeej et al., 1997; Lidov et al., 1995); Dp116 is expressed in Schwann cells (Byers et al., 1993); and Dp71 is ubiquitously expressed in non-muscle tissue (Bar et al., 1990; Lederfein et al., 1992).

Full-length dystrophin (Dp427), which is found in skeletal muscle, consists of an amino-terminal actin–binding domain adjacent to a rod domain, which contains 24 spectrin-like repeats interspersed with 4 proline-rich hinges (reviewed in (Ervasti, 2007)). The spectrin-like repeats and hinges are thought to give the protein a flexible, rod-like structure. Within this rod domain is a

second actin-binding domain. Following the 24th repeat of the rod domain is the fourth hinge, which together with the neighboring cysteine-rich (CR) domain binds β-dystroglycan. Lastly, the carboxy-terminal (CT) domain is the binding site of the dystrobrevins and syntrophins. β-dystroglycan, the syntrophins, and the dystrobrevins are members of the dystrophin-associated protein complex (Figure 1.1), which will be discussed in greater detail later. A schematic illustrating dystrophin and dystrophin-related proteins is shown in Figure 1.2.

Dystrophin-Associated Protein Complex (DPC) in skeletal muscle

Within a couple of years after the identification of the dystrophin gene and protein, digitonin-solubilized dystrophin from skeletal muscle membranes was found to bind to wheat germ agglutinin (WGA)-Sepharose (Campbell and Kahl, 1989). This technique, combined with additional purification steps, allowed for the identification of several proteins, including an integral membrane glycoprotein, later called β-dystroglycan, that form a complex with dystrophin. This complex was termed the dystrophin-glycoprotein complex (DGC), also known as the dystrophin-associated protein complex (DPC) (Figure 1.1). This finding provided the first evidence that dystrophin, by way of an interaction with an integral membrane associated glycoprotein, could link the cytoskeleton to the sarcolemma and possibly the extracellular matrix. Aside from dystrophin, the DPC in skeletal muscle is comprised of α- and β-dystroglycan, the sarcoglycans (α, β, γ, δ), sarcospan, the syntrophins, and α-dystrobrevin. The

proteins co-localize with dystrophin at the sarcolemma and are absent or greatly reduced in dystrophin-deficient (*mdx* and DMD) muscle, suggesting that a function of the DPC may be to provide structural integrity to the sarcolemma during muscle contraction (Butler et al., 1992; Crosbie et al., 1997; Ervasti et al., 1990; Mizuno et al., 1995; Mizuno et al., 1994a).

A. Dystroglycan

Dystroglycan was the first member of the DPC to be cloned. Derived from a single transcript that is proteolytically processed, α-dystroglycan (156 kDa) and β-dystroglycan (43 kDa) complete the link between dystrophin and the extracellular matrix (Ibraghimov-Beskrovnaya et al., 1992). β-dystroglycan spans the sarcolemma and binds to the CR region of dystrophin. α-dystroglycan, on the other hand, lies extracellularly and binds both β-dystroglycan and laminin in the extracellular matrix (Suzuki et al., 1994). The dystroglycans are essential members of the DPC as the lack of dystroglycan in mice results in embryonic lethality (Williamson et al., 1997).

B. Sarcospan and the Sarcoglycans

Sarcospan (25 kDa) resides in the sarcolemma and consists of four transmembrane spanning domains (Crosbie et al., 1997). The exact function of sarcospan is unknown. Tightly bound to sarcospan is the sarcoglycan sub-complex. The sarcoglycans (α, β, γ, δ) are single-pass transmembrane glycoproteins that form a tetrameric complex within the sarcolemma (Ozawa et al., 2005). Neither the sarcoglycans nor sarcospan interact directly with

dystrophin. However, the sarcoglycan complex binds α-dystrobrevin, and through an interaction with biglycan, is linked to α-dystroglycan (Bowe et al., 2000; Rafii et al., 2006). These interactions suggest that the sarcoglycan complex may help to stabilize the DPC.

C. The Dystrobrevins

The dystrobrevins were originally identified from postsynaptic membranes of the Torpedo electric organ (Carr et al., 1989). In mammals, they are encoded by two different genes to generate α- and β-dystrobrevin, both of which share sequence homology with the C-terminal end of dystrophin and both of which bind directly to the carboxy-terminal of dystrophin (Figures 1.1 and 1.2) (Ambrose et al., 1997; Blake et al., 1996; Carr et al., 1989; Peters et al., 1997b; Sadoulet-Puccio et al., 1996). β-dystrobrevin is expressed in several tissues, but not in cardiac or skeletal muscle (Peters et al., 1997b). Alternative splicing of α-dystrobrevin gives rise to six isoforms (α-dystrobrevin-1, -2a/b, -3, -4, -5) with complex expression patterns (Blake et al., 1996; Enigk and Maimone, 1999; Sadoulet-Puccio et al., 1996). Together the α-dystrobrevins are ubiquitously expressed. However, only α-dystrobrevin-1, -2, and -3 are found in skeletal muscle, and only α-dystrobrevin-4 and -5 are found in brain (Blake et al., 1996). In skeletal muscle, α-dystrobrevin-1 preferentially localizes to the neuromuscular junction (NMJ), whereas α-dystrobrevin-2 localizes to the NMJ as well as the extra-synaptic regions of the sarcolemma (Peters et al., 1998).

Because α-dystrobrevin-3 does not have a protein sequence unique from the other α-dystrobrevins, its expression pattern in skeletal muscle is not known.

The multiple splice variants and complex tissue distribution of the variants suggest different roles for the different isoforms depending on the tissue. The precise function of the dystrobrevins is unknown. However, mice lacking α-dystrobrevin have a mild muscular dystrophy and abnormalities of the NMJ (discussed below), suggesting a structural role for dystrobrevin and a role in the maintenance of the NMJ. How the loss of dystrobrevin leads to these muscle abnormalities is unknown. However, that syntrophins bind α-dystrobrevin as well as numerous signaling molecules (discussed below) and that syntrophins are decreased in α-dystrobrevin-null muscle (Grady et al., 1999; Grady et al., 2000) suggest that abnormal signaling may contribute to the abnormalities of the α-dystrobrevin-null mouse.

D. The Syntrophins

The syntrophins (58 kDa) are a family of five modular adapter proteins encoded by five separate genes (α, β1, β2, γ1, γ2). γ1- and γ2-syntrophin are the least characterized syntrophins. γ1-syntrophin is not found in skeletal muscle, but is highly expressed in brain and to a lesser extent in testes; whereas γ2-syntrophin is expressed in a number of tissues, including skeletal muscle where it is confined to the subsynaptic space beneath the neuromuscular junction (NMJ) in mice (Alessi et al., 2006). The most characterized syntrophins, α1-, β1-, and β2-, are expressed in a variety of

tissues, including skeletal muscle, although β1-syntrophin is only expressed in high levels in type IIb fast-twitch muscle fibers (Peters et al., 1997a). In skeletal muscle, all three are present at the NMJ, but only α-, and β1- syntrophin localize to the extra-synaptic regions of the sarcolemma where α-syntrophin predominates (Adams et al., 1993; Kramarcy and Sealock, 2000; Peters et al., 1997a; Peters et al., 1994). Protein interaction studies and studies using syntrophin-null mice suggest that syntrophins mediate cell signaling and are also important for proper maintenance of the NMJ (Adams et al., 2000).

E. Function of the DPC

The best-recognized and studied role of the DPC is in maintaining the structural integrity to the sarcolemma via its connection to intracellular actin. The most well-known example of this role comes from the loss of dystrophin, which forms a direct, physical link between the sarcolemma and actin. The fragility of muscle fibers is evident from elevated creatine kinase levels, reflecting damage to the sarcolemma, the uptake by muscle fibers of systemically-injected Evans blue dye following exercise, also reflecting damage to the sarcolemma, and reduced ability to maintain force production during sustained periods of muscle contraction (Head et al., 1994; Moens et al., 1993; Petrof et al., 1993). Although Duchenne muscular dystrophy may arguably be the most well-known, several forms of muscular dystrophy are also caused by mutations in other DPC members. For example, deletions of individual sarcoglycans cause limb-girdle muscular dystrophies (LGMD) in humans and

progressive muscular dystrophies in mice. These are characterized by myofiber degeneration, cell infiltration, and fibrosis and the influx of Evans blue dye and efflux of creatine kinase, suggesting damage to the sarcolemma (Ozawa et al., 2005). The connection between the dystroglycans and between dystrophin and β-dystroglycan are weakened by the loss of sarcoglycans, suggesting the damage to the sarcolemma may be due to disruption of the physical connection between the inside and outside of the fibers.

A second function of the DPC is to maintain the stability of the NMJ, which was determined based, in part, on mice generated to lack either α-dystrobrevin or α-syntrophin. Both knockout mice have abnormal appearing NMJs, characterized by reduced numbers of post-junctional folds, a reduction of acetylcholine receptors (AChR), and/or an abnormal distribution of AChR (Adams et al., 2000; Grady et al., 2000). The role of the DPC in the formation and maintenance of the NMJ will be discussed in a following section.

A third role for the DPC also appears to be in cell signaling. Syntrophin is likely one of the DPC's mediators of signaling. Syntrophins bind dystrophin and α-dystrobrevin directly (Ahn et al., 1996; Ahn and Kunkel, 1995; Dwyer and Froehner, 1995; Kramarcy et al., 1994; Yang et al., 1995). Both α-dystrobrevin and dystrophin contain two binding sites for syntrophin, allowing for four syntrophins to be bound to the DPC in muscle at any given time (Ahn and Kunkel, 1995; Newey et al., 2000). To date, several signaling molecules have

been shown to interact with syntrophin and therefore the DPC. Via its PDZ domain, the various syntrophins associate with signaling proteins such as voltage-activated sodium channels (Nav1.4 and Nav1.5) (Gee et al., 1998; Schultz et al., 1998), potassium channels (Connors et al., 2004; Leonoudakis et al., 2004), stress-activated protein kinase-3 (SAPK3) (Hasegawa et al., 1999), a microtubule-associated serine/threonine kinase (MAST) (Lumeng et al., 1999), a syntrophin-associated serine/threonine kinase (SAST) (Lumeng et al., 1999), ICA512 (Ort et al., 2000), Grb2 (Oak et al., 2001), α1D-adrenergic receptor (Chen et al., 2006), ATP-binding cassette A1 (ABCA1) (Buechler et al., 2002; Munehira et al., 2004), and perhaps the most well-studied DPC-interacting protein, neuronal nitric oxide synthase (nNOS), which regulates vasodilation during exercise (Brenman et al., 1996). In addition to the above interactions, β-dystroglycan binds caveolin-3, which is known to recruit signaling molecules (Sotgia et al., 2000). Caveolin-3, which is specifically expressed in skeletal muscle, has been shown to bind signaling molecules such as nNOS (Venema et al., 1997). Another example for the possible role of the DPC in signaling comes from studies using the α-dystrobrevin-null mouse, which is mildly dystrophic and has NMJ abnormalities. In this work, α-dystrobrevin-1, which can be tyrosine phosphorylated and is preferentially expressed at the NMJ, and α-dystrobrevin-2, which is not tyrosine phosphorylated and is normally present along the sarcolemma and NMJ, were independently transgenically expressed in α-dystrobrevin-null mice (Grady et al., 2003). While muscle fiber

degeneration was corrected by transgenic expression of either of these isoforms, only the transgenic expression of α-dystrobrevin-1 could correct the NMJ defects. This observation coupled with site-directed mutagenesis studies of the phosphorylation sites suggested the necessity of α-dystrobrevin phosphorylation for proper NMJ formation and the different signaling possibilities of the α-dystrobrevins.

Based upon the above-mentioned interactions and the number of syntrophins that can possibly bind the DPC at one time, it seems plausible that a role of the DPC is to bring signaling proteins into close contact with each other and/or tether signaling proteins to the sarcolemma for fast and efficient cell signaling. However, whether or not abnormalities in this putative signaling function of the DPC contribute to the pathophysiology of DMD patients or NMJ abnormalities of α-dystrobrevin-null or α-syntrophin-null mice is still unclear. In order to address these questions, gene expression analyses, described in Chapter 2, of α-dystrobrevin-null and α-syntrophin skeletal muscles were performed to identify alterations in expression of signaling molecules that might contribute to DMD and/or NMJ abnormalities, resulting from the loss of α-dystrobrevin or α-syntrophin.

Pathophysiology of DMD

Neither an effective treatment, much less a cure, for DMD exists. While much attention has focused on restoration of the DPC by bringing back

dystrophin or dystrophin-like proteins (discussed below in Therapeutic approaches to DMD), greater understanding of the mechanisms leading from dystrophin-deficiency to muscle degeneration could provide alternate areas of therapeutic focus. Several hypotheses have emerged as to the causes leading to degeneration, resulting from dystrophin loss (reviewed in (Deconinck et al., 2006). One long-standing hypothesis is that membrane damage causes the loss of calcium homeostasis, leading to calpain activation, cell and membrane proteolysis, and ultimately cell death. However, examination of intracellular calcium levels in mdx and DMD tissue has yielded inconsistent data (Collet et al., 1999; Gailly et al., 1993; Turner et al., 1991). Based upon knowledge of the DPC members and function, two other hypotheses seem plausible, although still under debate: a structural and a signaling hypothesis.

As noted above, one of the functions of the dystrophin complex is to link the intracellular cytoskeleton to the extracellular matrix. Early studies have shown that mice lacking dystrophin (*mdx*) exhibit increased tearing of the myofibers in response to muscle contractions (Petrof et al., 1993). Located on the cytoplasmic side of the sarcolemma, dystrophin sits in a rib-like lattice protein network, called costameres. Costameres contain large membrane-cytoskeletal complexes, which include the DPC, spectrin, ankyrin, and vinculin, and lie at the sarcolemma and over M-lines of nearby myofibrils (reviewed in (Bloch and Gonzalez-Serratos, 2003)). One theory of costameric function is that they transmit forces laterally from myofibril to myofibril out to the

sarcolemma, thereby reinforcing the sarcolemma by enabling it to move in unison with the myofibrils during contraction (Bloch and Gonzalez-Serratos, 2003). Studies in *mdx* mice have found that the distribution of the costameric protein, β-spectrin, is altered as is the organization of the costameric strands (Williams and Bloch, 1999). By losing dystrophin, the costameric link between the myofibers and sarcolemma is thus lost, which is believed to make the sarcolemma susceptible to tearing during contractions.

Whether or not the loss of costameric function is responsible for damage to the sarcolemma is still under debate. However, clearly, the integrity of the sarcolemmae is compromised in dystrophin-deficient muscle as it becomes permeable to macromolecules. Creatine kinase, for example, an enzyme normally found inside muscle, is elevated in serum of DMD patients. Evans Blue Dye (EBD) is also used to determine membrane permeability. In this case, EBD injected into the tail vein of mice became apparent in degenerating mdx myofibers, but not in intact or regenerating mdx fibers or wild-type mouse fibers (Matsuda et al., 1995). Similar results have been found using procion orange dye. Moreover, even greater uptake of orange dye was observed after forced muscle contractions than during rest in *mdx* muscles (Petrof et al., 1993).

Another area that could contribute to the disease course of DMD is altered signal transduction. The DPC members, syntrophins, bind numerous signaling molecules, as reviewed above. Given this and the fact that syntrophins have two binding sites on both dystrophin and dystrobrevin (Ahn

and Kunkel, 1995; Newey et al., 2000) and that syntrophin is absent from the sarcolemma in the absence of dystrophin (Butler et al., 1992), one could imagine that perturbations in signal transduction would arise from the absence of syntrophin at the membrane, contributing to the pathphysiology of DMD. A promising example of what might occur from the loss of syntrophin came from one of syntrophin's binding partners, nNOS, which produces nitric oxide (NO), an important regulator of vasodilation during exercise (Brenman et al., 1996). As nNOS is absent from the sarcolemma of dystrophin-deficient tissue and the vasodilation response during exercise is impaired in DMD muscle, one hypothesis of DMD pathophysiology was that the lack of NO production could cause muscle ischemia during exercise (Brenman et al., 1996; Crosbie, 2001; Sander et al., 2000). However, neither nNOS-null mice nor syntrophin-null mice show any signs of muscle disease (Adams et al., 2004; Adams et al., 2000; Huang et al., 1993). Intriguingly, though, transgenic overexpression of nNOS in *mdx* muscle alleviates the dystrophic phenotype (Wehling et al., 2001). A "two-hit" hypothesis has been proposed to explain this apparent paradox (Rando, 2001). According to the hypothesis, the pathogenic defects found in DMD muscle are likely caused by at least two biochemical consequences, such as enhanced ischemia, resulting from the loss of nNOS (first hit), in combination with an increased vulnerability of the muscle to ischemia, resulting from the disruption of the DPC in DMD (second hit). The hypothesis thus suggests that, while the loss of one protein alone might not be detrimental to muscle, it may, in

connection with the loss of dystrophin and the DPC, contribute to the DMD phenotype.

Mouse models of muscular dystrophy.

The understanding of DMD and the function of the DPC, as well as the research into therapies and treatments for DMD, have been greatly aided by the use of various animal models of muscular dystrophy. The most commonly used animal model is the *mdx* mouse, which arose from a spontaneous, nonsense mutation in exon 23 of the dystrophin gene (Bulfield et al., 1984; Sicinski et al., 1989). Like human DMD patients, the mutation is X-linked recessive and the *mdx* mice do not make the dystrophin protein (Hoffman et al., 1987). Muscles exhibit abnormal morphology beginning at approximately 3 weeks of age, at which time muscle weakness develops and muscle degeneration and regeneration events become evident (e.g. muscle fiber necrosis, fiber size variation, elevated serum creatine kinase and pyruvate kinase levels, accumulation of macrophages, proliferation of satellite cells and fibroblasts, and small, centrally-nucleated fibers) (Bulfield et al., 1984). However, for unknown reasons, the myopathology in *mdx* mice is much less severe than that of DMD patients with only the diaphragm displaying the severe myopathy seen in DMD patients (Sicinski et al., 1989), and the mice essentially live a normal lifespan, an obvious difference from human DMD patients. Despite the slight phenotypic

differences between humans and mice, the *mdx* mouse is an invaluable tool in the study of DMD.

In addition to *mdx* mice, mice lacking α-dystrobrevin (*Dtna*$^{-/-}$) also display a muscular dystrophy, albeit a milder form than that of *mdx* mice. *Dtna*$^{-/-}$ mice were created by deleting a 2.5kb segment, containing exon 3, of the α-dystrobrevin gene (Grady et al., 1999). The deletion results in the loss of α-dystrobrevin-1 and α-dystrobrevin-2, which are the only known *Dtna* splice variants in skeletal muscle (Peters et al., 1998). *Dtna*$^{-/-}$ muscles resemble *mdx* muscles but to a milder degree, e.g. less necrosis, fibrosis, and fiber size variability, and fewer centrally-nucleated fibers and macrophages. *Dtna*$^{-/-}$ muscles become dystrophic by one month of age, with the number of necrotic fibers reaching a plateau at six months of age and centrally-nucleated fibers at three months of age. Like *mdx* mice, *Dtna*$^{-/-}$ mice live a normal lifespan.

Therapeutic approaches to DMD

Despite the identification nearly 20 years ago of dystrophin as the gene affected in DMD, a therapy for DMD still has yet to be found. However, in 1996, Cox et al. showed that transgenically overexpressing full-length dystrophin in *mdx* mouse muscle effectively restored expression of dystrophin and the other DPC members at the sarcolemma and eliminated the dystrophic phenotype, as illustrated by restoration of the morphological, immunohistochemical, and functional aspects of the muscles (Cox et al., 1993). This work effectively

marked the beginning of the current, on-going effort to use gene therapy to treat DMD. Current efforts to restore functional dystrophin into humans include the use of antisense oligonucleotides (AO) to create short forms of dystrophin by modifying the *in vivo* processing of dystrophin, and the use of viral vectors for introducing short forms of dystrophin.

One approach to introducing dystrophin into muscle cells is to modify dystrophin pre-mRNA processing. Both Duchenne and Becker muscular dystrophies occur from mutations in the dystrophin gene. However, while DMD patients are diagnosed young, suffer from severe, progressive skeletal loss, and die by their early 20s, BMD patients are typically diagnosed later, have less severe muscle loss, and can live into mid- to late-adulthood. The phenotypic differences result from the types of genetic mutations giving rise to the two diseases, i.e. DMD is caused by out-of-frame mutations, resulting in the loss of the dystrophin protein, whereas BMD is caused by in-frame mutations, resulting in shortened, yet functional, dystrophin protein (Monaco et al., 1988). Current efforts aim to alter dystrophin pre-mRNA processing in order to restore the reading frame and create functional dystrophin protein (Mann et al., 2001). The goal of this method is to convert the DMD phenotype to that of BMD, as a shorter, but functional dystrophin protein would be generated. *In vitro* studies using DMD and *mdx* muscle cells have shown that AOs can block normal splice sites of dystrophin pre-mRNA, resulting in a skipping of the exon(s), restoration of the reading frame, and synthesis of dystrophin protein (Aartsma-Rus et al.,

2002; Mann et al., 2001; van Deutekom et al., 2001). Work in *mdx* mice, using intramuscular injection of AOs, has also shown effective dystrophin synthesis, as well as less dystrophic muscles (Williams et al., 2006; Yin et al., 2007).

As DMD is caused by various types of out-of-frame mutations, e.g. duplications, insertions, or single-point mutations, no one AO will be sufficient to treat all DMD cases. Each patient's mutations will need to be known and a tailor-made plan will need to be devised for each case. Additionally, some restorations of reading frames by exon-skipping will be easier than others. For example, single-exon duplication events appear easier to target than multiple-exon events. However, depending on the duplicated exon, sometimes attempting to skip the duplicated exon results in the inadvertent skipping of the original exon as well, generating out-of-frame mutations (Aartsma-Rus et al., 2007). In other cases, again depending on which exon the mutation is in, some single exons can be simply skipped while still staying in frame, whereas in other cases, adjacent exons must also be skipped in order to restore the open reading frame. Although many questions, like the safety and long-term effectiveness of this technology still need to be addressed, exon-skipping provides a promising treatment for DMD.

Adeno-associated virus (AAV)-based vectors are being explored as a means of delivering dystrophin to muscle cells. Because of the small genome size of the AAV vector and large size of the dystrophin gene, full-length dystrophin cannot be packaged efficiently into AAV vector (Hermonat et al.,

1997). Like in exon-skipping, efforts have therefore focused on the creation of shorter, yet still functional, dystrophins that can be inserted into the AAV genome and effectively packaged into the virion for delivery to muscle. These "micro-dystrophins" and "mini-dystrophins" lack various amounts of the central rod domain and/or carboxy-terminus and have shown to be an effective method of restoring dystrophin in and attenuating the phenotype of mdx muscle (Gregorevic et al., 2006; Liu et al., 2005; Ragot et al., 1993; Wang et al., 2000). Ultimately, the effective delivery of dystrophin to DMD muscle and the amelioration of DMD will require not only a functional dystrophin packaged into AAV, but also the lack of an immune response to the virus and an efficient mechanism and effective viral dose for long-term, widespread delivery of the virus to within and among muscles (Ragot et al., 1993). Efforts are currently underway to address these issues in the mdx mouse and canine models of DMD (Foster et al., 2006; Wang et al., 2007; Yuasa et al., 2007).

The DPC and the NMJ

To this point, the focus on the dystrophin complex has largely been on its components and their functions at the extra-synaptic regions of the sarcolemma, but the complex also has important roles at the NMJ, too. The complex members at the NMJ are the same or similar to those on the sarcolemma, but whereas the DPC members are significantly reduced or lost from the sarcolemma in the absence of dystrophin, they are retained at the

post-synaptic membrane of the NMJ (Crosbie et al., 1997; Grady et al., 1997b; Peters et al., 1997b; Peters et al., 1998). The most notable differences at the post-synaptic membrane from the rest of the sarcolemma are the presence of a dystrophin homolog, utrophin, the organization of the complex members, and the role of the complex in NMJ maturation and maintenance.

Utrophin was identified from human fetal muscle two years after the discovery of dystrophin (Love et al., 1989). Derived from an autosomal gene, utrophin shares approximately 80% amino acid identity with dystrophin (Figure 1.2). Utrophin is expressed in a number of tissues, including lung, which has high levels of expression, brain, nervous system, vascular endothelial and smooth muscle cells, and skeletal muscle (Karpati et al., 1993; Love et al., 1991; Matsumura et al., 1993). Immunohistochemical examination found utrophin expressed along the sarcolemma of fetal muscle fibers, as well as along the sarcolemma of adult muscle fibers after denervation (Takemitsu et al., 1991). In normal adult fibers, utrophin is only expressed at the NMJ, colocalizing with acetylcholine receptors (AChR). However, in dystrophin-deficient fibers, utrophin is found not only at the NMJ, but all along the sarcolemma in a manner similar to dystrophin in normal muscle (Karpati et al., 1993; Nguyen et al., 1991). Because utrophin binds to the same DPC proteins as dystrophin (Ahn et al., 1996; Chung and Campanelli, 1999; Matsumura et al., 1992; Peters et al., 1998), this suggests that utrophin is upregulated in order to compensate for the lack of dystrophin at the sarcolemma. Two lines of

evidence largely support this idea. First, mice lacking both dystrophin and utrophin exhibit a more severe dystrophy than mice lacking only dystrophin (Grady et al., 1997b). Second, transgenic overexpression of utrophin rescues the phenotype of dystrophin-null mouse (mdx) muscle (Tinsley et al., 1998).

The post-junctional membrane of skeletal muscle is arranged into a series of folds, and some DPC members localize to specific regions of those folds. Utrophin localizes to the crests of the folds with AChR, whereas dystrophin is found in the troughs of the folds with voltage-gated sodium channels (Bewick et al., 1992; Byers et al., 1991; Flucher and Daniels, 1989; Sealock et al., 1991). Along the extra-synaptic regions of the sarcolemma, β-dystroglycan binds to dystrophin, but at the NMJ, β-dystroglycan is also able to bind to utrophin (Chung and Campanelli, 1999). Yeast-two hybrid studies found that α-dystrobrevin-1, which is found exclusively at the NMJ, interacts with both utrophin and dystrophin, and α-dystrobrevin-2, which is found all along the sarcolemma, binds only to dystrophin (Peters et al., 1998). Accordingly, α-dystrobrevin-1 localizes to the crests and troughs of the folds with utrophin and dystrophin, and α-dystrobrevin-2 is found predominantly in the troughs with dystrophin (Peters et al., 1998). Like the dystrobrevins, the syntrophins also have distict localization patterns at the NMJs of adult muscle. Colocalization studies found α1-syntrophin staining at the crests and troughs, consistent with biochemical studies showing α1-syntrophin associating equally well with utrophin and dystrophin (Ahn et al., 1996; Kramarcy and Sealock, 2000). β2-

syntrophin stained strongly in the troughs, but weakly at the crests, a surprising result given that β2-syntrophin associates with utrophin and dystrophin in immunopurification assays (Ahn et al., 1996; Kramarcy and Sealock, 2000; Peters et al., 1997a). β1-syntrophin is detectable in only a subset of type IIb fast fibers in mice over six weeks of age, where it localizes exclusively to the troughs of the folds, again somewhat surprising given its interactions with both utrophin and dystrophin (Ahn et al., 1996; Kramarcy and Sealock, 2000). Lastly, γ2-syntrophin also preferentially localizes to the NMJ, but is actually in a subsynaptic space under the NMJ, thus not found in the folds at all (Alessi et al., 2006). These data show that DPC member localization at the NMJ is quite distinct, likely reflecting specialized functions for the different DPC combinations at the different regions of the NMJ.

The formation of the synapse requires the agrin-stimulated clustering of acetylcholine receptors (AChR) on the postsynaptic membrane (Gautum et al., 1996); however, the stabilization and maintenance of the NMJ depend upon the presence of the dystrophin complex, as suggested by mice lacking elements of the DPC. α-syntrophin null (Adams et al., 2000), β2-syntrophin-/α-syntrophin-null (Adams et al., 2004), α-dystrobrevin null (Grady et al., 2000), and utrophin-null mice (Deconinck et al., 1997; Grady et al., 1997a) each have structural defects at the neuromuscular junction (NMJ).

Despite utrophin's strict localization to the NMJ in adult skeletal muscle, suggesting its importance to NMJ structure, mice lacking utrophin display no

signs of dystrophy and have only mild neuromuscular defects (Deconinck et al., 1997; Grady et al., 1997a). These defects include a reduction in the number of acetylcholine receptors by 30-50%. The effect of this alteration on neuromuscular transmission is minimal, with only minor reductions in miniature end-plate current amplitudes observed.

The α-dystrobrevin-null and syntrophin-null mice have provided more convincing evidence of the importance of the DPC at the NMJ (Adams et al., 2000; Grady et al., 2000). In contrast to wild-type mice, the α-dystrobrevin-null and α-syntrophin-null mice have shallower gutters, abnormal and reduced numbers of folds (>50%), and abnormal distribution of AChRs. AChRs appear in patchy clusters both along the folds and extending beyond the gutters, and the numbers of AChRs are dramatically reduced. Mice doubly-deficient in α- and β2-syntrophin have more structurally abnormal NMJs and an even greater reduction in AChR levels than those in mice lacking just α-syntrophin (Adams et al., 2004). Moreover, unlike the α-syntrophin-null and α-dystrobrevin-null mice, the double knock-outs are unable to run as far as wild-type mice. The mechanisms leading to all these NMJ abnormalities are unclear. A plausible explanation, though, is that as a result of a loss of syntrophins, or a reduction of syntrophins, as occurs in the α-dystrobrevin-null mouse, signaling pathways are altered, affecting proper NMJ structure. Together with the observation that α-dystrobrevin is necessary for maintaining AChR clusters in myotubes following agrin withdrawal (Grady et al., 2000), these studies strongly suggest that the

DPC members, α–, β2-syntrophin and α-dystrobrevin, are required for stabilizing AChR at the NMJ.

Concluding Remarks

In an effort to gain a better understanding of the pathophysiology of muscular dystrophy, I have performed gene expression analyses of α-dystrobrevin-null skeletal muscle (Chapter 2). Gene expression studies were also performed on both α-dystrobrevin-null and α-syntrophin null skeletal muscles in order to elucidate the molecular mechanisms responsible for the NMJ abnormalities found in those mice (Chapter 2). The data revealed a highly significant decrease in the amount of Niemann-Pick C1 (*Npc1*) transcript in the α-dystrobrevin-null quadriceps muscle. Chapter 3 examines whether or not NPC1 downregulation may be contributing to the dystrophy and/or NMJ abnormalities associated with α-dystrobrevin-null mouse, by transgenically expressing *Npc1* in α-dystrobrevin-null skeletal muscles. Furthermore, Chapter 3 examines whether or not transgenically expressing *Npc1* alleviates the more severe dystrophy of *mdx* muscle, which could yield a potentially new therapeutic approach for treating DMD. Lastly, NPC1 is the gene mutated in NPC disease, a progressive and ultimately fatal neurodegenerative, lysosomal storage disorder. The results presented in this thesis are the first indication of a potential commonality between neuronal degeneration in NPC disease and muscle degeneration in muscular dystrophy. In Chapter 5, I examine if

transgenically expressing *Npc1* in NPC1-null mouse skeletal muscle can correct the wasting and shortened lifespan of these animals.

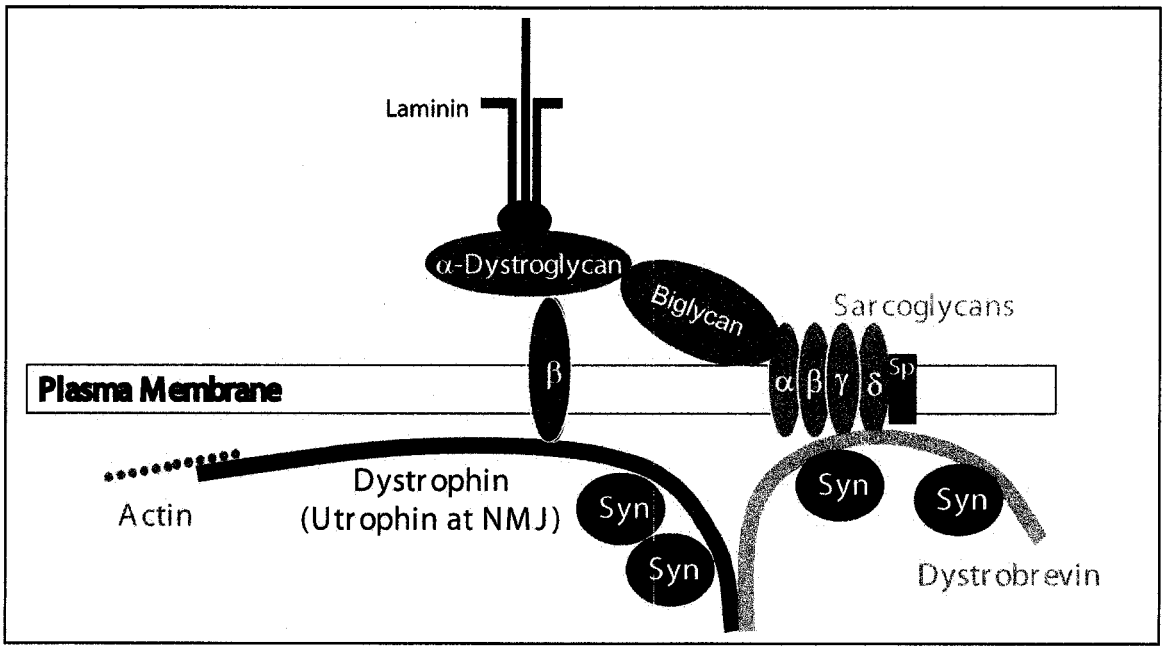

Figure 1.1: Diagram of the dystrophin-associated protein complex (DPC). The DPC links the intracellular actin cytoskeleton to laminin in the extracellular matrix. In addition to dystrophin, the DPC consists of the dystroglycans (α and β), the sarcoglycan subcomplex, consisting of the sarcoglycans (α,β,γ,δ) and sarcospan (Sp), and the syntrophin (Syn)-dystrobrevin subcomplex. In adult muscle, utrophin replaces dystrophin at the neuromuscular junction (NMJ) at the crests of the post-synaptic membrane folds, whereas dystrophin is found in the depths of the folds and extra-synaptically along the rest of the plasma membrane. Adapted from (Albrecht and Froehner, 2002)

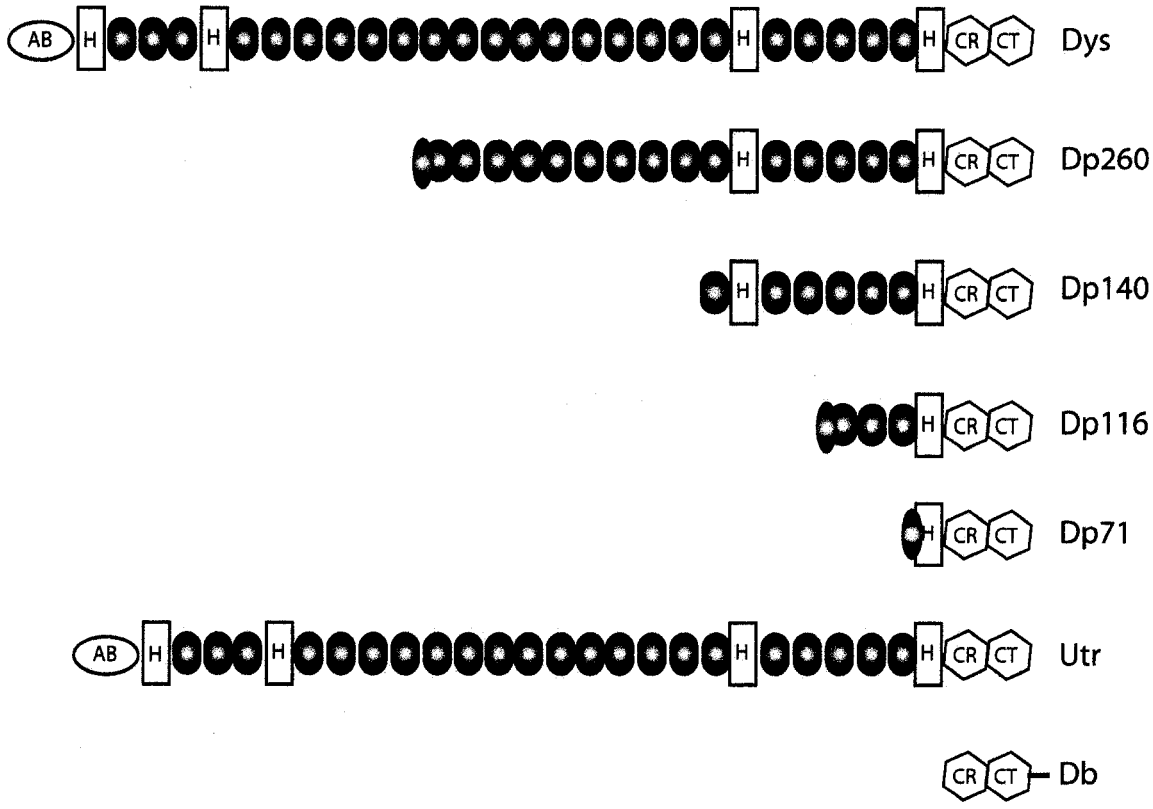

Figure 1.2: Diagram of the dystrophin protein, isoforms, and related family members. Dystrophin (Dys) contains an actin-binding (AB) amino-terminal, a rod domain comprised of spectrin-like repeats (shaded ellipses) and hinge domains (H), a cysteine-rich (CR) domain necessary for binding β-dystroglycan, and a carboxy-terminal (CT) necessary for binding dystrobrevins and syntrophins. Alternate promoters within the dystrophin gene create shorter isoforms of dystrophin found in various tissues: Dp260 (retina), Dp140 (brain), Dp116 (Schwann cells), and Dp71 (ubiquitously expressed). The dystrophin family members, utrophin and the dystrobrevins are encoded by distinct genes. Utrophin shares significant sequence similarity and identity to dystrophin. The dystrobrevins share sequence similarity only with the CR/CT domains of dystrophin.

CHAPTER 2:

Gene expression analyses of α-dystrobrevin-null and α-syntrophin-null skeletal muscles

Introduction

The dystrophin-associated protein complex (DPC), located throughout the sarcolemma of skeletal muscle, links the intracellular actin cytoskeleton to the extracellular matrix (Figure 1.1). Genetic defects in some of the proteins comprising the dystrophin complex result in several fatal skeletal muscle wasting diseases (Brown, 1997). The most well known of these diseases, Duchenne muscular dystrophy, results from mutations in the dystrophin gene (Hoffman et al., 1987). Although not as severe as DMD patients' muscles, *mdx* mouse muscles, which lack functional dystrophin, also exhibit dystrophy. Additionally, defects in any of the four sarcoglycans result in limb girdle muscular dystrophies (Bushby, 1999), and mice lacking α-dystrobrevin (*Dtna*$^{-/-}$) become moderately dystrophic by one month of age (Grady et al., 1999).

Members of the DPC are also necessary for the stabilization and maintenance of the neuromuscular synapse (Adams et al., 2004; Adams et al., 2000; Deconinck et al., 1997; Grady et al., 1997a; Grady et al., 2000). Emerging evidence supports the hypothesis that the proteins in this complex are parts of signaling pathways of which some, when abnormal, lead to muscular dystrophy, and others, when abnormal, result in defects of the neuromuscular junction (NMJ). Whereas the formation of the synapse requires

the agrin-stimulated clustering of acetylcholine receptors (AChR) on the postsynaptic membrane (Gautum et al., 1996), the stabilization of the synapse depends upon the presence of the dystrophin complex (Adams et al., 2000; Grady et al., 2000). α-syntrophin null (*Snta*$^{-/-}$) (Adams et al., 2000; Grady et al., 2000), α-dystrobrevin null (Grady et al., 2000), utrophin-null (Deconinck et al., 1997; Grady et al., 1997), α- and β2-syntrophin double mutants (Adams et al., 2004), and *mdx* mice (Lyons and Slater, 1991), for example, show structural defects at the NMJ. The underlying mechanism for this process is unclear. However, as the syntrophins bind signaling proteins such as nNOS (Brenman et al., 1996; Gee et al., 1998; Lumeng et al., 1999; Schultz et al., 1998), and syntrophins are greatly reduced at α-dystrobrevin-null NMJs (Grady et al., 2000) and absent at α-syntrophin-null NMJs, a plausible explanation for the NMJ defects in these mice is impaired signaling pathways.

As described previously in Chapter 1, the α-syntrophin-null (Adams et al., 2000) and α-dystrobrevin-null (Grady et al., 1999; Grady et al., 2000) mice exhibit NMJ abnormalities. Compared to wild-type mice, the *Snta*$^{-/-}$ and *Dtna*$^{-/-}$ have shallower synaptic gutters on the post-synaptic membrane, reduced numbers of folds (>50%), and abnormal distribution of AChRs. AChRs appear in patches at the synapse and in clusters extending beyond the synapse. In addition, *Snta*$^{-/-}$ mice had reduced numbers of AChRs. AChR levels in *Dtna*$^{-/-}$ muscle were not quantitated. Whereas the *Dtna*$^{-/-}$ muscle is mildly dystrophic (Grady et al., 1999), however, *Snta*$^{-/-}$ appears healthy. Thus, these mice exhibit

some phenotypic features in common, but differ in other features. Examination of gene expression levels in these mice may provide explanations for the observed similarities and differences. Genes involved in the formation of muscular dystrophy, for example, may be up- or down-regulated in the α-dystrobrevin-null mouse, but unchanged in the α-syntrophin-null mice, which is not dystrophic (Adams et al., 2000). Therefore, in order to elucidate genes whose misregulation may be responsible for the development of muscular dystrophy and/or abnormalities of the NMJ, I compared gene expression changes in skeletal muscles of the α-dystrobrevin-null and α-syntrophin-null mice.

Materials and Methods

Affymetrix GeneChip Arrays

RNA was isolated from the quadriceps muscles of individual six-week-old, male *Dtna*$^{-/-}$ mice (Grady et al., 1999), a gift of Joshua Sanes at Harvard University, and from the quadriceps muscles of *Snta*$^{-/-}$ mice (Adams et al., 2000) and compared to that of age- and sex-matched, homozygous wild-type littermates. We used the Affymetrix GeneChip microarray system (Center for Expression Arrays, University of Washington) to screen the genome for expression changes in *Dtna*$^{-/-}$ and *Snta*$^{-/-}$ mice. Total RNA from each muscle was isolated with Trizol reagent (Invitrogen), followed by a cleanup of the RNA with the RNeasy Mini Kit (Qiagen). 20μg RNA was subsequently processed for

gene expression analysis, using Affymetrix GeneChip U74Av2, U74Bv2, and U74Cv2 arrays, following suggested Affymetrix protocols (www.affymetrix.com). RNAs from eight experimental and eight control mice were analyzed on each of the U74 arrays. Samples were not pooled. Briefly, following isolation, the total RNA was converted to double-stranded cRNA (SuperScript Choice system, Invitrogen). Single-stranded, biotin-labeled cRNA (BioArray™ HighYield™ RNA Transcript Labeling Kit (T7), Enzo Life Sciences) was then synthesized by *in vitro* transcription, and fragmented. 15μg of fragmented, single-stranded, biotin-labeled cRNA was subsequently hybridized to the Affymetrix arrays, which were stained with the GeneChip® Fluidics Station 400 (Affymetrix) and scanned with the GeneChip® Scanner 3000 (Affymetrix) at the Center for Array Technologies at the University of Washington. Initial data analysis was performed with Affymetrix ® Microarray Suite 5.0. Student's paired *t* tests were performed on the signal intensities of all probe sets to identify significant differences between the control and experimental groups. $P<0.005$ was considered significant.

In addition to quadriceps muscles, we analyzed gene expression levels in the diaphragm muscles of six-week-old, male *Dtna*$^{-/-}$ mice and their age- and sex-matched littermates. Purification and processing of the RNA was performed as described above, with the following exceptions. Firstly, all processing of the RNA following RNA extraction was performed at the Center for Expression Arrays (University of Washington), following recommended

Affymetrix protocols. Secondly, RNA from ten experimental and ten control muscles were processed using Affymetrix GeneChip® 430 v.2 arrays. Lastly, initial data analysis was performed with Affymetrix GeneChip® Operating Software (GCOS).

Real-Time Quantitative RT-PCR

Changes in gene expression ($p<0.005$, using paired Student's *t* test) were confirmed by Real-Time quantitative RT-PCR, using TaqMan® chemistry and the ABI 7000 sequence detection system (Applied Biosystems). Muscles were dissected and total RNA was prepared, as described above, from six-week-old male *Dtna*$^{-/-}$ or *Snta*$^{-/-}$ mice and their age- and sex-matched wild-type littermates. Each sample was treated individually. Real-Time quantitative RT-PCR was performed on each sample with an ABI Prism 7000 Sequence Detection System (Applied Biosystems), using 50ng of total RNA, One-Step RT-PCR Master Mix reagents (Applied Biosystems), *18S* primers and probe (Applied Biosystems, P/N 4310893E), and primers (Integrated DNA Technologies; Applied Biosystems) and probes (Biosearch Technologies; Sigma; Applied Biosystems) for the respective experimental genes (Table 2.1). The relative expression of *NPC1* mRNA was normalized to the amount of *18S* RNA in the same sample. Each sample was run in duplicate. A Student's paired *t* test was performed to determine the significance of the difference in *Npc1* expression between the control and experimental groups.

Results

Expression levels in Dtna$^{-/-}$ and Snta$^{-/-}$ quadriceps muscles

Using Affymetrix GeneChip® technology, we have examined expression levels of RNA isolated from the quadriceps muscles of individual six-week-old, male homozygous null (*Dtna*$^{-/-}$ or *Snta*$^{-/-}$) and homozygous wild-type mice. Each knockout mouse, *Dtna*$^{-/-}$ or *Snta*$^{-/-}$, was compared to an age- and sex-matched wild-type littermate. Isolated cRNA was hydridized to, stained, and scanned on the Murine Genome U74A, B, and C arrays, which contain probe sets representing approximately 36,000 fully characterized genes and expressed sequence tags (EST). We have identified 93 upregulated probe sets (Table 2.2) and 87 downregulated (Table 2.3) probe sets in the *Snta*$^{-/-}$ muscle, and 116 upregulated probe sets (Table 2.4) and 87 downregulated probe sets (Table 2.5) in *Dtna*$^{-/-}$ muscle ($p<0.005$).

In the *Snta*$^{-/-}$ quadriceps, we have examined several of the expression changes ($p<0.005$) identified by the Affymetrix arrays, using real-time quantitative RT-PCR (Applied Biosystems 7000 Sequence Detection System) (Table 2.6). Using TaqMan® chemistry, we have confirmed ($p<0.05$) the decreased expression of α-syntrophin (*Snta*) and the increased expression of *Kcne1l (Kcne5)*, the epsilon subunit of the acetylcholine receptor (*Chrne*), and aquaporin 4 (*Aqp4*), in the *Snta*$^{-/-}$ quadriceps. However, contrary to the data from the Affymetrix arrays, RT-PCR analysis indicates that *Abcc3* levels are

elevated, rather than reduced, and that syndecan 4 (*Sdc4*) levels are unchanged, rather than decreased in *Snta*$^{-/-}$ muscle.

Additionally, we have confirmed ($p<0.05$) the decreased expression of α-dystrobrevin (*Dtna*), Niemann Pick Type C1 (*Npc1*), and *Ankrd1* in the *Dtna*$^{-/-}$ quadriceps muscle (Table 2.7). However, although the data from the Affymetrix arrays indicates decreased *Traf5* expression, ($p<0.005$), analysis of gene expression by quantitative RT-PCR instead suggests a significant increase ($p<0.05$) of *Traf5* expression in *Dtna*$^{-/-}$ quadriceps muscles by RT-PCR. Contrary to the Affymetrix array data as well, expression levels of β1-adrenergic receptor (*Adrb1*), *Sema4g*, *Efna5*, and the epsilon subunit of the acetylcholine receptor (*Chrne*), were not significantly different between the *Dtna*$^{-/-}$ and wild-type quadriceps muscles when examined by RT-PCR.

Because *Dtna*$^{-/-}$ and *Snta*$^{-/-}$ muscle have abnormalities of the NMJ, including reduced numbers of post-junctional folds and abnormal distributions of ACh receptors, gene expression alterations that the *Dtna*$^{-/-}$ and *Snta*$^{-/-}$ muscles have in common may indicate genes whose misregulation contributes to or causes the NMJ irregularities. Therefore, using the Affymetrix array data, we compared the genes, which were significantly changed ($p<0.005$) in the quadriceps muscle of the *Dtna*$^{-/-}$ mice to the genes, which were significantly changed ($p<0.005$) in the quadriceps muscle of the *Snta*$^{-/-}$ mice (Table 2.8). Expression levels of four transcripts were significantly elevated in both of the *Dtna*$^{-/-}$ and *Snta*$^{-/-}$ muscles: *Acot11* (acyl-CoA thioesterase 11), *Myl4* (myosin,

light polypeptide 4), *Prkar1a* (protein kinase, camp dependent regulatory, type I, alpha), and *Chrne* (cholinergic receptor, nicotinic, epsilon polypeptide). No down-regulated transcripts were held in common between the *Dtna*$^{-/-}$ and *Snta*$^{-/-}$ muscles.

Gene expression changes in the diaphragm of α-dystrobrevin-null mice.

Whereas normal muscle has similarly sized fibers with peripherally located nuclei, dystrophic muscle displays fibers of variable size with centrally located nuclei, indicating degenerating and regenerating fibers. Grady et al. (1999) have reported that the quadriceps femoris, tibialis anterior, soleus, and sternomastoid muscles of the α-dystrobrevin-null mouse become dystrophic by one month of age, and by three months of age, ~50% of all fibers within the muscles have centrally located nuclei. A more severe dystrophy was reported in the diaphragm muscle. In contrast, our lab has found that the severity of muscular dystrophy observed in the α-dystrobrevin-null mouse varies among the different muscles with a much smaller percentage of centrally-nucleated fibers found in the quadriceps muscle (10% and 35%) than in the diaphragm (~25% and ~70.5%) at eight and 16 weeks of age, respectively (Y. Tesch and D.E. Albrecht, personal communication). These data suggest that α-dystrobrevin-null diaphragm muscle may be a better muscular dystrophy model for gene expression analysis than the quadriceps muscle and that a comparison of gene expression changes found in these two muscles may provide an

explanation for why one muscle is more severely affected by dystrophy than the other.

We examined expression levels of RNA isolated from the diaphragms of individual six-week-old, male α-dystrobrevin-null mice and their age- and sex-matched wild-type littermates. The expression analyses were performed using Affymetrix GeneChip® 430 2.0 arrays, which consist of more than 45,000 probe sets interrogating over 34,000 well-characterized genes. We have identified 233 upregulated probe sets (Table 2.9) and 372 downregulated probe sets in the α-dystrobrevin-null diaphragms, compared to controls ($p<0.005$) (Table 2.10).

A comparison of the significant ($p<0.005$) changes in transcript expression levels in the diaphragm muscle to the quadriceps muscles identified 13 transcripts that are differentially expressed in both the diaphragm and quadriceps muscle (Table 2.11). Eight transcripts are down-regulated in both muscles, such as *Dtna* (α-dystrobrevin) and *Abcb4* (ATP-binding cassette, sub-family B, member 4), and three transcripts are up-regulated in both muscles, such as *Igf2* (Insulin-like growth factor 2) and *Myl4* (myosin, light polypeptide 4). Three transcripts are differentially affected in the two muscles. For example, *Mapk9* (mitogen activated protein kinase 9) is elevated in $Dtna^{-/-}$ quadriceps muscle but reduced in the diaphragm.

Discussion

Arguably the most well-known dystrophy, Duchenne Muscular Dystrophy, results from mutations in the dystrophin gene, causing the loss of the dystrophin protein. Although some of the effects of the loss of dystrophin are known, such as the loss of dystrobrevin, α-syntrophin, the sarcoglycans, and nNOS, the precise molecular consequences occurring downstream of these losses, culminating in the dystrophic phenotype, are largely unknown (Brenman et al., 1995; Butler et al., 1992; Ervasti et al., 1990; Mizuno et al., 1995; Mizuno et al., 1994b). Several gene expression analyses have previously been performed on muscles from DMD patients and *mdx* mice in order to elucidate the molecular pathways affected by the absence of dystrophin. The preponderance of transcriptional changes are related to inflammation, extracellular matrix biology, muscle regeneration, and cell signaling (Bakay et al., 2002; Haslett et al., 2002; Haslett et al., 2003; Porter et al., 2002; Porter et al., 2004; Tkatchenko et al., 2000; Tkatchenko et al., 2001).

The α-dystrobrevin-null mouse displays a much milder dystrophy than the *mdx* mouse. Because of this, we hypothesized that comparing gene expression levels in *Dtna*$^{-/-}$ muscle to wild-type muscle would identify genes whose misregulation contributes to the development of muscular dystrophy, but might otherwise be obscured by the significant inflammatory or regeneration genes that accompany severely dystrophic *mdx* and DMD muscles. In addition, by comparing the transcriptional changes in the α-dystrobrevin-null quadriceps

muscle to those in α-syntrophin-null quadriceps muscle, we hypothesized that we could further narrow the list of misregulated genes contributing to dystrophic muscle as well as identify misregulated genes and/or pathways contributing to NMJ abnormalities. Transcripts that are similarly differentially expressed between the *Snta*$^{-/-}$ and *Dtna*$^{-/-}$ mice may cause or contribute to the NMJ abnormalities that these mice share; whereas, transcriptional changes occurring only in *Dtna*$^{-/-}$ muscle may represent molecular alterations responsible for muscular dystrophy, as only *Dtna*$^{-/-}$ muscle is dystrophic.

Using Affymetrix expression arrays and a pre-determined significance level of $p<0.005$, we identified 180 differentially expressed probe sets in *Snta*$^{-/-}$ quadriceps muscle and 203 differentially expressed probe sets in *Dtna*$^{-/-}$ quadriceps muscle. Given the $p<0.005$ significance level and the fact that 36,701 probe sets were examined in the *Dtna*$^{-/-}$ and *Snta*$^{-/-}$ studies, conservatively, one would expect that the expression of 184 probe sets would be significantly altered just by chance alone. This suggests that all of the *Snta*$^{-/-}$ muscle changes and all but 19 of the *Dtna*$^{-/-}$ muscle changes identified, could theoretically be false positives, which may explain why several of the changes that were identified by the arrays could not be confirmed by RT-PCR. Of the 180 transcriptional changes identified in the *Snta*$^{-/-}$ muscle, we followed-up with quantitative RT-PCR analyses of the expression of six of those transcripts, but could confirm that only four of the six examined were indeed differentially expressed in the *Snta*$^{-/-}$ muscle. Similarly, of the changes identified by

Affymetrix arrays in the *Dtna*$^{-/-}$ muscle, we confirmed only three of the eight transcriptional changes that were examined further with RT-PCR analyses. A possible explanation for the relatively few significant transcriptional changes found in the *Snta*$^{-/-}$ mouse could be that, phenotypically, the lack of α-syntrophin appears only to affect the NMJ, a relatively small region of skeletal muscle (Adams et al., 2000; Kameya et al., 1999). A similar explanation could also be given for the *Dtna*$^{-/-}$ quadriceps muscle, which also has NMJ abnormalities. Although one might expect significantly more changes in *Dtna*$^{-/-}$ muscle, similar to the numbers that have been reported in other dystrophic muscle, e.g. *mdx* muscle (Haslett et al., 2005; Porter et al., 2002; Porter et al., 2004), our lab has found that the degree of dystrophy in the *Dtna*$^{-/-}$ quadriceps may not be as severe as previous studies have suggested (Grady et al., 1999).

As previously explained, we compared transcriptional changes, as identified by Affymetrix arrays ($p<0.005$), from *Dtna*$^{-/-}$ quadriceps muscle to *Snta*$^{-/-}$ quadriceps muscle in an effort to identify genes whose misregulation may result in NMJ abnormalities or muscular dystrophy. Four transcripts were differentially expressed in both *Dtna*$^{-/-}$ and *Snta*$^{-/-}$ muscle: *Prkar1a*, *Acot11*, *Myl4*, and *Chrne*. Acot11, also called BFIT (brown-fat-inducible thioesterase), was significantly elevated in both mutant mice. Elevated BFIT transcript has been found in brown adipose tissue (BAT) and skeletal muscle following exposure to cold, in BAT in food-restricted mice 4-6 hours post-feeding, and in obesity-resistant mouse strains (Adams et al., 2001). BFIT is a member of the

acyl-CoA thioesterase functional family and, as such, is postulated to be involved in fatty acid metabolism, regulation of cell signaling, and trafficking of proteins (Adams et al., 2001), Although a role for BFIT at the NMJ has not been studied, the study by Adams et al. (2001) suggests a potentially interesting role for syntrophin and/or dystrobrevin in lipid metabolism. The significant upregulation of *Chrne* (nicotinic cholinergic receptor, epsilon subunit) levels provided potentially the most interesting change with respect to the NMJ defects of the *Dtna*$^{-/-}$ and *Snta*$^{-/-}$ mice. *Chrne* is the epsilon subunit of the acetycholine receptor that replaces the gamma subunit in adult muscle to give the nAChR subunit stoichiometry, $(\alpha 1)_2\beta 1\varepsilon\tilde{\delta}$. However examination of *Chrne* transcript levels in the *Dtna*$^{-/-}$ muscle by RT-PCR did not confirm the change identified by the arrays. Of particular interest, a small, yet significant increase was found in *Prkar1a*, the R1α regulatory subunit of cAMP-dependent protein kinase. Recently, both α-dystrobrevin-1 and -2 were found to directly interact with *Prkar1a* (Ceccarini et al., 2007). Moreover, α-syntrophin was found in a complex with α-dystrobrevin and *Prkar1a*. In addition, the authors found that α-dystrobrevin is a substrate for PKA phosphorylation. As α-dystrobrevin is reduced at the NMJs of α-syntrophin mice (Adams et al., 2000), an increase in *Prkar1a* expression in *Dtna*$^{-/-}$ and *Snta*$^{-/-}$ muscle may suggest that the phosphorylation of dystrobrevin by PKA or the tethering of PKA by dystrobrevin to the DPC for phosphorylation of DPC or DPC-interacting proteins is necessary for maintaining NMJ structure.

We also compared transcriptional changes in the *Dtna*$^{-/-}$ quadriceps and diaphragm muscles. Our lab has found that *Dtna*$^{-/-}$ quadriceps exhibit a less severe dystrophy than diaphragm muscles (Y. Tesch and DE Albrecht, personal communication), consistent with reports from *mdx* muscle (Haslett et al., 2005). Therefore, not only could changes in common between the two muscles provide strong support for a role for these genes in the pathogenesis or progression of the disease, but changes exclusive to the diaphragm might provide valuable information toward understanding why some muscles are more severely affected than others. This knowledge could, in turn, aid in the creation of therapies that prevent a muscle from becoming severely dystrophic. The diaphragm and other respiratory muscles of DMD patients would most obviously benefit from this strategy, as DMD patients generally succumb to respiratory failure due to the severe damage to the respiratory muscles as a result of the disease.

Of the more than 200 differentially expressed transcripts in the quadriceps muscle and the more than 600 differentially expressed transcripts in the diaphragm muscle, 13 transcripts were differentially expressed in both muscles, but not necessarily in the same direction. In other words, expression of some transcripts was either upregulated or downregulated in both muscles; however, in the case of *Mapk3*, upregulation occurs in the quadriceps muscle while downregulation occurs in the diaphragm, which could contribute to the phenotypic differences of the two muscles. Insulin-like growth factor (Igf)-2 was

one transcript we found upregulated in the diaphragm and quadriceps muscles. Increased expression of *Igf-2* has also been shown in biopsy samples from DMD patients (Bakay et al., 2002) and the quadriceps and diaphragm muscles of *mdx* mice (Haslett et al., 2005; Porter et al., 2004). IGF-II stimulates myoblast proliferation and differentiation (Florini et al., 1996), and overexpression of IGF-II in mdx mice has been shown to ameliorate the dystrophic phenotype (Smith et al., 2000). Together these data suggest that the upregulation of *Igf-2* in dystrophic muscle is part of the regenerative process of the muscle. Interestingly, *Myl4* (a.k.a. *Mlc1a*), whose expression was upregulated in the quadriceps muscles of both the $Dtna^{-/-}$ and $Snta^{-/-}$ mice, was upregulated in the $Dtna^{-/-}$ diaphragm as well. During the fetal skeletal muscle development in the mouse, *Myl4* is the most abundantly expressed myosin light chain, but after birth Myl4 transcripts are detectable only in slow muscle (Washabaugh et al., 1998), suggesting that this transcript is upregulated as a result of the regenerative process in the $Dtna^{-/-}$ muscles. As $Snta^{-/-}$ muscle is not dystrophic and histologically does not appear to have a higher than normal number of regenerated fibers, the reason for the elevation of *Myl4* is unclear, although a shift in fiber type composition as a result of α-syntrophin loss is an intriguing possibility. On the other hand, $Snta^{-/-}$ muscles treated with cardiotoxin to damage sarcolemmae show hypertrophy of, decreased exercise capacity and contractile force of, and NMJ abnormalities in regenerating fibers, similar to what has been found in *mdx* muscle (Hosaka et al., 2002). Taking the "two-hit"

hypothesis described in chapter 1 into consideration (Rando, 2001), the loss of α-syntrophin by itself, as in *Snta*$^{-/-}$ muscles, may not impair the ability of muscle to regenerate, but the reduction of α-syntrophin in combination with the sarcolemmal damage found in *Dtna*$^{-/-}$ and *mdx* may adversely affect the regenerative capacity of dystrophic muscle.

At first glance, the few similarities in transcriptional changes between the *Dtna*$^{-/-}$ quadriceps and diaphragms muscles may lead one to conclude that gene expression studies do not provide useful information toward furthering the understanding of the molecular events leading to muscular dystrophy. For example, *Npc1*, which was altered in the quadriceps muscle was statistically unchanged in the more affected diaphragm and *Snta*$^{-/-}$ quadriceps, leading one to surmise that *Npc1* expression changes may be uninvolved in either the dystrophic process or the disruption of the NMJ. However, we have found evidence suggesting that the reduction of *Npc1* may contribute to muscular dystrophy (See Chapter 3). An explanation for the lack of similar expression patterns between the two muscles may simply be that muscles are different from each other. Not only do various wild-type skeletal muscles have significantly different expression patterns from each other (Haslett et al., 2005), but gene expression studies of dystrophin-deficient mouse and human skeletal muscle also show different molecular responses of individual muscles to the dystrophin deficiency (Haslett et al., 2005; Porter et al., 2004). The loss of α-dystrobrevin likely then has different downstream consequences in the

diaphragm than the quadriceps. As *Dtna*$^{-/-}$ diaphragm is more dystrophic than quadriceps, transcriptional decreases in skeletal muscle genes, such as *Npc1*, may be missed in the diaphragm analyses due to the presence of those same transcripts in the infiltrating inflammatory cells, for example.

Here we provide gene expression analyses of *Snta*$^{-/-}$ quadriceps, *Dtna*$^{-/-}$ quadriceps, and *Dtna*$^{-/-}$ diaphragm muscle and their littermate controls. We hypothesized that transcriptional differences between the aforementioned muscles and their respective controls would help to identify molecular changes that occur downstream of the loss of α-dystrobrevin or α-syntrophin and result in the dystrophy and/or NMJ defects seen in these muscles. An obvious limitation of this approach is that the list of changes identified include not only those that may contribute to the phenotype(s), but also those that are secondary to, i.e. arise from the abnormalities themselves. These data therefore serve to provide lists of candidate genes for further study. In the following chapter, I take a closer look at one such gene, *Npc1*, found here to be downregulated in *Dtna*$^{-/-}$ muscle, and examine the effect that transgenically expressing *Npc1* in skeletal muscle has on the phenotype, i.e. NMJ abnormalities and dystrophy, typical to the *Dtna*$^{-/-}$ muscle.

Table 2.1: Quantitative RT-PCR primers and probes

Gene Symbol	**Primers** (Integrated DNA Technologies)	**Probe** (Biosearch Technologies)
Npc1	5'-AAT GCG GTC TCC TTG GTC AA-3' 5'-GCT CTC GTT ATA TGG CTG CAG AA-3'	5' 6-FAM d(CAC AGA AAT GCC ACA GCT CAT CAC CAA) BHQ-1 3'
Dtna	5'- CCC CTA CTG CAG GTC TTA ACT AAC A -3' 5'- AAC ATA CAT TAG AGG CCA AAG CAA T -3'	5' 6-FAM d(AGG GCT GCT GTC CTG CTG ACC TTC T) BHQ-1 3'
Snta1	5'- GAT GCA CCA GCC CTG AAG AG -3' 5'- CCA GAC GAG CAG GCA GTC A -3'	5' 6-FAM d(TTC ATC TTG TGG CCT GAC CTG TCC TTC) BHQ-1 3'
Sdc4	5'- GGC TCC TGG GCC TGC TT -3' 5'- GCC ACA CGA GGC CAC TGT AT -3'	5' 6-FAM d(CTC CAG GCG CTC TAG ATG CAC AAT CC) BHQ-1 3'
Abcc3	5'- AGG GCT TGT GGG TCT TTC TGT -3' 5'- CCA AGT CGG ATA TCA TTC GTA TCA -3'	5' 6-FAM d(TCC TAT GCC TTA CAG GTG ACC ATG GCT TT) BHQ-1 3'
Adrb1	5'- CAA GAC ACT GGG CAT CAT CAT G -3' 5'- CCA CGT TGG CCA GGA AGA -3'	5' 6-FAM d(TGT GTT CAC GCT CTG CTG GCT GC) BHQ-1 3'
EphA5	5'- TGT CTG TAT CAA TGA CTA CCT GGA TGT -3' 5'- CGT AGC GCT CAG TCT TGT CTT C -3'	5' 6-FAM d(TTC TGC CCT CAC TAT GAG GAC TCT GTC CC) BHQ-1 3'
Aqp4	5'- TGG AGC CAG CAT GAA TCC A -3' 5'- CCA GTG GTT TGC CCA GTT TC -3'	5' 6-FAM d(CTC GAT CTT TTG GAC CCG CAG TTA TCA TG) BHQ-1 3'

Gene Symbol	**Primers** (Applied Biosystems)	**Probe** (Sigma)
Chrne	5'- TGC CCA GAA AAT TCC AGA GAC T -3' 5'- GGC AAC CAC CAT GAC GAA TAT -3'	5' 6-FAM d(CTG CTG GGC AGG TAT) MGBNFQ 3'

Gene Symbol	**Primers/Probe** (Applied Biosystems)
Sema4g	P/N Mm00442518_m1
Kcne1l	P/N Mm00517596_s1
Ankrd1	P/N Mm 00495767_m1
Traf5	P/N Mm00496512_m1

Table 2.2: Up-regulated transcripts in *Snta*$^{-/-}$ versus wild-type quadriceps muscle, with expression fold changes indicated

Probe ID	Gene symbol	Gene name	p value	Change
165433_at	Prmt2	protein arginine N-methyltransferase 2	3.38E-06	1.23
103617_at	Cd55	CD55 antigen	0.00009	1.35
113555_at	Loh12cr1	loss of heterozygosity, 12, chromosomal region 1 homolog (human)	0.00015	1.16
162688_at	Coq10b	coenzyme Q10 homolog B (S. cerevisiae)	0.00016	1.50
104548_at	Phlda2	pleckstrin homology-like domain, family A, member 2	0.00017	1.58
136066_at	---	Transcribed locus	0.00019	1.29
104092_at	LOC674195 /// Usp48	ubiquitin specific peptidase 48 /// hypothetical protein LOC674195	0.00021	1.19
105098_at	Sfi1	Sfi1 homolog, spindle assembly associated (yeast)	0.00040	2.84
134064_at	Twistnb	TWIST neighbor	0.00046	1.73
93892_at	Cugbp2	CUG triplet repeat, RNA binding protein 2	0.00056	1.21
100306_at	2700007P21Rik	RIKEN cDNA 2700007P21 gene	0.00057	1.30
110689_at	B4galt7	xylosylprotein beta1,4-galactosyltransferase, polypeptide 7 (galactosyltransferase I)	0.00059	1.36
110406_at	Nek1	NIMA (never in mitosis gene a)-related expressed kinase 1	0.00072	1.12
168221_f_at	Lrrc48	leucine rich repeat containing 48	0.00074	1.49
161316_f_at	---	---	0.00089	1.39
92550_at	Krt19	keratin 19	0.00100	1.36
101408_at	Gamt	guanidinoacetate methyltransferase	0.00109	1.12
96030_at	Csn1s1	casein alpha s1	0.00109	1.31
94545_at	Rtn1	reticulon 1	0.00115	1.33
96023_at	Vac14	Vac14 homolog (S. cerevisiae)	0.00122	1.30
163236_at	6720467C03Rik	RIKEN cDNA 6720467C03 gene	0.00124	1.29
170021_i_at	Snx10	Sorting nexin 10	0.00125	1.96
96852_at	Prkar1a	protein kinase, cAMP dependent regulatory, type I, alpha	0.00127	1.12
94838_r_at	LOC630663 /// OTTMUSG00000000651 /// Prl2c2 /// Prl2c3	prolactin family 2, subfamily c, member 2 /// prolactin family 2, subfamily c, member 3 /// similar to Proliferin 3 precursor (Mitogen-regulated protein 3) /// predicted gene, OTTMUSG00000000651	0.00136	3.02
99194_at	LOC641190 /// Pnpt1	polyribonucleotide nucleotidyltransferase 1 /// similar to polyribonucleotide nucleotidyltransferase 1	0.00142	1.16

Table 2.2 continued:

160487_at	Myl4	myosin, light polypeptide 4	0.00150	1.27
93993_at	Lman2	lectin, mannose-binding 2	0.00157	1.17
102703_s_at	Aqp4	aquaporin 4	0.00174	1.48
165661_i_at	4922501K12Rik	RIKEN cDNA 4922501K12 gene	0.00185	2.08
95854_at	C76332	expressed sequence C76332	0.00193	1.90
171328_at	---	---	0.00193	1.39
165124_r_at	---	---	0.00208	3.06
160160_at	Dedd	death effector domain-containing	0.00209	1.32
135807_r_at	---	Transcribed locus	0.00209	1.78
100907_at	Kcne1l	potassium voltage-gated channel, Isk-related family, member 1-like	0.00210	2.25
170186_i_at	Odz2	Odd Oz/ten-m homolog 2 (Drosophila)	0.00212	1.93
114244_at	Zfp11	zinc finger protein 11	0.00225	1.17
161181_f_at	Dusp16	dual specificity phosphatase 16	0.00229	2.42
106580_at	Magee1	melanoma antigen, family E, 1	0.00232	1.12
102237_at	Cd28	CD28 antigen	0.00237	1.39
93776_at	Ngdn	neuroguidin, EIF4E binding protein	0.00248	1.42
96861_at	Mrpl50	mitochondrial ribosomal protein L50	0.00248	1.10
130745_at	Ppp1r13b	protein phosphatase 1, regulatory (inhibitor) subunit 13B	0.00248	1.34
165806_at	Jazf1	JAZF zinc finger 1	0.00251	2.47
103603_at	Eftud1	elongation factor Tu GTP binding domain containing 1	0.00260	1.50
166304_f_at	Atp6ap2	ATPase, H+ transporting, lysosomal accessory protein 2	0.00260	1.98
167461_r_at	Prdm16	PR domain containing 16	0.00267	1.10
166368_at	Txndc8	thioredoxin domain containing 8	0.00273	1.24
165250_at	---	---	0.00275	1.34
95523_at	2900062L11Rik	RIKEN cDNA 2900062L11 gene	0.00276	1.43
168479_at	---	---	0.00292	1.15
135322_at	Fancl	Fanconi anemia, complementation group L	0.00293	2.00
111986_at	Vti1a	Vesicle transport through interaction with t-SNAREs homolog 1A (yeast)	0.00297	2.40
169187_at	Eml4	Echinoderm microtubule associated protein like 4	0.00307	1.39
170398_r_at	Psme4	proteasome (prosome, macropain) activator subunit 4	0.00310	1.98
104743_at	Cdh13	cadherin 13	0.00313	1.21
95961_at	Nbeal2	neurobeachin-like 2	0.00315	1.43

Table 2.2 continued:

104199_at	Tigd5	tigger transposable element derived 5	0.00320	1.20
160078_at	Ppp1r14b	protein phosphatase 1, regulatory (inhibitor) subunit 14B	0.00333	1.15
103921_i_at	Cyb5r1	cytochrome b5 reductase 1	0.00340	1.18
103657_i_at	Mtf2	metal response element binding transcription factor 2	0.00341	1.34
166309_at	Katnb1	katanin p80 (WD40-containing) subunit B 1	0.00343	1.47
136750_at	Acot11	Acyl-CoA thioesterase 11	0.00350	1.40
137680_at	Clasp1	CLIP associating protein 1	0.00359	1.64
115439_at	4732473B16Rik	RIKEN cDNA 4732473B16 gene	0.00363	1.45
116855_at	Clstn1	calsyntenin 1	0.00366	1.16
114690_at	Mthfs	5, 10-methenyltetrahydrofolate synthetase	0.00369	1.23
92247_at	Arhgap5	Rho GTPase activating protein 5	0.00378	1.65
92282_at	2610304G08Rik	RIKEN cDNA 2610304G08 gene	0.00378	1.29
92966_g_at	Chrne	cholinergic receptor, nicotinic, epsilon polypeptide	0.00379	1.53
97360_at	Cmtm3	CKLF-like MARVEL transmembrane domain containing 3	0.00386	1.87
94739_at	Trpc1	transient receptor potential cation channel, subfamily C, member 1	0.00389	1.45
94238_at	Prss23	protease, serine, 23	0.00392	1.16
109377_at	Rapgef3	Rap guanine nucleotide exchange factor (GEF) 3	0.00405	1.24
162702_at	Dusp14	dual specificity phosphatase 14	0.00416	1.10
93664_at	Atp1b2	ATPase, Na+/K+ transporting, beta 2 polypeptide	0.00419	1.16
115685_at	4632428C04Rik	RIKEN cDNA 4632428C04 gene	0.00425	1.20
110121_at	Sema3a	sema domain, immunoglobulin domain (Ig), short basic domain, secreted, (semaphorin) 3A	0.00426	1.39
170970_i_at	Fuk	fucokinase	0.00428	1.51
129284_at	9630023C09Rik	RIKEN cDNA 9630023C09 gene	0.00432	1.51
113452_at	Obfc2a	oligonucleotide/oligosaccharide-binding fold containing 2A	0.00440	2.01
167870_at	2900016G23Rik	RIKEN cDNA 2900016G23 gene	0.00441	3.58
98462_s_at	Klc4	kinesin light chain 4	0.00448	1.13
140782_f_at	Nek4	NIMA (never in mitosis gene a)-related expressed kinase 4	0.00453	1.40
114767_at	Acsm1	acyl-CoA synthetase medium-chain family member 1	0.00459	1.42
102416_at	Cyp17a1	cytochrome P450, family 17, subfamily a, polypeptide 1	0.00467	1.35
92393_at	Kcna3	potassium voltage-gated channel, shaker-related subfamily, member 3	0.00470	1.30
92796_at	Akp2	alkaline phosphatase 2, liver	0.00470	1.32
94380_at	Ide	insulin degrading enzyme	0.00471	1.12

Table 2.2 continued:

105495_at	Ddx59	DEAD (Asp-Glu-Ala-Asp) box polypeptide 59	0.00482	1.56
115427_at	Asph	aspartate-beta-hydroxylase	0.00485	1.30
137727_at	Ssh1	slingshot homolog 1 (Drosophila)	0.00488	1.45
161905_r_at	---	---	0.00498	1.37

Table 2.3: Down-regulated transcripts in *Snta*$^{-/-}$ versus wild-type quadriceps muscle, with expression fold changes indicated

Probe ID	Gene symbol	Gene name	p value	Change
102890_at	Snta1	syntrophin, acidic 1	1.08E-07	-4.18
104089_at	2810026P18Rik	RIKEN cDNA 2810026P18 gene	0.00010	-1.28
162147_f_at	Snta1	syntrophin, acidic 1	0.00011	-2.19
166865_f_at	Stau1	Staufen (RNA binding protein) homolog 1 (Drosophila)	0.00011	-1.29
102922_at	Pitpnc1	phosphatidylinositol transfer protein, cytoplasmic 1	0.00022	-1.11
111332_at	Ift52	intraflagellar transport 52 homolog (Chlamydomonas)	0.00027	-1.47
104934_at	---	Transcribed locus	0.00035	-1.80
114971_at	Rnf11	ring finger protein 11	0.00038	-1.28
115237_at	2410127E16Rik	RIKEN cDNA 2410127E16 gene	0.00039	-1.22
96299_at	---	Transcribed locus, moderately similar to XP_580165.1 hypothetical protein XP_580165 [Rattus norvegicus]	0.00040	-1.58
110320_at	Elk4	ELK4, member of ETS oncogene family	0.00050	-1.09
97447_at	Map1lc3a	microtubule-associated protein 1 light chain 3 alpha	0.00057	-1.30
114997_at	Lass4	longevity assurance homolog 4 (S. cerevisiae)	0.00065	-1.35
98590_at	Sdc4	syndecan 4	0.00073	-1.59
166097_at	Ccdc70	coiled-coil domain containing 70	0.00080	-1.94
139748_at	9330129D05Rik	RIKEN cDNA 9330129D05 gene	0.00085	-1.19
101161_at	Mc1r	melanocortin 1 receptor	0.00093	-1.49
105188_at	4632419I22Rik	RIKEN cDNA 4632419I22 gene	0.00107	-1.15
99833_at	Capn9 /// LOC639715	calpain 9 (nCL-4) /// similar to calpain 9 (nCL-4)	0.00109	-1.86
165943_f_at	Igl-V1	immunoglobulin lambda chain, variable 1	0.00121	-1.78
113519_r_at	1700081L11Rik	RIKEN cDNA 1700081L11 gene	0.00123	-1.40
138963_r_at	Sept3	septin 3	0.00127	-1.63
135301_at	---	Transcribed locus	0.00127	-1.71
105904_at	---	---	0.00129	-1.17
170017_r_at	Ciapin1	cytokine induced apoptosis inhibitor 1	0.00129	-1.95
167652_i_at	1700007N14Rik	RIKEN cDNA 1700007N14 gene	0.00136	-1.44
160566_at	Prss8	protease, serine, 8 (prostasin)	0.00142	-2.07
105569_at	---	---	0.00149	-1.17
168604_r_at	Nat13	N-acetyltransferase 13	0.00157	-1.12

Table 2.3 continued:

135241_g_at	---	Transcribed locus	0.00169	-1.09
171526_r_at	---	---	0.00171	-3.48
113396_f_at	Ccdc22	coiled-coil domain containing 22	0.00181	-1.27
93598_at	Snx5	sorting nexin 5	0.00186	-1.17
171175_at	Dock6 /// LOC670024	dedicator of cytokinesis 6 /// similar to Dedicator of cytokinesis protein 6	0.00198	-1.21
137535_at	Elk4	ELK4, member of ETS oncogene family	0.00202	-1.35
113986_at	Egln3	EGL nine homolog 3 (C. elegans)	0.00208	-1.28
100151_at	Serinc3	serine incorporator 3	0.00212	-1.78
100702_at	Shbg	sex hormone binding globulin	0.00222	-1.26
108373_at	B930006L02Rik	RIKEN cDNA B930006L02 gene	0.00228	-1.81
105610_at	Pitpnc1	phosphatidylinositol transfer protein, cytoplasmic 1	0.00229	-1.21
100059_at	Cyba	cytochrome b-245, alpha polypeptide	0.00231	-1.13
102836_at	RP23-136K12.4	putative phosphatase	0.00232	-1.10
103689_at	Abcc3	ATP-binding cassette, sub-family C (CFTR/MRP), member 3	0.00255	-2.40
163736_at	Neurl2	neuralized-like 2 (Drosophila)	0.00256	-1.38
107419_at	Accn2	Amiloride-sensitive cation channel 2, neuronal	0.00268	-1.43
115983_at	---	---	0.00269	-2.24
171280_i_at	Pus7	pseudouridylate synthase 7 homolog (S. cerevisiae)	0.00280	-3.14
160432_at	U2af1l4	U2 small nuclear RNA auxiliary factor 1-like 4	0.00281	-1.18
161584_r_at	Elf1	E74-like factor 1	0.00290	-2.83
169068_i_at	4930434J08Rik	RIKEN cDNA 4930434J08 gene	0.00293	-1.21
98135_r_at	Otud6b	OTU domain containing 6B	0.00315	-1.59
169922_at	Asahl	N-acylsphingosine amidohydrolase (acid ceramidase)-like	0.00316	-2.01
99556_s_at	Sry	sex determining region of Chr Y	0.00317	-1.38
93323_at	Plp2	proteolipid protein 2	0.00326	-1.08
169231_at	Hsd17b10	Hydroxysteroid (17-beta) dehydrogenase 10	0.00329	-1.70
110030_at	Dgkb	Diacylglycerol kinase, beta	0.00343	-1.77
137122_at	AA409587	expressed sequence AA409587	0.00343	-1.19
102396_at	Ift172	intraflagellar transport 172 homolog (Chlamydomonas)	0.00352	-1.11
135609_at	Egln3	EGL nine homolog 3 (C. elegans)	0.00356	-1.28
135389_at	E330016A19Rik	RIKEN cDNA E330016A19 gene	0.00357	-2.10
93780_at	Them2	thioesterase superfamily member 2	0.00357	-1.23
114170_at	Rgag4	retrotransposon gag domain containing 4	0.00362	-1.87

Table 2.3 continued:

160376_at	Trp53inp2	transformation related protein 53 inducible nuclear protein 2	0.00364	-1.32
103555_at	Chmp4b	chromatin modifying protein 4B	0.00372	-1.15
167887_at	---	Adult male testis cDNA, RIKEN full-length enriched library, clone:4930515K13 product:unclassifiable, full insert sequence	0.00374	-1.19
108886_at	Zer1	zer-1 homolog (C. elegans)	0.00384	-1.64
161197_r_at	D10Wsu52e	DNA segment, Chr 10, Wayne State University 52, expressed	0.00387	-1.74
133560_at	Ap1gbp1	AP1 gamma subunit binding protein 1	0.00390	-1.27
170613_r_at	4933430H16Rik	RIKEN cDNA 4933430H16 gene	0.00394	-3.18
136758_at	---	Transcribed locus	0.00396	-1.46
92549_at	Pkig	protein kinase inhibitor, gamma	0.00404	-1.35
171359_at	Smarca2	SWI/SNF related, matrix associated, actin dependent regulator of chromatin, subfamily a, member 2	0.00405	-1.23
168401_f_at	Pld4	phospholipase D family, member 4	0.00421	-1.40
167810_r_at	Vapb	Vesicle-associated membrane protein, associated protein B and C	0.00422	-1.40
115506_at	Hbp1	high mobility group box transcription factor 1	0.00432	-1.25
135298_at	---	---	0.00433	-1.91
164338_f_at	Sord	sorbitol dehydrogenase	0.00436	-1.35
164300_i_at	Sparc	secreted acidic cysteine rich glycoprotein	0.00452	-1.31
163064_at	Elavl2	ELAV (embryonic lethal, abnormal vision, Drosophila)-like 2 (Hu antigen B)	0.00455	-1.57
167929_at	EG546166	predicted gene, EG546166	0.00458	-1.89
94857_at	Mpg	N-methylpurine-DNA glycosylase	0.00466	-1.28
138398_at	---	Transcribed locus	0.00466	-1.83
164045_at	BC087945	cDNA sequence BC087945	0.00473	-1.19
106171_at	A230083H22Rik	RIKEN cDNA A230083H22 gene	0.00481	-1.47
165846_r_at	1700027D21Rik	RIKEN cDNA 1700027D21 gene	0.00482	-2.79
163117_at	Eif4e2	eukaryotic translation initiation factor 4E member 2	0.00490	-1.24
107283_at	LOC669042 /// Zfp467	zinc finger protein 467 /// similar to zinc finger protein EZI	0.00491	-1.28

Table 2.4: Up-regulated transcripts in *Dtna*$^{-/-}$ versus wild-type quadriceps muscle, with expression fold changes indicated

Probe ID	Gene Symbol	Gene Name	p value	Change
116686_at	Acot11	acyl-CoA thioesterase 11	0.00004	1.40
95706_at	Lgals3	lectin, galactose binding, soluble 3	0.00006	2.99
102048_at	Ankrd1	ankyrin repeat domain 1 (cardiac muscle)	0.00007	2.10
97459_at	Psma4	proteasome (prosome, macropain) subunit, alpha type 4	0.00013	1.12
160925_at	Nras	neuroblastoma ras oncogene	0.00013	1.25
171091_f_at	1700010B08Rik	RIKEN cDNA 1700010B08 gene	0.00015	1.22
160156_at	0910001A06Rik	RIKEN cDNA 0910001A06 gene	0.00021	1.23
101464_at	Timp1	tissue inhibitor of metalloproteinase 1	0.00024	1.93
99175_at	Gng10	guanine nucleotide binding protein (G protein), gamma 10	0.00024	1.30
98008_at	Cx3cl1	chemokine (C-X3-C motif) ligand 1	0.00034	1.38
97519_at	Spp1	secreted phosphoprotein 1	0.00037	2.39
100281_at	Gmcl1	Germ cell-less homolog 1 (Drosophila)	0.00041	1.73
163977_at	---	---	0.00046	1.39
164112_at	4632415L05Rik	RIKEN cDNA 4632415L05 gene	0.00046	1.44
162738_at	Tfrc	transferrin receptor	0.00052	1.32
94282_at	Asah1	N-acylsphingosine amidohydrolase 1	0.00061	1.24
98473_at	Arg2	arginase type II	0.00070	1.93
98604_at	Rrp1	ribosomal RNA processing 1 homolog (S. cerevisiae)	0.00070	1.13
105369_at	---	---	0.00075	1.36
161045_at	Lrrn1	leucine rich repeat protein 1, neuronal	0.00077	1.37
134289_r_at	Stx11	syntaxin 11	0.00077	1.74
167635_r_at	Matn3	matrilin 3	0.00081	3.21
114811_at	4930430E16Rik	RIKEN cDNA 4930430E16 gene	0.00082	1.91
97952_at	Tsc2	tuberous sclerosis 2	0.00083	1.30
98623_g_at	Igf2	insulin-like growth factor 2	0.00083	1.22
111911_at	Yif1b	Yip1 interacting factor homolog B (S. cerevisiae)	0.00084	1.06
168835_s_at	Colec11	collectin sub-family member 11	0.00085	1.91
100828_at	Myl4	myosin, light polypeptide 4	0.00086	1.37
97319_at	Rrad	Ras-related associated with diabetes	0.00087	2.00
105197_at	---	Transcribed locus	0.00091	4.22
97885_at	Tmem176b	transmembrane protein 176B	0.00095	1.16

Table 2.4 continued:

98535_at	Comt	catechol-O-methyltransferase	0.00104	1.14
94972_at	Rbms1	RNA binding motif, single stranded interacting protein 1	0.00106	1.26
92966_g_at	Chrne	cholinergic receptor, nicotinic, epsilon polypeptide	0.00107	1.87
116249_at	Rps6ka5	ribosomal protein S6 kinase, polypeptide 5	0.00108	1.35
165648_i_at	Sept6	septin 6	0.00118	1.15
101281_at	Olfr49	olfactory receptor 49	0.00122	1.44
99463_at	Cyp3a13	cytochrome P450, family 3, subfamily a, polypeptide 13	0.00126	1.40
114584_at	C87482	expressed sequence C87482	0.00128	2.49
96695_at	Ube2a	ubiquitin-conjugating enzyme E2A, RAD6 homolog (S. cerevisiae)	0.00135	1.12
111406_at	LOC676546 /// Mmd	monocyte to macrophage differentiation-associated /// similar to monocyte to macrophage differentiation-associated	0.00150	1.21
160963_at	9630050M13Rik	RIKEN cDNA 9630050M13 gene	0.00157	1.21
92441_at	Fap	fibroblast activation protein	0.00162	1.26
108788_at	Zfp553	zinc finger protein 553	0.00173	2.05
138487_at	Arpp21	Cyclic AMP-regulated phosphoprotein, 21	0.00174	1.11
170018_r_at	Manba	mannosidase, beta A, lysosomal	0.00179	1.11
108295_at	Rab11fip4	RAB11 family interacting protein 4 (class II)	0.00182	1.75
170804_at	Serpinb1b	serine (or cysteine) peptidase inhibitor, clade B, member 1b	0.00189	1.60
101793_at	Fcgr1	Fc receptor, IgG, high affinity I	0.00191	1.24
113308_at	Stard8	START domain containing 8	0.00196	1.21
169266_at	Prdm2	PR domain containing 2, with ZNF domain	0.00200	1.52
162911_at	C030048B08Rik	RIKEN cDNA C030048B08 gene	0.00202	1.21
92611_at	Caprin1	cell cycle associated protein 1	0.00205	1.19
98042_at	Scpep1	serine carboxypeptidase 1	0.00206	1.22
102297_at	Zkscan6	zinc finger with KRAB and SCAN domains 6	0.00206	1.88
102896_at	Dok1	docking protein 1	0.00215	1.41
95283_at	Abcc2	ATP-binding cassette, sub-family C (CFTR/MRP), member 2	0.00224	1.79
161650_at	Slpi	secretory leukocyte peptidase inhibitor	0.00228	1.18
99677_at	2610042O14Rik	RIKEN cDNA 2610042O14 gene	0.00231	1.20
103335_at	Lgals9	lectin, galactose binding, soluble 9	0.00239	1.28
114610_at	Birc6	Baculoviral IAP repeat-containing 6	0.00241	2.38
129843_at	Tmtc2	Transmembrane and tetratricopeptide repeat containing 2	0.00248	1.22
160461_f_at	Tubb6	tubulin, beta 6	0.00254	1.45
94850_at	Acot9	acyl-CoA thioesterase 9	0.00259	1.19

Table 2.4 continued:

162927_at	Dner	delta/notch-like EGF-related receptor	0.00265	1.16
104338_r_at	Pkp2	plakophilin 2	0.00274	2.61
160487_at	Myl4	myosin, light polypeptide 4	0.00274	2.46
162083_f_at	Ntan1	N-terminal Asn amidase	0.00274	1.92
104578_f_at	Actn1	actinin, alpha 1	0.00284	1.16
132812_at	5230400M03Rik	RIKEN cDNA 5230400M03 gene	0.00287	1.48
103549_at	Nes	nestin	0.00294	1.25
116590_at	Appl1	adaptor protein, phosphotyrosine interaction, PH domain and leucine zipper containing 1	0.00294	1.17
105420_at	Rab14	RAB14, member RAS oncogene family	0.00305	1.26
166358_at	Catsper1	cation channel of sperm 1	0.00309	1.59
100775_at	---	---	0.00310	1.42
97426_at	Emp1	epithelial membrane protein 1	0.00316	1.36
101753_s_at	Lyz /// Lyzs	lysozyme	0.00316	1.83
104116_at	D5Ertd593e	DNA segment, Chr 5, ERATO Doi 593, expressed	0.00326	1.24
101926_at	Pim2	proviral integration site 2	0.00326	1.25
164317_f_at	---	---	0.00334	1.27
103890_at	Unc45a	unc-45 homolog A (C. elegans)	0.00341	1.45
97909_at	Stmn1	stathmin 1	0.00344	1.35
94047_at	0610031J06Rik	RIKEN cDNA 0610031J06 gene	0.00351	1.09
116600_at	2610203C20Rik	RIKEN cDNA 2610203C20 gene	0.00361	1.24
169741_at	Lce1i	late cornified envelope 1I	0.00361	2.30
138075_at	Mapk9	mitogen activated protein kinase 9	0.00366	1.19
100300_at	Cybb	cytochrome b-245, beta polypeptide	0.00371	1.53
100593_at	Tnnt2	troponin T2, cardiac	0.00381	2.02
104355_at	Fus	fusion, derived from t(12;16) malignant liposarcoma (human)	0.00388	2.63
167301_r_at	1700025F22Rik	RIKEN cDNA 1700025F22 gene	0.00389	1.77
162856_at	Leprotl1	leptin receptor overlapping transcript-like 1	0.00396	1.16
170143_at	Zfp40	Zinc finger protein 40	0.00397	1.82
130749_at	Thrap5	thyroid hormone receptor associated protein 5	0.00397	1.22

Table 2.4 continued:

101049_at	EG622589 /// EG633570 /// EG668844 /// LOC622098 /// LOC630855 /// LOC639477 /// LOC668706 /// Rpl12 /// Snora65	small nucleolar RNA, H/ACA box 65 /// ribosomal protein L12 /// similar to 60S ribosomal protein L12 /// predicted gene, EG622589 /// predicted gene, EG633570 /// predicted gene, EG668844	0.00401	1.29
109403_at	Cd44	CD44 antigen	0.00404	1.71
163038_at	Itgb1bp2	integrin beta 1 binding protein 2	0.00405	1.05
108822_at	Gpnmb	glycoprotein (transmembrane) nmb	0.00415	1.62
109824_f_at	Gatm	glycine amidinotransferase (L-arginine:glycine amidinotransferase)	0.00421	1.29
94785_at	---	---	0.00423	1.82
163814_r_at	Plagl1	pleiomorphic adenoma gene-like 1	0.00428	1.78
167278_f_at	Prkra	protein kinase, interferon inducible double stranded RNA dependent activator	0.00432	1.45
96852_at	Prkar1a	protein kinase, cAMP dependent regulatory, type I, alpha	0.00435	1.12
99887_at	Efna5	ephrin A5	0.00437	2.54
111239_at	Pvrl3	poliovirus receptor-related 3	0.00442	2.08
105412_at	Slc25a21	solute carrier family 25 (mitochondrial oxodicarboxylate carrier), member 21	0.00454	3.60
112378_at	Sh3kbp1	SH3-domain kinase binding protein 1	0.00459	1.14
161001_at	AA407270	expressed sequence AA407270	0.00483	1.67
93143_at	1190005I06Rik	RIKEN cDNA 1190005I06 gene	0.00484	1.39
93327_at	Tax1bp3	Tax1 (human T-cell leukemia virus type I) binding protein 3	0.00489	1.23
105960_at	4930431J08Rik	RIKEN cDNA 4930431J08 gene	0.00489	1.41
139163_at	B3galt1	UDP-Gal:betaGlcNAc beta 1,3-galactosyltransferase, polypeptide 1	0.00491	1.16
102169_at	Olfr93	olfactory receptor 93	0.00491	2.56
134330_at	Trim55	Tripartite motif-containing 55	0.00494	1.16
99910_at	Accn1	amiloride-sensitive cation channel 1, neuronal (degenerin)	0.00496	1.69
161805_r_at	Nsun2	NOL1/NOP2/Sun domain family 2	0.00497	1.67
113574_at	Htra3	HtrA serine peptidase 3	0.00498	1.16

Table 2.5: Down-regulated transcripts in *Dtna*$^{-/-}$ versus wild-type quadriceps muscle, with expression fold changes indicated

Probe ID	Gene Symbol	Gene Name	p value	Change
98114_at	Npc1	Niemann Pick type C1	3.02E-07	-1.80
108855_at	Dtna	dystrobrevin alpha	1.32E-06	-4.53
92183_at	Dtna	dystrobrevin alpha	0.00005	-2.35
168336_at	Dtna	dystrobrevin alpha	0.00010	-2.39
168745_at	4930596D02Rik	RIKEN cDNA 4930596D02 gene	0.00013	-1.40
92888_s_at	Styx	phosphoserine/threonine/tyrosine interaction protein	0.00023	-1.21
103255_at	Traf5	Tnf receptor-associated factor 5	0.00024	-2.30
136760_at	Dtna	dystrobrevin alpha	0.00030	-2.57
163706_at	Tpmt	thiopurine methyltransferase	0.00032	-2.23
115762_at	Esco1	establishment of cohesion 1 homolog 1 (S. cerevisiae)	0.00037	-1.68
168651_at	1700112M02Rik	RIKEN cDNA 1700112M02 gene	0.00042	-1.45
100984_at	Atf1	activating transcription factor 1	0.00053	-1.25
92308_at	Ptprm	protein tyrosine phosphatase, receptor type, M	0.00058	-1.32
104101_at	Slc9a8	solute carrier family 9 (sodium/hydrogen exchanger), member 8	0.00061	-1.11
103499_at	Vwf	Von Willebrand factor homolog	0.00071	-1.34
108957_at	2700023E23Rik	RIKEN cDNA 2700023E23 gene	0.00077	-2.39
93316_at	Osbpl1a	oxysterol binding protein-like 1A	0.00078	-1.22
98848_at	Sorbs3	sorbin and SH3 domain containing 3	0.00080	-1.27
170263_f_at	Tmem79	transmembrane protein 79	0.00081	-2.26
164095_i_at	Zscan29	zinc finger SCAN domains 29	0.00087	-1.36
115811_at	AI449310	expressed sequence AI449310	0.00099	-1.79
110090_at	---	Transcribed locus	0.00109	-2.90
136559_at	Tmem98	Transmembrane protein 98	0.00112	-1.91
101198_at	Cplx1	complexin 1	0.00135	-1.24
92806_at	Pdrg1	p53 and DNA damage regulated 1	0.00140	-1.08
112093_at	---	Transcribed locus	0.00141	-1.66
115425_at	AI118064	Expressed sequence AI118064	0.00147	-1.51
162945_at	Dexi	dexamethasone-induced transcript	0.00150	-1.09
99970_at	Ptpn21	protein tyrosine phosphatase, non-receptor type 21	0.00155	-1.12
93560_at	Acyp1	acylphosphatase 1, erythrocyte (common) type	0.00160	-1.21

Table 2.5 continued:

92941_at	1110054M08Rik	RIKEN cDNA 1110054M08 gene	0.00161	-1.24
170608_at	Hdac11	histone deacetylase 11	0.00161	-1.84
92527_at	Adcy9	adenylate cyclase 9	0.00166	-1.15
95040_at	Pdcd6ip	programmed cell death 6 interacting protein	0.00169	-1.32
137234_i_at	Rnf10	Ring finger protein 10	0.00170	-1.31
102151_at	Adrb1	adrenergic receptor, beta 1	0.00174	-1.82
94733_at	Abcb4	ATP-binding cassette, sub-family B (MDR/TAP), member 4	0.00175	-1.22
96255_at	Bnip3l	BCL2/adenovirus E1B interacting protein 3-like	0.00178	-1.17
92507_at	Utrn	utrophin	0.00182	-1.48
95071_at	Kcmf1	potassium channel modulatory factor 1	0.00186	-1.16
166454_at	Brp44l	Brain protein 44-like	0.00189	-1.77
99978_s_at	Mapk14	mitogen activated protein kinase 14	0.00204	-1.12
116207_at	Calb1	calbindin-28K	0.00211	-1.53
103297_at	Pfkfb1	6-phosphofructo-2-kinase/fructose-2,6-biphosphatase 1	0.00215	-1.25
137352_at	---	Transcribed locus	0.00223	-1.50
94257_at	Rraga	Ras-related GTP binding A	0.00226	-1.13
106939_at	AI931714	expressed sequence AI931714	0.00226	-1.19
160535_at	Nfe2l1	nuclear factor, erythroid derived 2,-like 1	0.00227	-1.08
96747_at	Rhou	ras homolog gene family, member U	0.00234	-1.24
97104_g_at	Rfk	riboflavin kinase	0.00235	-1.12
166431_at	Herc2	hect (homologous to the E6-AP (UBE3A) carboxyl terminus) domain and RCC1 (CHC1)-like domain (RLD) 2	0.00243	-1.24
101027_s_at	Pttg1	pituitary tumor-transforming 1	0.00247	-1.14
165937_r_at	Tm4sf20	Transmembrane 4 L six family member 20	0.00261	-1.90
95328_at	Fut9	fucosyltransferase 9	0.00263	-1.47
109152_g_at	Nek9	NIMA (never in mitosis gene a)-related expressed kinase 9	0.00264	-1.07
167307_i_at	Prickle1	prickle like 1 (Drosophila)	0.00267	-1.38
162697_at	6430604K15Rik /// 9130019O22Rik /// Zfp764	RIKEN cDNA 9130019O22 gene /// zinc finger protein 764 /// RIKEN cDNA 6430604K15 gene	0.00274	-1.50
168785_at	4930402K13Rik	RIKEN cDNA 4930402K13 gene	0.00279	-2.55
94507_at	Acsl1	acyl-CoA synthetase long-chain family member 1	0.00281	-1.12
103238_at	Wnt4	wingless-related MMTV integration site 4	0.00294	-1.28
170067_i_at	---	---	0.00300	-1.80

Table 2.5 continued:

93689_at	Emid1	EMI domain containing 1	0.00307	-1.08
96680_at	Dnajb9	DnaJ (Hsp40) homolog, subfamily B, member 9	0.00316	-1.25
99471_at	Stard7	START domain containing 7	0.00318	-1.15
133981_at	Ugdh	UDP-glucose dehydrogenase	0.00321	-1.21
171309_r_at	Lix1	limb expression 1 homolog (chicken)	0.00325	-2.05
140638_at	Cox4nb	COX4 neighbor	0.00330	-1.37
116927_at	Rai1	retinoic acid induced 1	0.00336	-1.20
166829_at	Ttc28	tetratricopeptide repeat domain 28	0.00339	-1.26
129330_at	Hoxb13	homeo box B13	0.00349	-1.98
163869_at	Ndel1	nuclear distribution gene E-like homolog 1 (A. nidulans)	0.00351	-1.46
108358_at	Stch	stress 70 protein chaperone, microsome-associated, human homolog	0.00359	-1.28
168781_at	ORF9	open reading frame 9	0.00360	-1.53
137123_at	Ctns	Cystinosis, nephropathic	0.00366	-1.49
94319_at	Rab18	RAB18, member RAS oncogene family	0.00374	-1.11
115187_at	Sema4g	sema domain, immunoglobulin domain (Ig), transmembrane domain (TM) and short cytoplasmic domain, (semaphorin) 4G	0.00379	-1.54
160921_at	Acss1	acyl-CoA synthetase short-chain family member 1	0.00381	-1.17
95035_at	Ipo4	importin 4	0.00385	-1.16
94940_at	Mccc1	methylcrotonoyl-Coenzyme A carboxylase 1 (alpha)	0.00391	-1.15
164483_r_at	Alkbh1	alkB, alkylation repair homolog 1 (E. coli)	0.00420	-1.17
96650_at	Auh	AU RNA binding protein/enoyl-coenzyme A hydratase	0.00427	-1.17
101292_f_at	---	---	0.00431	-1.86
101884_at	Xlr4a	X-linked lymphocyte-regulated 4A	0.00431	-2.54
160716_at	2410018C17Rik	RIKEN cDNA 2410018C17 gene	0.00451	-1.08
160301_at	Riok3	RIO kinase 3 (yeast)	0.00457	-1.16
115747_at	Ctsm	cathepsin M	0.00487	-1.40
94405_at	Slc6a6	solute carrier family 6 (neurotransmitter transporter, taurine), member 6	0.00489	-1.65

Table 2.6: Comparison of *Snta*$^{-/-}$ quadriceps gene expression changes, using Affymetrix arrays ($p<0.005$) versus RT-PCR ($p<0.05$)

Gene Symbol	Change vs. WT (Affymetrix)	Change vs. WT (RT-PCR)
Snta	-54% to -76%	-82%
Kcne1l	+125%	+96%
Sdc4	-37%	not significant
Abcc3	+140%	-18.0%
Chrne	+53%	+35%
Aqp4	+48%	+23%

Table 2.7: Comparison of *Dtna*$^{-/-}$ quadriceps gene expression changes, using Affymetrix arrays ($p<0.005$) versus RT-PCR ($p<0.05$)

Gene Symbol	Change vs. WT (Affymetrix)	Change vs. WT (RT-PCR)
Chrne	+87%	not significant
Npc1	-45%	-50%
Dtna	-57% to -78%	-78%
Adrb1	-45%	not significant
Ankrd	+110%	-26%
Sema4g	-35%	not significant
Traf5	-57%	+26%
Efna5	+154%	not significant

Table 2.8: Gene expression changes in common between *Dtna*$^{-/-}$ and *Snta*$^{-/-}$ quadriceps muscles ($p<0.005$)

Gene Symbol	Gene Name	Change in *Snta*$^{-/-}$, vs. WT	Change in *Dtna*$^{-/-}$, vs. WT
Acot11	acyl-CoA thioesterase 11	+39.7%	+39.9%
Myl4	myosin, light polypeptide 4	+27.0%	+146.2%
Prkar1a	protein kinase, cAMP dependent regulatory, type I, alpha	+12.5%	+11.9%
Chrne	cholinergic receptor, nicotinic, epsilon polypeptide	+53.1%	+87.5%

Table 2.9: Up-regulated transcripts in *Dtna*$^{-/-}$ versus wild-type diaphragm muscle, with expression fold changes indicated

Probe ID	Gene Symbol	Gene Name	p value	Change
1435290_x_at	H2-Aa	histocompatibility 2, class II antigen A, alpha	1.21E-05	1.63
1457296_at	Cilp	cartilage intermediate layer protein, nucleotide pyrophosphohydrolase	1.23E-05	1.26
1438858_x_at	H2-Aa	Histocompatibility 2, class II antigen A, alpha	3.76E-05	1.79
1442279_at	Epc1	Enhancer of polycomb homolog 1 (Drosophila)	4.24E-05	2.19
1425519_a_at	Cd74	CD74 antigen (invariant polypeptide of major histocompatibility complex, class II antigen-associated)	5.61E-05	1.60
1443783_x_at	H2-Aa	Histocompatibility 2, class II antigen A, alpha	6.24E-05	2.08
1435767_at	Scn3b	sodium channel, voltage-gated, type III, beta	8.18E-05	1.38
1451721_a_at	H2-Ab1	histocompatibility 2, class II antigen A, beta 1	0.00010	1.77
1417676_a_at	Ptpro	protein tyrosine phosphatase, receptor type, O	0.00010	1.72
1452431_s_at	H2-Aa	histocompatibility 2, class II antigen A, alpha	0.00010	2.06
1423607_at	Lum	lumican	0.00011	1.24
1459515_at	2610037D02Rik	RIKEN cDNA 2610037D02 gene	0.00012	1.56
1418457_at	Cxcl14	chemokine (C-X-C motif) ligand 14	0.00013	1.41
1424086_at	Oaf	OAF homolog (Drosophila)	0.00013	1.23
1417025_at	H2-Eb1	histocompatibility 2, class II antigen E beta	0.00015	1.55
1418937_at	Dio2	deiodinase, iodothyronine, type II	0.00017	1.49
1453246_at	Rab39b	RAB39B, member RAS oncogene family	0.00018	2.01
1437753_at	AW742931	Expressed sequence AW742931	0.00020	1.30
1446059_at	St6galnac5	ST6 (alpha-N-acetyl-neuraminyl-2,3-beta-galactosyl-1,3)-N-acetylgalactosaminide alpha-2,6-sialyltransferase 5	0.00021	1.72
1424131_at	Col6a3 /// LOC674521	procollagen, type VI, alpha 3 /// similar to alpha 3 type VI collagen isoform 1 precursor	0.00024	1.31
1452795_at	Fcf1	FCF1 small subunit (SSU) processome component homolog (S. cerevisiae)	0.00024	1.33
1422527_at	H2-DMa	histocompatibility 2, class II, locus DMa	0.00026	1.61
1449127_at	Selplg	selectin, platelet (p-selectin) ligand	0.00027	1.63
1436193_at	Man1c1	mannosidase, alpha, class 1C, member 1	0.00028	1.27
1425145_at	Il1rl1	interleukin 1 receptor-like 1	0.00029	1.53
1425477_x_at	H2-Ab1	histocompatibility 2, class II antigen A, beta 1	0.00032	2.02

Table 2.9 continued:

1455161_at	AI504432	expressed sequence AI504432	0.00038	1.90
1433840_a_at	C330006K01Rik	RIKEN cDNA C330006K01 gene	0.00038	1.20
1460447_at	Pus7l	pseudouridylate synthase 7 homolog (S. cerevisiae)-like	0.00039	1.18
1421597_a_at	Msx3	homeo box, msh-like 3	0.00039	1.91
1426306_a_at	Maged2	melanoma antigen, family D, 2	0.00043	1.59
1428727_at	Cep192	centrosomal protein 192	0.00046	1.41
1443356_at	Arpp21	Cyclic AMP-regulated phosphoprotein, 21	0.00048	1.87
1431038_at	Rassf4	Ras association (RalGDS/AF-6) domain family 4	0.00049	1.22
1433583_at	LOC674611 /// Zfp365	zinc finger protein 365 /// similar to zinc finger protein 365	0.00050	1.60
1415976_a_at	Carhsp1	calcium regulated heat stable protein 1	0.00052	1.48
1426202_at	H2-Ea	Histocompatibility 2, class II antigen E alpha /// MHC class II E-sub-alpha (E-sub-alpha) mRNA, 5' flanking region and partial cds	0.00055	1.95
1456605_at	Cebpd	CCAAT/enhancer binding protein (C/EBP), delta	0.00059	1.30
1449856_at	Rgs18	regulator of G-protein signaling 18	0.00059	1.34
1434244_x_at	Htf9c	HpaII tiny fragments locus 9c	0.00061	1.15
1441635_at	Olfml2a	Olfactomedin-like 2A	0.00062	1.21
1450569_a_at	Rbm14	RNA binding motif protein 14	0.00062	1.14
1423783_at	Tor2a	torsin family 2, member A	0.00064	1.32
1416407_at	Pea15a	phosphoprotein enriched in astrocytes 15A	0.00068	1.16
1456107_x_at	Eftud2	elongation factor Tu GTP binding domain containing 2	0.00069	1.19
1456133_x_at	Itgb5	integrin beta 5	0.00070	1.13
1428800_a_at	Pus7l	pseudouridylate synthase 7 homolog (S. cerevisiae)-like	0.00071	1.23
1450437_a_at	Ncam1	neural cell adhesion molecule 1	0.00072	1.88
1418223_at	Sec11a	SEC11 homolog A (S. cerevisiae)	0.00073	1.17
1416318_at	Serpinb1a	serine (or cysteine) peptidase inhibitor, clade B, member 1a	0.00075	1.36
1451209_at	Lass5	longevity assurance homolog 5 (S. cerevisiae)	0.00075	1.13
1450138_a_at	Serpinb6a	serine (or cysteine) peptidase inhibitor, clade B, member 6a	0.00076	1.31
1416723_at	Tcf4	transcription factor 4	0.00082	1.13
1426501_a_at	T2bp	Traf2 binding protein	0.00087	1.36
1446532_at	---	---	0.00088	1.77
1427892_at	Myo1g	myosin IG	0.00096	1.67

Table 2.9 continued:

1449273_at	Cyfip2	cytoplasmic FMR1 interacting protein 2	0.00100	1.70
1425942_a_at	Gpm6b	glycoprotein m6b	0.00101	1.17
1420876_a_at	Sept6	septin 6	0.00102	1.56
1431122_at	Armc9	armadillo repeat containing 9	0.00103	2.80
1428347_at	Cyfip2	cytoplasmic FMR1 interacting protein 2	0.00106	1.40
1441230_at	Fndc3b	Fibronectin type III domain containing 3B	0.00107	1.51
1454443_at	4833411I10Rik	RIKEN cDNA 4833411I10 gene	0.00107	1.32
1439226_at	Dock8	Dedicator of cytokinesis 8	0.00109	1.46
1418638_at	H2-DMb1	histocompatibility 2, class II, locus Mb1	0.00110	1.58
1428942_at	Mt2	metallothionein 2	0.00111	2.01
1447759_x_at	Ccdc22	coiled-coil domain containing 22	0.00114	1.22
1449285_at	Cst9	cystatin 9	0.00115	1.48
1429328_at	Nsfl1c	NSFL1 (p97) cofactor (p47)	0.00116	1.44
1439191_at	---	---	0.00121	1.15
1457261_at	A930025H08Rik	RIKEN cDNA A930025H08 gene	0.00124	2.36
1427512_a_at	Lama3 /// LOC669814	laminin, alpha 3 /// similar to Laminin alpha-3 chain precursor (Nicein alpha subunit)	0.00125	1.35
1450513_at	Cd33	CD33 antigen	0.00128	1.28
1426926_at	Plcg2	phospholipase C, gamma 2	0.00134	1.37
1415741_at	Tmem165	transmembrane protein 165	0.00135	1.15
1448126_at	Tera	teratocarcinoma expressed, serine rich	0.00136	1.18
1452181_at	Ckap4	cytoskeleton-associated protein 4	0.00140	1.27
1441484_at	---	---	0.00141	1.45
1436837_at	Mael	maelstrom homolog (Drosophila)	0.00145	1.95
1451244_a_at	Zfp422	zinc finger protein 422	0.00146	1.14
1457819_at	LOC671835 /// Scn9a	sodium channel, voltage-gated, type IX, alpha /// similar to sodium channel 25	0.00148	1.73
1435172_at	Eomes	eomesodermin homolog (Xenopus laevis)	0.00151	1.49
1426172_a_at	Cd209a	CD209a antigen	0.00152	1.34
1418758_a_at	Pscd3	pleckstrin homology, Sec7 and coiled-coil domains 3	0.00155	1.17
1416333_at	Dok2	docking protein 2	0.00160	1.36
1435731_x_at	---	Transcribed locus, moderately similar to XP_001067603.1 similar to peroxiredoxin 1 [Rattus norvegicus]	0.00165	1.32

Table 2.9 continued:

1455726_at	Gm71	gene model 71, (NCBI)	0.00168	1.64
1418778_at	Ccdc109b	coiled-coil domain containing 109B	0.00170	1.44
1450498_at	Mthfr	5,10-methylenetetrahydrofolate reductase	0.00171	1.39
1448698_at	Ccnd1	cyclin D1	0.00172	1.20
1451268_at	Tram1l1	translocation associated membrane protein 1-like 1	0.00173	2.81
1453467_s_at	Rps15a	ribosomal protein S15a	0.00176	1.24
1419631_at	Was	Wiskott-Aldrich syndrome homolog (human)	0.00182	1.68
1429135_at	1110059M19Rik	RIKEN cDNA 1110059M19 gene	0.00193	1.81
1445919_at	AA409261	expressed sequence AA409261	0.00194	1.23
1426465_at	Dlgap4	discs, large homolog-associated protein 4 (Drosophila)	0.00196	1.29
1417268_at	Cd14	CD14 antigen	0.00199	1.51
1435795_at	Glb1	galactosidase, beta 1	0.00201	1.35
1453001_at	Rnaseh2b	ribonuclease H2, subunit B	0.00202	1.33
1446432_at	B530045E10Rik	RIKEN cDNA B530045E10 gene	0.00204	1.53
1442118_at	---	Transcribed locus	0.00205	1.44
1422440_at	Cdk4 /// LOC640611	cyclin-dependent kinase 4 /// similar to Cell division protein kinase 4 (Cyclin-dependent kinase 4) (PSK-J3) (CRK3)	0.00206	1.26
1442086_at	Mta3	Metastasis associated 3	0.00207	1.91
1439426_x_at	Lyz	lysozyme	0.00207	1.46
1420421_s_at	Klrb1b	killer cell lectin-like receptor subfamily B member 1B	0.00208	1.62
1460067_at	Ccr2	chemokine (C-C motif) receptor 2	0.00209	1.95
1440972_at	Nsd1	nuclear receptor-binding SET-domain protein 1	0.00209	1.25
1456880_at	Sfrs8	Splicing factor, arginine/serine-rich 8	0.00210	1.15

Table 2.9 continued:

1454627_a_at	EG666642 /// EG667466 /// LOC433350 /// LOC433941 /// LOC622707 /// LOC626772 /// LOC665032 /// LOC669999 /// LOC670334 /// LOC675846 /// Rpl29	ribosomal protein L29 /// similar to 60S ribosomal protein L29 /// predicted gene, EG666642 /// predicted gene, EG667466 /// hypothetical protein LOC669999	0.00212	1.32
1422443_at	Xpnpep1	X-prolyl aminopeptidase (aminopeptidase P) 1, soluble	0.00214	1.07
1440519_at	Sp8	trans-acting transcription factor 8	0.00218	1.78
1430252_at	3110027N22Rik	RIKEN cDNA 3110027N22 gene	0.00218	1.46
1447150_at	Phr1	pam, highwire, rpm 1	0.00219	1.20
1453107_s_at	4933413G19Rik /// Foxm1 /// Pebp1	forkhead box M1 /// phosphatidylethanolamine binding protein 1 /// RIKEN cDNA 4933413G19 gene	0.00220	1.89
1433611_s_at	Bud31	BUD31 homolog (yeast)	0.00223	1.15
1452156_a_at	Nisch	nischarin	0.00223	1.09
1450195_at	Ndst4	N-deacetylase/N-sulfotransferase (heparin glucosaminyl) 4	0.00231	1.31
1451017_at	Ergic3	ERGIC and golgi 3	0.00232	1.12
1422650_a_at	Riok3	RIO kinase 3 (yeast)	0.00246	1.23
1432023_a_at	1700019H03Rik	RIKEN cDNA 1700019H03 gene	0.00247	1.51
1426618_a_at	Pomgnt1	protein O-linked mannose beta1,2-N-acetylglucosaminyltransferase	0.00248	1.12
1452106_at	Npnt	nephronectin	0.00249	1.42
1454825_at	1110014N23Rik	RIKEN cDNA 1110014N23 gene	0.00258	1.17
1443245_at	---	---	0.00259	1.37
1421043_s_at	Arhgef2	rho/rac guanine nucleotide exchange factor (GEF) 2	0.00260	1.40
1426784_at	Trim47	tripartite motif protein 47	0.00260	1.18
1459083_at	A330084C13Rik	RIKEN cDNA A330084C13 gene	0.00260	2.73
1418605_at	Nr2c1	nuclear receptor subfamily 2, group C, member 1	0.00260	1.06

Table 2.9 continued:

1451161_a_at	Emr1	EGF-like module containing, mucin-like, hormone receptor-like sequence 1	0.00262	1.44
1452896_at	Gtl3	gene trap locus 3	0.00265	1.23
1443777_at	---	---	0.00265	2.22
1451775_s_at	Il13ra1	interleukin 13 receptor, alpha 1	0.00270	1.40
1457686_at	B230333C21Rik	RIKEN cDNA B230333C21 gene	0.00271	1.39
1428132_at	Cdc42se1	CDC42 small effector 1	0.00273	1.27
1436953_at	Wipf1	WAS/WASL interacting protein family, member 1	0.00275	1.29
1425340_a_at	Ptpra	protein tyrosine phosphatase, receptor type, A	0.00276	1.18
1438764_at	Anxa7	annexin A7	0.00278	1.14
1449388_at	Thbs4	thrombospondin 4	0.00279	1.60
1448152_at	Igf2	insulin-like growth factor 2	0.00283	1.78
1442787_at	---	---	0.00285	2.07
1455117_at	Mcm9	minichromosome maintenance complex component 9	0.00286	1.67
1445267_at	EG382161	Predicted gene, EG382161	0.00286	1.21
1449873_at	Bmp8a	bone morphogenetic protein 8a	0.00286	1.76
1419315_at	Slamf9	SLAM family member 9	0.00292	1.76
1428655_at	Ccdc128	coiled-coil domain containing 128	0.00296	1.18
1450200_s_at	Csf2rb1 /// Csf2rb2	colony stimulating factor 2 receptor, beta 1, low-affinity (granulocyte-macrophage) /// colony stimulating factor 2 receptor, beta 2, low-affinity (granulocyte-macrophage)	0.00296	1.88
1450652_at	Ctsk	cathepsin K	0.00301	1.33
1438626_x_at	Rpl14	ribosomal protein L14	0.00305	1.13
1438598_at	Shc2	src homology 2 domain-containing transforming protein C2	0.00309	2.21
1424879_at	Sap25	mSin3A-binding protein	0.00310	1.75
1438999_a_at	Nfat5	nuclear factor of activated T-cells 5	0.00310	1.12
1451978_at	Loxl1	lysyl oxidase-like 1	0.00311	1.23
1458550_at	Myo1d	myosin ID	0.00317	1.19
1440300_at	---	Transcribed locus	0.00322	1.16
1440873_at	---	---	0.00324	1.43
1434788_at	D930050A07Rik	RIKEN cDNA D930050A07 gene	0.00325	1.73
1430395_at	Ankrd45	ankyrin repeat domain 45	0.00326	2.33
1425374_at	Oas3	2'-5' oligoadenylate synthetase 3	0.00326	1.93

Table 2.9 continued:

1456716_s_at	3110002H16Rik	RIKEN cDNA 3110002H16 gene	0.00327	1.18
1429159_at	Itih5	inter-alpha (globulin) inhibitor H5	0.00328	1.25
1439409_x_at	Tyrp1	tyrosinase-related protein 1	0.00330	1.71
1443586_at	Fip1l1	FIP1 like 1 (S. cerevisiae)	0.00330	1.21
1419100_at	Serpina3n	serine (or cysteine) peptidase inhibitor, clade A, member 3N	0.00337	1.95
1441027_at	---	Transcribed locus	0.00341	2.05
1460021_at	EG626231	predicted gene, EG626231	0.00341	1.48
1426804_at	Smarca4	SWI/SNF related, matrix associated, actin dependent regulator of chromatin, subfamily a, member 4	0.00344	1.11
1448922_at	Dusp19	dual specificity phosphatase 19	0.00346	1.17
1416328_a_at	Atp6v0e	ATPase, H+ transporting, lysosomal V0 subunit E	0.00349	1.23
1458781_at	Kcnk13	Potassium channel, subfamily K, member 13	0.00349	1.73
1433067_at	6330582A15Rik	RIKEN cDNA 6330582A15 gene	0.00353	1.37
1456531_x_at	Prpf19	PRP19/PSO4 pre-mRNA processing factor 19 homolog (S. cerevisiae)	0.00355	1.16
1429265_a_at	Rnf130	ring finger protein 130	0.00355	1.09
1417830_at	Smc1a	structural maintenance of chromosomes 1A	0.00356	1.13
1426789_s_at	Ssrp1	structure specific recognition protein 1	0.00357	1.22
1420643_at	Lfng	lunatic fringe gene homolog (Drosophila)	0.00360	1.42
1444213_at	1700012D14Rik	RIKEN cDNA 1700012D14 gene	0.00363	1.76
1452250_a_at	Col6a2	procollagen, type VI, alpha 2	0.00363	1.12
1454448_at	2900018E21Rik	RIKEN cDNA 2900018E21 gene	0.00374	1.46
1426347_at	2010321M09Rik	RIKEN cDNA 2010321M09 gene	0.00375	1.13
1449708_s_at	Chek1	checkpoint kinase 1 homolog (S. pombe)	0.00377	2.85
1456752_at	---	13 days embryo heart cDNA, RIKEN full-length enriched library, clone:D330038P10 product:Mus musculus Nespas mRNA, full insert sequence	0.00380	1.20
1443982_at	Rgnef	Rho-guanine nucleotide exchange factor	0.00381	2.28
1438643_at	Camk1d	Calcium/calmodulin-dependent protein kinase ID	0.00384	1.21
1422519_at	Cask	calcium/calmodulin-dependent serine protein kinase (MAGUK family)	0.00384	1.13
1440999_at	Zfp697	zinc finger protein 697	0.00386	1.35
1456241_a_at	1810073N04Rik	RIKEN cDNA 1810073N04 gene	0.00388	1.04

Table 2.9 continued:

1425541_at	Ddx27	DEAD (Asp-Glu-Ala-Asp) box polypeptide 27	0.00388	1.24
1449939_s_at	Dlk1	delta-like 1 homolog (Drosophila)	0.00392	1.44
1424089_a_at	Tcf4	transcription factor 4	0.00392	1.28
1458644_at	AI661708 /// Ccdc62	expressed sequence AI661708 /// coiled-coil domain containing 62	0.00394	1.24
1433390_at	A230105L22Rik	RIKEN cDNA A230105L22 gene	0.00398	1.73
1426866_at	Chst14	carbohydrate (N-acetylgalactosamine 4-0) sulfotransferase 14	0.00401	1.45
1422580_at	Myl4	myosin, light polypeptide 4	0.00403	12.61
1441029_at	Axin1	Axin 1	0.00404	1.46
1426525_at	Arid2	AT rich interactive domain 2 (Arid-rfx like)	0.00405	1.14
1459080_at	---	---	0.00408	1.57
1415935_at	Smoc2	SPARC related modular calcium binding 2	0.00410	1.14
1456694_x_at	Ptpn6	protein tyrosine phosphatase, non-receptor type 6	0.00411	1.20
1432253_at	4921523P09Rik	RIKEN cDNA 4921523P09 gene	0.00412	1.61
1416188_at	Gm2a	GM2 ganglioside activator protein	0.00412	1.27
1448182_a_at	Cd24a	CD24a antigen	0.00412	1.18
1431436_a_at	Katnal2	katanin p60 subunit A-like 2	0.00417	1.88
1418454_at	Mfap5	microfibrillar associated protein 5	0.00419	1.22
1455899_x_at	Socs3	suppressor of cytokine signaling 3	0.00428	1.38
1422467_at	Ppt1	palmitoyl-protein thioesterase 1	0.00428	1.20
1451181_at	Tmem121	transmembrane protein 121	0.00429	2.87
1441673_at	Pllp	plasma membrane proteolipid	0.00430	1.52
1428156_at	Gng2	guanine nucleotide binding protein (G protein), gamma 2 subunit	0.00431	1.31
1417756_a_at	Lsp1	lymphocyte specific 1	0.00432	1.34
1442809_at	LOC671835 /// Scn9a	sodium channel, voltage-gated, type IX, alpha /// similar to sodium channel 25	0.00436	2.20
1439527_at	ENSMUSG00000074510 /// Pgr	progesterone receptor /// predicted gene, ENSMUSG00000074510	0.00437	1.19
1443668_x_at	C79407	expressed sequence C79407	0.00447	1.40
1452648_at	Tbrg1	transforming growth factor beta regulated gene 1	0.00448	1.14
1428621_a_at	Vps25	vacuolar protein sorting 25 (yeast)	0.00451	1.08
1426266_s_at	Zbtb8os	zinc finger and BTB domain containing 8 opposite strand	0.00452	1.13

Table 2.9 continued:

1452729_at	Dpm3	dolichyl-phosphate mannosyltransferase polypeptide 3	0.00454	1.94
1441120_at	Ceacam16	CEA-related cell adhesion molecule 16	0.00454	1.55
1423224_at	4432405B04Rik	RIKEN cDNA 4432405B04 gene	0.00455	1.36
1457515_at	Hipk1	Homeodomain interacting protein kinase 1	0.00459	1.23
1441436_at	Dusp12	dual specificity phosphatase 12	0.00465	1.26
1447819_x_at	Col8a1	procollagen, type VIII, alpha 1	0.00469	1.33
1436416_x_at	Fxc1	fractured callus expressed transcript 1	0.00473	1.20
1426591_at	Gfm2	G elongation factor, mitochondrial 2	0.00481	1.35
1440624_at	Ptprd	Protein tyrosine phosphatase, receptor type, D	0.00482	1.38
1451394_at	Dpp6	dipeptidylpeptidase 6	0.00486	1.40
1418296_at	Fxyd5	FXYD domain-containing ion transport regulator 5	0.00487	1.36
1436996_x_at	Lyz	lysozyme	0.00488	1.36
1460245_at	Klrd1	killer cell lectin-like receptor, subfamily D, member 1	0.00489	1.78
1434754_at	Garnl4	GTPase activating RANGAP domain-like 4	0.00494	1.19
1435830_a_at	5430435G22Rik	RIKEN cDNA 5430435G22 gene	0.00495	1.38
1426615_s_at	Ndrg4	N-myc downstream regulated gene 4	0.00496	1.46
1437185_s_at	Tmsb10	thymosin, beta 10	0.00499	1.44

Table 2.10: Down-regulated transcripts in *Dtna*$^{-/-}$ versus wild-type diaphragm muscle, with expression fold changes indicated

Probe ID	Gene Symbol	Gene Name	p value	Change
1419223_a_at	Dtna	dystrobrevin alpha	3.24E-09	-5.00
1456069_at	Dtna	dystrobrevin alpha	8.49E-08	-3.31
1427588_a_at	Dtna	dystrobrevin alpha	1.05E-06	-3.19
1426066_a_at	Dtna	dystrobrevin alpha	1.69E-06	-2.83
1416666_at	Serpine2	serine (or cysteine) peptidase inhibitor, clade E, member 2	1.77E-06	-1.23
1429768_at	Dtna	dystrobrevin alpha	2.78E-06	-4.55
1425292_at	Dtna	dystrobrevin alpha	3.31E-06	-2.27
1420612_s_at	Ptp4a2	protein tyrosine phosphatase 4a2	1.61E-05	-1.16
1422315_x_at	Phkg1	phosphorylase kinase gamma 1	2.21E-05	-1.34
1460325_at	Pum1	pumilio 1 (Drosophila)	2.96E-05	-1.13
1422063_a_at	Pex5	peroxisome biogenesis factor 5	7.79E-05	-1.14
1460670_at	Riok3	RIO kinase 3 (yeast)	8.29E-05	-2.97
1416215_at	Gosr1	golgi SNAP receptor complex member 1	8.30E-05	-1.20
1425164_a_at	Phkg1	phosphorylase kinase gamma 1	8.55E-05	-1.38
1418592_at	Dnaja4	DnaJ (Hsp40) homolog, subfamily A, member 4	8.90E-05	-1.29
1437207_at	Rnf170	ring finger protein 170	9.35E-05	-1.28
1418563_at	Serbp1	Serpine1 mRNA binding protein 1	9.36E-05	-1.10
1418915_at	Mmachc	methylmalonic aciduria cblC type, with homocystinuria	9.95E-05	-1.16
1434682_at	Zfp770	zinc finger protein 770	0.00013	-1.23
1455475_at	3110057O12Rik	RIKEN cDNA 3110057O12 gene	0.00013	-1.31
1458087_at	Stac3	SH3 and cysteine rich domain 3	0.00013	-1.22
1425185_at	5830417C01Rik	RIKEN cDNA 5830417C01 gene	0.00014	-1.10
1454976_at	Sod2	superoxide dismutase 2, mitochondrial	0.00016	-1.16
1426578_s_at	Snapap	SNAP-associated protein	0.00016	-1.10
1455473_at	Usp13	ubiquitin specific peptidase 13 (isopeptidase T-3)	0.00017	-1.20
1455014_at	AV009015	expressed sequence AV009015	0.00018	-1.25
1424324_at	Esco1	establishment of cohesion 1 homolog 1 (S. cerevisiae)	0.00019	-2.14
1424946_a_at	Mtfr1	mitochondrial fission regulator 1	0.00019	-1.24
1454987_a_at	H2-Ke6	H2-K region expressed gene 6	0.00019	-1.17
1449078_at	St3gal6	ST3 beta-galactoside alpha-2,3-sialyltransferase 6	0.00021	-1.25
1421529_a_at	Txnrd1	thioredoxin reductase 1	0.00023	-1.13

Table 2.10 continued:

1423200_at	Ncor1	nuclear receptor co-repressor 1	0.00024	-1.08
1425196_a_at	Hint2	histidine triad nucleotide binding protein 2	0.00024	-1.17
1430786_at	1110002E22Rik	RIKEN cDNA 1110002E22 gene	0.00024	-1.34
1455252_at	Tsc1	tuberous sclerosis 1	0.00029	-1.18
1435430_at	Tmem1	transmembrane protein 1	0.00030	-1.08
1426912_at	EG621205 /// Rfwd2	ring finger and WD repeat domain 2 /// predicted gene, EG621205	0.00032	-1.10
1434537_at	Slco3a1	solute carrier organic anion transporter family, member 3a1	0.00033	-1.30
1415747_s_at	Riok3	RIO kinase 3 (yeast)	0.00034	-1.18
1436387_at	C330006P03Rik	RIKEN cDNA C330006P03 gene	0.00034	-1.57
1429615_at	Zfp91	zinc finger protein 91	0.00034	-1.16
1449818_at	Abcb4	ATP-binding cassette, sub-family B (MDR/TAP), member 4	0.00035	-1.23
1448918_at	Slco3a1	solute carrier organic anion transporter family, member 3a1	0.00036	-1.29
1416180_a_at	Rdx	radixin	0.00037	-1.29
1452213_at	Tex2	testis expressed gene 2	0.00037	-1.17
1460241_a_at	St3gal5	ST3 beta-galactoside alpha-2,3-sialyltransferase 5	0.00037	-1.34
1447870_x_at	1110002E22Rik	RIKEN cDNA 1110002E22 gene	0.00038	-1.18
1449028_at	Rhou	ras homolog gene family, member U	0.00039	-1.33
1452791_at	Coq2	coenzyme Q2 homolog, prenyltransferase (yeast)	0.00039	-1.15
1449079_s_at	St3gal6	ST3 beta-galactoside alpha-2,3-sialyltransferase 6	0.00039	-1.28
1444504_at	Dhrs7c	dehydrogenase/reductase (SDR family) member 7C	0.00039	-1.22
1427414_at	Prkar2a	protein kinase, cAMP dependent regulatory, type II alpha	0.00040	-1.35
1434717_at	Cul3	cullin 3	0.00042	-1.21
1436088_at	0910001A06Rik	RIKEN cDNA 0910001A06 gene	0.00043	-1.20
1423176_at	Tob1	transducer of ErbB-2.1	0.00043	-1.22
1423266_at	2810405K02Rik	RIKEN cDNA 2810405K02 gene	0.00044	-1.15
1428473_at	Ppp3cb	protein phosphatase 3, catalytic subunit, beta isoform	0.00044	-1.09
1434549_at	Rab11a	RAB11a, member RAS oncogene family	0.00044	-1.19
1460741_x_at	D17Wsu92e	DNA segment, Chr 17, Wayne State University 92, expressed	0.00046	-1.27
1427073_at	Lace1	lactation elevated 1	0.00047	-1.19
1444502_at	Pet112l	PET112-like (yeast)	0.00049	-1.28
1454840_at	Mccc2	methylcrotonoyl-Coenzyme A carboxylase 2 (beta)	0.00049	-1.23
1419145_at	Smtnl1	smoothelin-like 1	0.00051	-1.20
1449944_a_at	Sec61a2	Sec61, alpha subunit 2 (S. cerevisiae)	0.00052	-1.13

Table 2.10 continued:

1415909_at	Stip1	stress-induced phosphoprotein 1	0.00053	-1.22
1435787_at	Ppm1l	protein phosphatase 1 (formerly 2C)-like	0.00054	-1.20
1428164_at	Nudt9	nudix (nucleoside diphosphate linked moiety X)-type motif 9	0.00055	-1.11
1417206_at	Urod	uroporphyrinogen decarboxylase	0.00055	-1.11
1434002_at	Ches1	checkpoint suppressor 1	0.00058	-1.13
1438031_at	Rasgrp3	RAS, guanyl releasing protein 3	0.00058	-1.70
1437637_at	Phtf2	putative homeodomain transcription factor 2	0.00058	-1.30
1427718_a_at	Mdm2	transformed mouse 3T3 cell double minute 2	0.00060	-1.08
1421938_at	Serhl	serine hydrolase-like	0.00061	-1.12
1441863_x_at	Krt13	keratin 13	0.00064	-1.22
1425891_a_at	Grtp1	GH regulated TBC protein 1	0.00064	-1.39
1450386_at	Kpna3	karyopherin (importin) alpha 3	0.00065	-1.10
1421891_at	St3gal2	ST3 beta-galactoside alpha-2,3-sialyltransferase 2	0.00068	-1.11
1436070_at	Glo1	glyoxalase 1	0.00069	-1.28
1454637_at	Klhl8	kelch-like 8 (Drosophila)	0.00070	-1.23
1434410_at	BC043118	cDNA sequence BC043118	0.00070	-1.23
1438030_at	Rasgrp3	RAS, guanyl releasing protein 3	0.00077	-1.26
1434042_s_at	Mtmr3	myotubularin related protein 3	0.00078	-1.06
1436421_s_at	Arpc5l	actin related protein 2/3 complex, subunit 5-like	0.00078	-1.20
1426483_at	Prkrir	protein-kinase, interferon-inducible double stranded RNA dependent inhibitor, repressor of (P58 repressor)	0.00078	-1.15
1423047_at	Tollip	toll interacting protein	0.00079	-1.08
1435384_at	Ube2n	ubiquitin-conjugating enzyme E2N	0.00082	-1.25
1454168_a_at	Clpb	ClpB caseinolytic peptidase B homolog (E. coli)	0.00084	-1.34
1448484_at	Amd1	S-adenosylmethionine decarboxylase 1	0.00085	-1.24
1427189_at	Arih1	ariadne ubiquitin-conjugating enzyme E2 binding protein homolog 1 (Drosophila)	0.00086	-1.16
1452442_at	Usp13	Ubiquitin specific peptidase 13 (isopeptidase T-3)	0.00087	-1.18
1423536_at	Strn3	striatin, calmodulin binding protein 3	0.00087	-1.16
1446978_at	---	---	0.00090	-1.66
1451638_s_at	Armc1 /// LOC634390	armadillo repeat containing 1 /// similar to armadillo repeat-containing protein	0.00091	-1.15
1419374_at	Wbp4	WW domain binding protein 4	0.00093	-1.10

Table 2.10 continued:

1438022_at	Rab11fip3	RAB11 family interacting protein 3 (class II)	0.00100	-1.28
1430656_a_at	Asnsd1	asparagine synthetase domain containing 1	0.00102	-1.14
1423652_at	Isca1	iron-sulfur cluster assembly 1 homolog (S. cerevisiae)	0.00103	-1.17
1420909_at	Vegfa	vascular endothelial growth factor A	0.00103	-1.25
1437728_at	Alkbh5	alkB, alkylation repair homolog 5 (E. coli)	0.00103	-1.16
1441069_at	Zdhhc23	zinc finger, DHHC domain containing 23	0.00104	-1.45
1425352_at	Rcor3	REST corepressor 3	0.00105	-1.26
1426921_at	Abcf1	ATP-binding cassette, sub-family F (GCN20), member 1	0.00105	-1.29
1428576_at	Hif1an	hypoxia-inducible factor 1, alpha subunit inhibitor	0.00106	-1.14
1436440_at	Slc25a12	solute carrier family 25 (mitochondrial carrier, Aralar), member 12	0.00109	-1.16
1420072_s_at	---	---	0.00109	-1.72
1450768_at	Dlg1	discs, large homolog 1 (Drosophila)	0.00111	-1.17
1428293_at	2310022M17Rik	RIKEN cDNA 2310022M17 gene	0.00111	-1.15
1452887_at	Traf3ip1	TNF receptor-associated factor 3 interacting protein 1	0.00112	-1.20
1436079_s_at	Vapb	vesicle-associated membrane protein, associated protein B and C	0.00112	-1.20
1419359_at	Hexim1	hexamethylene bis-acetamide inducible 1	0.00113	-1.21
1420932_at	Mapk8	mitogen activated protein kinase 8	0.00114	-1.08
1428461_at	Ppp2r5e	protein phosphatase 2, regulatory subunit B (B56), epsilon isoform	0.00114	-1.13
1449505_at	Kpna1	karyopherin (importin) alpha 1	0.00114	-1.22
1455568_at	2310015A05Rik	RIKEN cDNA 2310015A05 gene	0.00114	-2.09
1430474_a_at	Mtch2	mitochondrial carrier homolog 2 (C. elegans)	0.00115	-1.12
1435364_at	Cyhr1	cysteine and histidine rich 1	0.00116	-1.17
1460519_a_at	Mettl5	methyltransferase like 5	0.00118	-1.10
1449036_at	Rnf128	ring finger protein 128	0.00119	-1.15
1422293_a_at	Kctd1	potassium channel tetramerisation domain containing 1	0.00119	-1.65
1448100_at	4833439L19Rik	RIKEN cDNA 4833439L19 gene	0.00120	-1.11
1418782_at	Rxrg	retinoid X receptor gamma	0.00121	-1.28
1417183_at	Dnaja2	DnaJ (Hsp40) homolog, subfamily A, member 2	0.00122	-1.15
1433113_at	4921504P20Rik	RIKEN cDNA 4921504P20 gene	0.00124	-1.37
1423168_at	Prei3	preimplantation protein 3	0.00125	-1.23
1455794_at	D130058I21Rik	RIKEN cDNA D130058I21 gene	0.00125	-1.27
1416946_a_at	Acaa1a /// Acaa1b	acetyl-Coenzyme A acyltransferase 1A /// acetyl-Coenzyme A acyltransferase 1B	0.00126	-1.18

Table 2.10 continued:

1437987_at	---	---	0.00126	-1.28
1457596_at	---	---	0.00127	-1.49
1456869_at	Zfp787	zinc finger protein 787	0.00128	-1.28
1427212_at	Mapkap1	mitogen-activated protein kinase associated protein 1	0.00130	-1.16
1457281_at	4930461P20Rik	RIKEN cDNA 4930461P20 gene	0.00130	-1.32
1449576_at	Eif1ay	eukaryotic translation initiation factor 1A, Y-linked	0.00131	-1.34
1453796_a_at	Ergic2	ERGIC and golgi 2	0.00132	-1.17
1438196_at	Gpd1l	glycerol-3-phosphate dehydrogenase 1-like	0.00133	-1.18
1422743_at	Phka1	phosphorylase kinase alpha 1	0.00134	-1.35
1438006_at	4933439F18Rik	RIKEN cDNA 4933439F18 gene	0.00136	-1.16
1452300_at	2410005O16Rik	RIKEN cDNA 2410005O16 gene	0.00136	-1.27
1428309_s_at	Pdrg1	p53 and DNA damage regulated 1	0.00137	-1.14
1424563_at	Slc25a4	solute carrier family 25 (mitochondrial carrier, adenine nucleotide translocator), member 4	0.00138	-1.21
1424422_s_at	Flad1 /// Lenep	lens epithelial protein /// RFad1, flavin adenine dinucleotide synthetase, homolog (yeast)	0.00140	-1.17
1425190_a_at	Phospho2	phosphatase, orphan 2	0.00142	-1.29
1423096_at	Capn7	calpain 7	0.00143	-1.15
1453406_a_at	Rab28	RAB28, member RAS oncogene family	0.00143	-1.20
1418589_a_at	Mlf1	myeloid leukemia factor 1	0.00144	-1.16
1447827_x_at	Spop	speckle-type POZ protein	0.00146	-1.48
1453744_a_at	Ankrd40	ankyrin repeat domain 40	0.00147	-1.25
1454730_at	Tapt1	transmembrane anterior posterior transformation 1	0.00149	-1.15
1436939_at	Unc45b	unc-45 homolog B (C. elegans)	0.00149	-1.17
1444644_x_at	Tatdn1	TatD DNase domain containing 1	0.00149	-1.11
1416452_at	Oat	ornithine aminotransferase	0.00149	-1.15
1434552_at	Wdr77	WD repeat domain 77	0.00150	-1.12
1425399_at	9630055N22Rik	RIKEN cDNA 9630055N22 gene	0.00152	-1.21
1460576_at	Exoc6	exocyst complex component 6	0.00152	-1.10
1450756_s_at	Cul3	cullin 3	0.00153	-1.23
1444091_a_at	6430571L13Rik	RIKEN cDNA 6430571L13 gene	0.00154	-1.46
1420056_s_at	Jmjd6	jumonji domain containing 6	0.00159	-1.19
1454960_at	Smad3	MAD homolog 3 (Drosophila)	0.00160	-1.19

Table 2.10 continued:

1416846_a_at	Pdzrn3	PDZ domain containing RING finger 3	0.00161	-1.19
1443304_at	Mtl5	metallothionein-like 5, testis-specific (tesmin)	0.00162	-1.46
1415910_s_at	Ciapin1	cytokine induced apoptosis inhibitor 1	0.00163	-1.27
1416230_at	Rfk	riboflavin kinase	0.00164	-1.17
1438012_at	Ppm1l	protein phosphatase 1 (formerly 2C)-like	0.00166	-1.32
1435841_s_at	Suclg2	succinate-Coenzyme A ligase, GDP-forming, beta subunit	0.00166	-1.13
1447845_s_at	Vnn1	vanin 1	0.00169	-1.51
1418117_at	Ndufs4	NADH dehydrogenase (ubiquinone) Fe-S protein 4	0.00170	-1.19
1425610_s_at	Galnt2	UDP-N-acetyl-alpha-D-galactosamine:polypeptide N-acetylgalactosaminyltransferase 2	0.00172	-1.20
1433487_at	Clcn3	chloride channel 3	0.00173	-1.20
1449504_at	Kpna1	karyopherin (importin) alpha 1	0.00173	-1.41
1419365_at	Pex11a	peroxisomal biogenesis factor 11a	0.00173	-1.29
1418649_at	Egln3	EGL nine homolog 3 (C. elegans)	0.00173	-1.27
1416541_at	Clpb	ClpB caseinolytic peptidase B homolog (E. coli)	0.00175	-1.24
1434738_at	Tarsl2	threonyl-tRNA synthetase-like 2	0.00176	-1.20
1431398_at	5730446D14Rik	RIKEN cDNA 5730446D14 gene	0.00176	-1.45
1420631_a_at	Blcap	bladder cancer associated protein homolog (human)	0.00181	-1.19
1455412_at	9330180L21Rik	RIKEN cDNA 9330180L21 gene	0.00182	-1.18
1425002_at	Sectm1a	secreted and transmembrane 1A	0.00186	-1.73
1439708_at	Myom3	myomesin family, member 3	0.00188	-1.16
1451744_a_at	Zadh1	zinc binding alcohol dehydrogenase, domain containing 1	0.00188	-1.15
1434023_at	Ccdc100	coiled-coil domain containing 100	0.00190	-1.13
1428971_at	Ccny	cyclin Y	0.00190	-1.27
1420727_a_at	Tmlhe	trimethyllysine hydroxylase, epsilon	0.00191	-1.30
1418038_s_at	Dusp19	dual specificity phosphatase 19	0.00191	-1.09
1433545_s_at	Acad11	acyl-Coenzyme A dehydrogenase family, member 11	0.00191	-1.18
1457936_at	Mapk8	mitogen activated protein kinase 8	0.00192	-1.25
1436891_at	Usp15	ubiquitin specific peptidase 15	0.00192	-1.34
1424393_s_at	Adhfe1	alcohol dehydrogenase, iron containing, 1	0.00193	-1.22
1433486_at	Clcn3	chloride channel 3	0.00195	-1.16
1448133_at	Nmd3	NMD3 homolog (S. cerevisiae)	0.00198	-1.12
1451652_a_at	5033428A16Rik	RIKEN cDNA 5033428A16 gene	0.00199	-1.07

Table 2.10 continued:

1432158_a_at	Trappc2	trafficking protein particle complex 2	0.00199	-1.10
1457275_at	Dmn	desmuslin	0.00199	-1.27
1434556_at	---	Bone marrow macrophage cDNA, RIKEN full-length enriched library, clone:I830003K21 product:unclassifiable, full insert sequence	0.00200	-1.14
1448882_at	Tmem93	transmembrane protein 93	0.00203	-1.08
1430637_at	2210016H18Rik	RIKEN cDNA 2210016H18 gene	0.00206	-1.78
1440989_at	Mrpl35	Mitochondrial ribosomal protein L35	0.00206	-1.15
1439730_at	Ncald	Neurocalcin delta	0.00207	-2.00
1429146_at	6620401M08Rik	RIKEN cDNA 6620401M08 gene	0.00210	-1.18
1418170_a_at	Zcchc14	zinc finger, CCHC domain containing 14	0.00210	-1.26
1426531_at	Zmynd11	zinc finger, MYND domain containing 11	0.00214	-1.09
1444774_at	Det1	de-etiolated homolog 1 (Arabidopsis)	0.00214	-2.28
1427153_at	Bckdhb	branched chain ketoacid dehydrogenase E1, beta polypeptide	0.00215	-1.22
1436705_at	Tmem32	transmembrane protein 32	0.00216	-1.10
1423492_at	Mrpl45	mitochondrial ribosomal protein L45	0.00216	-1.16
1433526_at	Klhl8	kelch-like 8 (Drosophila)	0.00217	-1.48
1442148_at	Psip1	PC4 and SFRS1 interacting protein 1	0.00217	-1.39
1416229_at	Rfk	riboflavin kinase	0.00219	-1.14
1460436_at	Ndst1	N-deacetylase/N-sulfotransferase (heparan glucosaminyl) 1	0.00220	-1.10
1451943_a_at	Ppm1a	protein phosphatase 1A, magnesium dependent, alpha isoform	0.00221	-1.21
1434071_a_at	Pelo	pelota homolog (Drosophila)	0.00221	-1.30
1420858_at	Pkia	protein kinase inhibitor, alpha	0.00221	-1.25
1415920_at	Cstf2t	cleavage stimulation factor, 3' pre-RNA subunit 2, tau	0.00224	-1.08
1436982_at	Tnrc6b	trinucleotide repeat containing 6b	0.00225	-1.10
1422524_at	Abcb6	ATP-binding cassette, sub-family B (MDR/TAP), member 6	0.00227	-1.17
1438322_x_at	Fdft1	farnesyl diphosphate farnesyl transferase 1	0.00228	-1.21
1452785_at	1700034H14Rik	RIKEN cDNA 1700034H14 gene	0.00232	-1.16
1434135_at	B3galnt2	UDP-GalNAc:betaGlcNAc beta 1,3-galactosaminyltransferase, polypeptide 2	0.00233	-1.21
1419352_at	l7Rn6	lethal, Chr 7, Rinchik 6	0.00236	-1.16
1448835_at	E2f6	E2F transcription factor 6	0.00237	-1.14
1427677_a_at	Sox6	SRY-box containing gene 6	0.00239	-1.16
1420859_at	Pkia	protein kinase inhibitor, alpha	0.00239	-1.13

Table 2.10 continued:

1424109_a_at	Glo1	glyoxalase 1	0.00240	-1.12
1442325_at	Tbc1d24	TBC1 domain family, member 24	0.00242	-1.27
1436224_at	---	18-day embryo whole body cDNA, RIKEN full-length enriched library, clone:1110061F19 product:unclassifiable, full insert sequence	0.00242	-1.16
1460531_at	2900069M18Rik	RIKEN cDNA 2900069M18 gene	0.00244	-1.67
1418432_at	Cab39	calcium binding protein 39	0.00248	-1.25
1449469_at	Pkd2l2	polycystic kidney disease 2-like 2	0.00248	-1.62
1421491_a_at	Tmem49	transmembrane protein 49	0.00250	-1.15
1443872_at	March2	Membrane-associated ring finger (C3HC4) 2	0.00251	-1.20
1429188_at	Cox11	COX11 homolog, cytochrome c oxidase assembly protein (yeast)	0.00251	-1.10
1441371_at	Plxna4	plexin A4	0.00252	-1.36
1427407_s_at	Trip11	thyroid hormone receptor interactor 11	0.00253	-1.16
1451508_at	Larp2	La ribonucleoprotein domain family, member 2	0.00255	-1.13
1417456_at	Gnpat	glyceronephosphate O-acyltransferase	0.00257	-1.18
1428991_at	Hrasls	HRAS-like suppressor	0.00257	-1.18
1452937_s_at	Ccdc28b	coiled coil domain containing 28B	0.00258	-1.16
1437067_at	Phtf2	putative homeodomain transcription factor 2	0.00272	-1.21
1426880_at	Etl4	enhancer trap locus 4	0.00272	-1.13
1453657_at	2310065F04Rik	RIKEN cDNA 2310065F04 gene	0.00273	-1.33
1435836_at	Pdk1	pyruvate dehydrogenase kinase, isoenzyme 1	0.00275	-1.15
1425730_at	Cacng6	calcium channel, voltage-dependent, gamma subunit 6	0.00277	-1.19
1427400_at	Lbx1	ladybird homeobox homolog 1 (Drosophila)	0.00280	-1.24
1421815_at	Epdr1	ependymin related protein 1 (zebrafish)	0.00282	-1.22
1458081_at	---	13 days embryo heart cDNA, RIKEN full-length enriched library, clone:D330025O06 product:unclassifiable, full insert sequence	0.00283	-1.40
1455723_at	D1Ertd448e	DNA segment, Chr 1, ERATO Doi 448, expressed	0.00284	-1.22
1448630_a_at	Sdhc	succinate dehydrogenase complex, subunit C, integral membrane protein	0.00285	-1.16
1450651_at	Myo10	myosin X	0.00286	-1.34
1428323_at	Gpd2	glycerol phosphate dehydrogenase 2, mitochondrial	0.00287	-1.30
1416993_at	Cog4	component of oligomeric golgi complex 4	0.00287	-1.11
1430154_at	4930543C13Rik	RIKEN cDNA 4930543C13 gene	0.00289	-1.15
1416204_at	Gpd1	glycerol-3-phosphate dehydrogenase 1 (soluble)	0.00290	-1.26

Table 2.10 continued:

1420116_s_at	Golph3	golgi phosphoprotein 3	0.00290	-1.16
1424147_at	Ahsa1	AHA1, activator of heat shock protein ATPase homolog 1 (yeast)	0.00291	-1.14
1444956_at	Gabarapl2	Gamma-aminobutyric acid (GABA-A) receptor-associated protein-like 2	0.00292	-1.19
1448743_at	Ssx2ip	synovial sarcoma, X breakpoint 2 interacting protein	0.00297	-1.23
1423780_at	Hibadh	3-hydroxyisobutyrate dehydrogenase	0.00297	-1.12
1439010_at	D330037H05Rik /// LOC673040 /// LOC677019	RIKEN cDNA D330037H05 gene /// similar to La-related protein 4 (La ribonucleoprotein domain family member 4)	0.00297	-1.15
1435333_at	1110007M04Rik	RIKEN cDNA 1110007M04 gene	0.00298	-1.17
1433860_at	6030458C11Rik	RIKEN cDNA 6030458C11 gene	0.00299	-1.18
1454858_x_at	Mettl7a	methyltransferase like 7A	0.00301	-1.19
1449257_at	D11Wsu99e	DNA segment, Chr 11, Wayne State University 99, expressed	0.00303	-1.19
1418502_a_at	Oxr1	oxidation resistance 1	0.00304	-1.15
1419616_at	Bmpr2	bone morphogenic protein receptor, type II (serine/threonine kinase)	0.00304	-1.19
1457861_at	A230009B12Rik	RIKEN cDNA A230009B12 gene	0.00308	-1.82
1435923_at	Gm237	gene model 237, (NCBI)	0.00309	-1.20
1429194_at	Tigd2	tigger transposable element derived 2	0.00313	-1.10
1421456_at	P2ry1	purinergic receptor P2Y, G-protein coupled 1	0.00314	-1.47
1422261_a_at	Msh3	mutS homolog 3 (E. coli)	0.00318	-1.43
1425020_at	EG621629 /// Ubxd4	UBX domain containing 4 /// predicted gene, EG621629	0.00319	-1.21
1422795_at	Cul3	cullin 3	0.00322	-1.19
1431416_a_at	Jam2	junction adhesion molecule 2	0.00323	-1.79
1421878_at	Mapk9	mitogen activated protein kinase 9	0.00324	-1.29
1419371_s_at	Gosr2	golgi SNAP receptor complex member 2	0.00325	-1.08
1425918_at	Egln3	EGL nine homolog 3 (C. elegans)	0.00325	-1.40
1418947_at	Nek3	NIMA (never in mitosis gene a)-related expressed kinase 3	0.00331	-1.16
1458302_at	---	Transcribed locus	0.00334	-1.18
1424917_a_at	Wipi1	WD repeat domain, phosphoinositide interacting 1	0.00336	-1.16
1453732_at	Ccdc90a	coiled-coil domain containing 90A	0.00336	-1.24
1425439_a_at	Slc41a3	solute carrier family 41, member 3	0.00337	-1.32
1445655_at	---	Transcribed locus	0.00337	-1.36
1417315_at	Gripap1	GRIP1 associated protein 1	0.00340	-1.18

Table 2.10 continued:

1431980_a_at	As3mt	arsenic (+3 oxidation state) methyltransferase	0.00340	-1.19
1435567_at	Phka1	phosphorylase kinase alpha 1	0.00341	-1.29
1452157_at	Eprs /// LOC633677	glutamyl-prolyl-tRNA synthetase /// similar to Bifunctional aminoacyl-tRNA synthetase	0.00343	-1.16
1448924_at	Tmem186	transmembrane protein 186	0.00344	-1.10
1421872_at	Rab24	RAB24, member RAS oncogene family	0.00344	-1.11
1454838_s_at	AW548124	expressed sequence AW548124	0.00344	-1.25
1418152_at	Nsbp1	nucleosome binding protein 1	0.00346	-1.26
1418586_at	Adcy9	adenylate cyclase 9	0.00346	-1.18
1427441_a_at	Suclg2	succinate-Coenzyme A ligase, GDP-forming, beta subunit	0.00346	-1.17
1418763_at	Nit2	nitrilase family, member 2	0.00349	-1.11
1434977_at	4933403F05Rik	RIKEN cDNA 4933403F05 gene	0.00350	-1.19
1416192_at	Napa	N-ethylmaleimide sensitive fusion protein attachment protein alpha	0.00351	-1.22
1450910_at	Cap2	CAP, adenylate cyclase-associated protein, 2 (yeast)	0.00354	-1.10
1450858_a_at	Ube2d3	ubiquitin-conjugating enzyme E2D 3 (UBC4/5 homolog, yeast)	0.00355	-1.07
1419866_s_at	Atxn2	ataxin 2	0.00356	-1.11
1421158_at	Cgnl1	cingulin-like 1	0.00356	-1.79
1453307_a_at	Anapc5	anaphase-promoting complex subunit 5	0.00360	-1.20
1432472_a_at	Mccc2	methylcrotonoyl-Coenzyme A carboxylase 2 (beta)	0.00361	-1.21
1435556_at	Zfp597	zinc finger protein 597	0.00362	-1.18
1435280_at	AI452195	expressed sequence AI452195	0.00364	-1.24
1420644_a_at	Sec61a2	Sec61, alpha subunit 2 (S. cerevisiae)	0.00365	-1.14
1422208_a_at	Gnb5	guanine nucleotide binding protein, beta 5	0.00368	-1.10
1424013_at	Etf1	eukaryotic translation termination factor 1	0.00370	-1.06
1455558_at	Gm114	gene model 114, (NCBI)	0.00370	-1.21
1433819_s_at	Agpat3	1-acylglycerol-3-phosphate O-acyltransferase 3	0.00371	-1.24
1455991_at	Ccbl2	cysteine conjugate-beta lyase 2	0.00374	-1.14
1460213_at	Golga4	golgi autoantigen, golgin subfamily a, 4	0.00376	-1.28
1428025_s_at	Pitpnc1	phosphatidylinositol transfer protein, cytoplasmic 1	0.00376	-1.14
1421018_at	1110018J18Rik	RIKEN cDNA 1110018J18 gene	0.00377	-1.27
1416007_at	Satb1	special AT-rich sequence binding protein 1	0.00384	-1.17
1437398_a_at	Aldh9a1	aldehyde dehydrogenase 9, subfamily A1	0.00385	-1.20
1451921_a_at	Nfat5	nuclear factor of activated T-cells 5	0.00386	-2.48

Table 2.10 continued:

1435679_at	Optn	optineurin	0.00392	-1.23
1421914_s_at	Mrpl19	mitochondrial ribosomal protein L19	0.00393	-1.09
1417247_at	AI597479	expressed sequence AI597479	0.00396	-1.13
1439855_at	Tmtc1	transmembrane and tetratricopeptide repeat containing 1	0.00397	-1.24
1427565_a_at	Abcc5	ATP-binding cassette, sub-family C (CFTR/MRP), member 5	0.00398	-1.23
1422744_at	Phka1	phosphorylase kinase alpha 1	0.00399	-1.32
1445841_at	Lrrc39	leucine rich repeat containing 39	0.00400	-1.25
1453208_at	2700089E24Rik	RIKEN cDNA 2700089E24 gene	0.00405	-1.14
1426146_a_at	Chpt1	choline phosphotransferase 1	0.00406	-1.22
1418412_at	Tpd52l1	tumor protein D52-like 1	0.00409	-1.20
1420826_at	Letm1	leucine zipper-EF-hand containing transmembrane protein 1	0.00410	-1.20
1425597_a_at	Qk	quaking	0.00413	-1.25
1427152_at	Qser1	glutamine and serine rich 1	0.00414	-1.18
1438553_x_at	---	---	0.00416	-1.17
1432429_at	8430437N05Rik	RIKEN cDNA 8430437N05 gene	0.00416	-1.93
1448844_at	Cyb5b	cytochrome b5 type B	0.00417	-1.13
1435071_at	Zfyve1	zinc finger, FYVE domain containing 1	0.00417	-1.32
1433453_a_at	Abtb2	ankyrin repeat and BTB (POZ) domain containing 2	0.00418	-1.30
1455062_at	AU017455	expressed sequence AU017455	0.00418	-1.41
1420967_at	Slc25a15	solute carrier family 25 (mitochondrial carrier ornithine transporter), member 15	0.00419	-1.18
1426773_at	Mfn1	mitofusin 1	0.00421	-1.20
1423442_a_at	Fbxw2	F-box and WD-40 domain protein 2	0.00422	-1.13
1454680_at	D5Ertd579e	DNA segment, Chr 5, ERATO Doi 579, expressed	0.00422	-1.14
1438011_at	Pcyt1a	phosphate cytidylyltransferase 1, choline, alpha isoform	0.00431	-1.17
1425115_at	Rbbp6	retinoblastoma binding protein 6	0.00435	-1.17
1424892_at	Zkscan5	zinc finger with KRAB and SCAN domains 5	0.00435	-1.15
1435591_at	AI426330	expressed sequence AI426330	0.00438	-1.14
1429430_at	Pcmtd1	protein-L-isoaspartate (D-aspartate) O-methyltransferase domain containing 1	0.00440	-1.16
1424488_a_at	Ppa2	pyrophosphatase (inorganic) 2	0.00443	-1.14
1435501_at	2410024A21Rik	RIKEN cDNA 2410024A21 gene	0.00445	-1.20
1448486_at	Mut	methylmalonyl-Coenzyme A mutase	0.00447	-1.16

Table 2.10 continued:

1431020_a_at	Fgfr1op2	FGFR1 oncogene partner 2	0.00447	-1.17
1417241_at	X83328	EST X83328	0.00449	-1.10
1434307_at	Tmem64	transmembrane protein 64	0.00450	-1.14
1439332_at	Ddit4l	DNA-damage-inducible transcript 4-like	0.00450	-1.37
1426216_at	Cog6	component of oligomeric golgi complex 6	0.00453	-1.08
1459048_s_at	Zfp142	zinc finger protein 142	0.00454	-1.19
1435656_at	Gmps	guanine monphosphate synthetase	0.00455	-1.25
1450676_at	Tceb3	transcription elongation factor B (SIII), polypeptide 3	0.00457	-1.15
1423566_a_at	Hsp110	heat shock protein 110	0.00458	-1.28
1455700_at	Mterfd3	MTERF domain containing 3	0.00459	-1.15
1435006_s_at	Abcb7	ATP-binding cassette, sub-family B (MDR/TAP), member 7	0.00469	-1.12
1431827_a_at	Tlk2	tousled-like kinase 2 (Arabidopsis)	0.00469	-1.13
1417265_s_at	Coq5	coenzyme Q5 homolog, methyltransferase (yeast)	0.00472	-1.22
1456063_at	ORF34	open reading frame 34	0.00473	-1.16
1449823_at	Dach2	dachshund 2 (Drosophila)	0.00474	-1.35
1427114_at	Ttc19	tetratricopeptide repeat domain 19	0.00474	-1.22
1424347_at	Ppp6c	protein phosphatase 6, catalytic subunit	0.00474	-1.13
1426945_at	Ranbp5	RAN binding protein 5	0.00477	-1.09
1440228_at	Ranbp6	RAN binding protein 6	0.00478	-1.25
1423114_at	Ube2d3	ubiquitin-conjugating enzyme E2D 3 (UBC4/5 homolog, yeast)	0.00480	-1.11
1453156_s_at	Zadh1	zinc binding alcohol dehydrogenase, domain containing 1	0.00482	-1.16
1451398_at	Cbr4	carbonyl reductase 4	0.00484	-1.12
1423592_at	Rock2	Rho-associated coiled-coil containing protein kinase 2	0.00491	-1.24
1416743_at	LOC640502 /// Uap1	UDP-N-acetylglucosamine pyrophosphorylase 1 /// similar to UDP-N-acetylhexosamine pyrophosphorylase	0.00494	-1.16
1426043_a_at	Capn3	calpain 3	0.00495	-1.16
1434979_at	4933403F05Rik	RIKEN cDNA 4933403F05 gene	0.00496	-1.33
1460556_at	---	---	0.00497	-1.08
1430177_at	Ube2b	ubiquitin-conjugating enzyme E2B, RAD6 homology (S. cerevisiae)	0.00499	-1.26
1443849_x_at	Urod	uroporphyrinogen decarboxylase	0.00499	-1.08

Table 2.11: Gene expression changes in common between *Dtna*$^{-/-}$ diaphragm and quadriceps muscles ($p<0.005$)

Gene Symbol	Gene Name	Change in Dtna$^{-/-}$ quad, vs. WT	Change in Dtna$^{-/-}$ diaphragm, vs. WT
Dtna	dystrobrevin alpha	-51.2% to -77.9%	-56.0% to -80.0%
0910001A06Rik	RIKEN cDNA 0910001A06 gene	+22.6%	-16.4%
Esco1	establishment of cohesion 1 homolog 1 (S. cerevisiae)	-40.3%	-52.2%
Igf2	Insulin-like growth factor 2	+22.0%	+78.4%
Myl4	myosin, light polypeptide 4	+37.1% to +146.2%	+12.6%
Pdrg1	p53 and DNA damage regulated 1	-7.6%	-12.2%
Adcy9	adenylate cyclase 9	-13.4%	-15.4%
Arpp21	Cyclic AMP-regulated phosphoprotein, 21	+10.9%	+87.4%
Abcb4	ATP-binding cassette, sub-family B (MDR/TAP), member 4	-17.8%	-18.5%
Rhou	ras homolog gene family, member U	-19.4%	-24.7%
Rfk	riboflavin kinase	-10.6%	-14.8%
Mapk9	mitogen activated protein kinase 9	+19.0%	-22.7%
Riok3	RIO kinase 3 (yeast)	-13.7%	-66.3%

CHAPTER 3:

NPC1 overexpression attenuates muscular dystrophy in α-dystrobrevin-null and *mdx* mice

Introduction

Duchenne muscular dystrophy (DMD) is a fatal, muscle wasting disease, affecting approximately 1 in 3500 live male births. Patients with DMD display muscle weakness early in life, eventually progressing to loss of mobility due to severe muscle degeneration and ultimately death by the early twenties, usually from respiratory or cardiac failure. DMD results from the loss of functional dystrophin, a large intracellular membrane protein that is required for the formation of a large complex of transmembrane glycoproteins, adaptor proteins, and signaling proteins (Hoffman et al., 1987). Despite significant advances in gene therapy aimed at replacing the defective dystrophin gene (Cox et al., 1993; Gregorevic et al., 2006; Mann et al., 2001; Ragot et al., 1993; van Deutekom et al., 2001; Wang et al., 2000), DMD still remains without an effective treatment.

Dystrophin is a member the dystrophin-associated protein complex (DPC), which forms a physical link between the intracellular actin cytoskeleton and the extracellular matrix. Members of the DGC include the dystroglycans, which provide transmembrane linkage between dystrophin and laminin, γ-actin, the sarcoglycans, and the syntrophin-dystrobrevin scaffold for signaling proteins (reviewed in (Ervasti, 2007)). Disruptions in several of the DPC proteins cause

other forms of muscular dystrophies, particularly the limb-girdle muscular dystrophies (reviewed in (Ozawa et al., 2005)). Although the DPC complex has been extensively studied, the downstream molecular and cellular alterations that lead to muscle degeneration in DMD are largely unknown. A more complete understanding of these pathways may reveal new therapeutic targets that slow the progression of muscle degeneration.

In this study, we performed gene expression analyses on skeletal muscle from mice lacking α-dystrobrevin (*Dtna*$^{-/-}$), which display neuromuscular junction (NMJ) abnormalities and a mild dystrophic phenotype compared to *mdx* mice (Grady et al., 1999; Grady et al., 2000), in order to identify genes whose misregulation may contribute to the phenotype of this mouse. We identified a highly significant reduction in Niemann-Pick C1 (Npc1) transcript, which we confirmed at the protein level. Mutations in Npc1 are responsible for NPC disease, a progressive and ultimately fatal, autosommal recessive, neurodegenerative disease, affecting ~1 in 150,000 live births. The function of NPC1 is not well understood but appears to be involved in regulating intracellular cholesterol transport (Liscum et al., 1989). Cells lacking NPC1 exhibit an accumulation of LDL-derived unesterified cholesterol in the endosomal/lysosomal pathway, which may impair trafficking or other cellular functions (Sokol et al., 1988). NPC1 has been studied extensively in brain and liver, the tissues more severely affected by the disease. In contrast, skeletal muscle has not been studied, to our knowledge.

To determine if the restoration of NPC1 could reverse the NMJ defects of the *Dtna*$^{-/-}$ muscle or muscular dystrophy, we transgenically expressed *Npc1* specifically in skeletal muscle of both α-dystrobrevin-null and *mdx* mice. Here, we show that NPC1 overexpression significantly ameliorates the dystrophic phenotype in both of these mouse models of muscular dystrophy. These findings provide the first evidence for a mechanistic link between diseases of neuronal and skeletal muscles, i.e. the involvement of NPC1, a cholesterol and/or sphingolipid trafficking protein. Furthermore, these results reveal a potential new therapeutic target for muscle degeneration diseases.

Materials and Methods

Animals

We obtained breeding pairs of BALB/c mice heterozygous for the Niemann Pick type C1 mutant allele (The Jackson Laboratory). The mutant allele contains the insertion of a retroposon, resulting in a premature truncation, deleting 11 out of the 13 transmembrane domains. Breeding pairs were maintained and bred to produce *Npc1*-null (*Npc*$^{-/-}$), *Npc1*-heterozygous (*Npc*$^{+/-}$), and wild-type offspring. Genotyping was performed according to suggested Jackson Laboratory protocols (jaxmice.jax.org). *Dtna*$^{-/-}$ mice (α-dystrobrevin-null) (Grady et al., 1999) were a generous gift of Joshua Sanes (Harvard University). Mice lacking dystrophin (*mdx*) were obtained from The Jackson

Laboratory. All animal experiments were performed with the approval of the Institutional Animal Care and Use Committee at the University of Washington.

Affymetrix GeneChip Assays

Quadriceps muscles were dissected from individual six-week-old male α-dystrobrevin-null mice (*Dtna*$^{-/-}$) (Grady et al., 1999) and their wild-type, sex-matched littermates. Total RNA was isolated from each quadriceps muscle with Trizol Reagent (Invitrogen) and purified with the RNeasy Mini Kit (Qiagen). For each sample, 20μg of total RNA was processed for gene expression analysis, using Affymetrix Murine Genome U74Av2, U74Bv2, and U74Cv2 arrays, following suggested Affymetrix protocols (www.affymetrix.com). RNAs from eight experimental and eight control mice were analyzed on each of the U74v2 arrays. Samples were not pooled. Briefly, double-stranded cDNA was synthesized from total RNA (SuperScript Choice system, Invitrogen). Single-stranded, biotin-labeled cRNA (BioArray™ HighYield™ RNA Transcript Labeling Kit (T7), Enzo Life Sciences) was then synthesized by *in vitro* transcription, and fragmented. The resulting fragmented, biotin-labeled cRNA (15μg) was hybridized to the Affymetrix arrays, which were stained with the GeneChip® Fluidics Station 400 (Affymetrix) and scanned with the GeneChip® Scanner 3000 (Affymetrix) at the Center for Array Technologies at the University of Washington. Initial data analysis was performed with Affymetrix® Microarray Suite 5.0. Student's paired *t* tests were performed on the signal

intensities of all probe sets to identify significant differences between the control and experimental groups. $p<0.005$ was considered significant.

Real-Time quantitative RT-PCR

We confirmed the change in *Npc1* expression by Real-Time quantitative RT-PCR, using TaqMan® chemistry and the ABI 7000 sequence detection system (Applied Biosystems). Quadriceps muscles were dissected from nine individual six-week-old male *Dtna*$^{-/-}$ mice (Grady et al., 1999) and their wild-type, sex-matched littermates. Each sample was treated individually. Total RNA was isolated as described above. Real-Time quantitative RT-PCR was performed on each sample with an ABI Prism 7000 Sequence Detection System (Applied Biosystems), using 50ng of RNA, One-Step RT-PCR Master Mix reagents (Applied Biosystems), and *Npc1* primers (5'-AAT GCG GTC TCC TTG GTC AA-3' and 5'-GCT CTC GTT ATA TGG CTG CAG AA-3', Integrated DNA Technologies) and probe (5' 6-FAM d(CAC AGA AAT GCC ACA GCT CAT CAC CAA) BHQ-1 3', Biosearch Technologies, Inc.), or 18S primers and probe (Applied Biosystems, P/N 4310893E). The relative expression of *Npc1* mRNA was normalized to the amount of 18S RNA in the same sample. Each sample was run in duplicate. A Student's paired *t* test was performed to determine the significance of the difference in *Npc1* expression between the control and experimental groups.

Generation of NPC1 antibody

A 16-amino acid peptide, corresponding to the cytosolic carboxy-terminal domain of murine NPC1 ((GenBank Acc. No. BC052437, residues 1256-1271); KAKRHTTYERYRGTER) was synthesized (Macromolecular Resources, Colorado State University), conjugated to maleimide-activated mcKLH (Pierce), and injected into three New Zealand White rabbits (Covance Research Products). Antibodies were affinity purified using UltraLink Iodoacetyl Gel columns (Pierce) bound with the peptide.

Membrane enrichment and immunoblots

Tissues were dissected and quick frozen in liquid nitrogen. Membrane preparations and immunoblotting were performed as previously described (Garver et al., 2000) with the following modifications. Following homogenization in 25 mM MES, pH 6.5, 150 mM NaCl, and protease inhibitors, the tissues were centrifuged for 30 min at 100,000 g, generating a cytosolic fraction (supernatant) and membrane-enhanced fraction (pellet). Pellets were subsequently homogenized in 25 mM MES, pH 6.5, 150 mM NaCl, 1.0% Triton X-100, and protease inhibitors and centrifuged at 2,000 *g* for 10 min. Sample protein content was determined using the bicinchoninic acid (BCA) protein assay (Pierce). Gels (4-15% Tris-HCl gradient, BioRad) were loaded with 5-20 μg of protein. The separated proteins were transferred to nitrocellulose membrane (Schleicher and Schuell) at 100V for 1-hour. Immunoblots were

blocked for 1-hour at room temperature in 10 mM sodium phosphate, pH 7.4, 150 mM NaCl, 0.05% Tween-20, and 4% non-fat dry milk. Immunoblots were incubated at 4°C overnight in 10 mM sodium phosphate, pH 7.4, 150 mM NaCl, 0.05% Tween-20, and 1% non-fat dry milk, containing primary antibodies, followed by three 10-min washes. Primary antibody was detected using HRP-conjugated secondary antibody (Jackson ImmunoResearch Laboratories) in 10 mM sodium phosphate, pH 7.4, 150 mM NaCl, 0.05% Tween-20, and 1% non-fat dry milk. Protein bands were detected using SuperSignal® West Femto Maximum Sensitivity Substrate (Pierce) and a CCD camera (AlphaInnotech).

Immunofluorescence

Muscle fiber preparations were adapted from Percival et al. (2007) (Percival et al., 2007). Briefly, dissected muscles were rinsed in 1 mM EDTA, pH 7.4 for 3 min. Muscles were then pinned to Sylgaard-coated Petri dishes, fixed for 30 min in 1% paraformaldehyde, and teased apart into individual and small groups of fibers. Fibers were subsequently incubated for 20 min in 50 mM NH_4Cl followed by 30 min in blocking buffer (0.05% saponin, 10% goat serum in PBS) and 2 hr in anti-NPC1 primary antibody diluted (1:100) in blocking buffer. Following three 15-min washes in 0.05% saponin in PBS, the fibers were incubated for 45 min in Alexa-Fluor-488-conjugated donkey anti-rabbit secondary antibody (Molecular Probes) diluted in blocking buffer and washed. Labeled fibers were separated on glass slides in ProLong® Gold

antifade mounting media, containing DAPI (Invitrogen) for visualization of nuclei. Confocal microscopy images were obtained using a Zeiss LSM 510 META at the W.M. Keck Center for Advanced Studies in Neural Signaling at the University of Washington. Stacks of 40 serial optical sections measuring 0.44 μm in thickness were obtained at 0.44 μm intervals through the muscle fibers, using a Plan-Neofluar 40x/1.3 Oil objective at 2x zoom. The sections were merged into a single image using the "maximum" projection method.

Generation of transgenic mice

The cDNA encoding full-length *Npc1* was obtained from ATCC (cat. no. 9890203). Upon sequence comparison of this clone (GenBank BC052437) with that of another published mouse *Npc1* sequence (GenBank AF003348), multiple ESTs, and the mouse genome, we observed several sequence discrepancies. We considered the consensus sequence generated from all of the sequences to be correct. Therefore, by PCR, we made a single base mutation, a3963g, and consequently an amino acid alteration, K1273E, to match the ATCC sequence to that of the consensus. The *Npc1* cDNA was then cloned into the NotI site of the previously described pBSX-HSAvpA expression vector (Crawford et al., 2000), a generous gift from Dr. Jeffrey Chamberlain, University of Washington, and confirmed by sequencing. The linearized construct was injected into the pronuclei of *C57BL/6 x C3H* embryos (University of Washington, Department of Comparative Medicine, Transgenic Resources

Program), and the resulting progeny were genotyped by PCR (5'-GAT GAA GCA GAC AGT ATT CAG C-3' and 5'-CAG TTC GGC TCG CGG AGC AC-3'). Four founder lines carrying the *Npc1* transgene were identified (Tg(*Npc*1)) and bred onto *Dtna*$^{-/-}$ (*Dtna*$^{-/-}$-Tg(*Npc*1)) and *mdx* (*mdx*-Tg(*Npc*1)) backgrounds.

Central nuclei counts and fiber diameter measurements

Tibialis anterior (fast-twitch), soleus (slow-twitch), and diaphragm muscles were dissected, embedded in O.C.T. (TissueTek) in cryomolds, and quick-frozen in liquid nitrogen-cooled isopentane. Eight-μm cross-sections taken from the mid-belly of the muscles were fixed in 95% ethanol and stained with Gill's No. 3 hematoxylin and eosin Y. We used a Zeiss Axioscope 2 microscope to take cross-sectional images of the whole muscle. Each fiber in each muscle was assessed for the presence of centrally or peripherally-located nuclei. The percentage of muscle fibers with central nuclei was determined for each muscle by dividing the number of fibers with central nuclei by the total number of fibers. A minimum of five mice per genotype was analyzed. *Dtna*$^{-/-}$-Tg(*Npc*1) were examined at three months of age, and *mdx*-Tg(*Npc*1) at eight weeks of age. Additionally, we used ImageJ software to measure the Feret's diameter (Briguet et al., 2004) of muscle fibers. Measurements were taken from an entire cross-section of soleus muscle from each of three mice per genotype examined. Coefficients of variation (%) of the fiber diameters were calculated as standard deviation of the muscle fiber size/ mean fiber size x 100.

We performed one-way ANOVA tests with Tukey's post test for determination of statistical significance, using GraphPad Prism version 4.00 (GraphPad Software, San Diego, California).

Creatine kinase assay

Blood (50-100μl) was collected from the saphenous vein and allowed to clot for 20 minutes. Serum was obtained following centrifugation of the blood at 5,000g for 8 minutes at room temperature. We used the CK Liqui-UV Test (StanBio) and followed the manufacturer's protocol for the determination of serum creatine kinase activity. A minimum of five mice per genotype was analyzed, independently. A one-way ANOVA with Tukey's post test was performed for determination of statistical significance, using GraphPad Prism version 4.00 (GraphPad Software, San Diego, California).

Results

Reduction of NPC1 in Dtna$^{-/-}$ muscle

In order to identify genes whose misregulation results from the loss of *Dtna*, we compared gene expression levels from quadriceps muscle of six-week old, male *Dtna*$^{-/-}$ mice to sex-matched, wild-type littermate controls. The goal of these studies was to identify gene expression that is altered prior to the onset of muscle degeneration. To improve the chances of identifying early gene expression changes, we selected a muscle (quadriceps) that is only mildly

affected (based on histological analysis) and then analyzed large numbers of muscle samples independently so that even small, but statistically significant changes would be revealed. We analyzed expression levels using the Affymetrix Murine GeneChip U74v2 expression arrays, which probe approximately 36,000 full-length genes and ESTs. Using Student's *t* tests and a predetermined cutoff for statistical significance of $p<0.005$, we identified more than 200 transcripts that were differentially regulated in *Dtna*$^{-/-}$ muscle (See Chapter 2, Figures 2.4 and 2.5). Because of its high level of statistical significance ($p = 3.0e^{-7}$) and its involvement in a known neurodegenerative disease, our attention was directed toward *Npc1*. The expression level of *Npc1* was reduced by approximately 50% in the *Dtna*$^{-/-}$ muscle. Real-time quantitative RT-PCR confirmed the 50% reduction ($p<0.05$) of *Npc1* in *Dtna*$^{-/-}$ quadriceps muscle (Figure 3.1a).

We generated a rabbit polyclonal anti-peptide antibody to mouse NPC1 to determine if NPC1 protein levels are also reduced in *Dtna*$^{-/-}$ muscle. NPC1 is a 1278 amino acid, multi-pass transmembrane protein with a luminal amino-terminus and a cytosolic carboxy-terminus. The NPC1 antibody, generated against a 16 amino acids located in the carboxy-terminal region, was tested on quadriceps muscle from wild-type, *Npc1*-heterozygous (*Npc*$^{+/-}$), and NPC1-homozygous-null (*NPC*$^{-/-}$) mice (Figure 3.1b). Immunoblot analysis of membrane-enriched fractions of quadriceps muscle identified an ~180-kD band in wild-type tissue. This band was absent in *NPC*$^{-/-}$ tissue and at intermediate

levels in *NPC*$^{+/-}$ tissue (Figure 3.1b). These results confirm a previous study using a similarly designed antibody on *Npc*$^{-/-}$, *Npc*$^{+/-}$, and wild-type cultured mouse fibroblasts and mouse liver homogenates (Garver et al., 2000). Further evidence to support the specificity of our antibody comes from immunofluorescence staining of wild-type quadriceps muscle that is absent in *Npc*$^{-/-}$ tissue (Figure 3.1c).

Using this antibody, we compared NPC1 protein levels in *Dtna*$^{-/-}$ and wild-type quadriceps muscle. Like the *Npc1* transcript levels, NPC1 protein levels are also markedly decreased in *Dtna*$^{-/-}$ muscle, compared to wild-type samples (Figure 3.1d).

Generation of transgenic mice

To test the idea that restoration of NPC1 levels in dystrophic muscle would ameliorate the phenotype, we produced transgenic mice expressing *Npc1* driven by the human skeletal α-actin promoter to achieve expression specifically in skeletal muscle. We identified four transgenic founder lines (Tg(*Npc1*)19, Tg(*Npc1*)55, Tg(*Npc1*)56, and Tg(*Npc1*)58) (Figure 3.2a). Skeletal muscle from two (Tg(*Npc1*)19 and Tg(*Npc1*)58) of the four transgenic lines showed high expression of NPC1 (Figure 3.3b). The transgenic lines showed no adverse effects of high levels on NPC1 in muscle. Each of the Tg(*Npc1*) lines was crossed subsequently onto the *Dtna*$^{-/-}$ (Grady et al., 1999) and *mdx* backgrounds.

Examination of the effects of NPC1 overexpression on the NMJ abnormalities of the α-dystrobrevin-null mouse

In addition to a mild muscular dystrophy, α-dystrobrevin-null mice exhibit abnormalities of the NMJ, including abnormal distribution of acetylcholine receptors, giving the NMJ a "fuzzy" appearance as AChRs extend beyond the gutters where they are normally confined (Grady et al., 2000). Using α-bungarotoxin-stained, single-teased fiber preparations from sternomastoid muscles, we examined the distribution of ACh receptors at the NMJs of wild-type, *Dtna*$^{-/-}$, and *Dtna*$^{-/-}$-Tg(*NPC1*) mice. Although the abnormal AChR distribution did not appear as severe in the *Dtna*$^{-/-}$-Tg(*NPC1*)19 mice as in the *Dtna*$^{-/-}$ mice, overexpression of NPC1 in *Dtna*$^{-/-}$ skeletal muscle does not restore the distribution of ACh receptors to normal (data not shown).

Amelioration of muscular dystrophy in Dtna$^{-/-}$*-Tg(Npc1) mice*

Three-month-old *Dtna*$^{-/-}$-Tg(*Npc1*) mice, as well as age-matched *Dtna*$^{-/-}$ and wild-type controls of similar genetic backgrounds were analyzed. Muscular dystrophy is characterized, in part, by increased numbers of regenerating muscle fibers, which are identified by central nucleation, as well as damaged muscle membranes. The latter leads to elevated levels of serum creatine kinase, which provides a body-wide assessment of myofiber sarcolemmal integrity.

We determined the percentage of centrally-nucleated muscle fibers from H&E-stained cross-sections of soleus, TA, and diaphragm muscles of each genotype (Figure 3.3b). In both the soleus and diaphragm muscles, transgenic expression of NPC1 restored central nuclei counts to wild-type. Compared to *Dtna*$^{-/-}$, we observed large, statistically significant ($p<0.001$) reductions (83% and 76%) in the percentage of centrally-nucleated myofibers in the soleus muscle of the two transgenic lines expressing high levels of NPC1 (*Dtna*$^{-/-}$-Tg(*NPC1*)19 and *Dtna*$^{-/-}$-Tg(*NPC1*)58, respectively). We also observed smaller, but still statistically significant ($p<0.01$), reductions (42% and 34%) in the two lines expressing NPC1 at lower levels (*Dtna*$^{-/-}$-Tg(*NPC1*)55 and *Dtna*$^{-/-}$-Tg(*NPC1*)56, respectively). In the diaphragm muscle, the two transgenic lines expressing NPC1 at low levels did not show significant decreases in centrally-nucleated myofibers. However, both high NPC1-expressing transgenic lines (*Dtna*$^{-/-}$-Tg(*NPC1*)19 and *Dtna*$^{-/-}$-Tg(*NPC1*)58) had highly significant reductions (89% and 93%, respectively). In the TA muscle, the percentage of myofibers with central nuclei was unchanged in all four transgenic lines compared to *Dtna*$^{-/-}$ mice. *Dtna*$^{-/-}$ transgenic mice expressing high levels of NPC1 also exhibited marked reductions in serum creatine kinase activity. As shown in Figure 3.3c, transgenic expression of NPC1 in *Dtna*$^{-/-}$ mice restored creatine kinase levels to wild-type levels in both the *Dtna*$^{-/-}$-Tg(*NPC1*)19 and *Dtna*$^{-/-}$-Tg(*NPC1*)58 lines. These results show that the dystrophic phenotype is markedly reduced by

transgenic expression of NPC1, the response is dose dependent, and the phenotype amelioration is dependent on the muscle type.

Amelioration of muscular dystrophy in mdx-Tg(Npc1) mice

The dystrophic phenotype of the *Dtna*$^{-/-}$ mouse has been attributed to defects in the signaling function of the dystrophin complex (Grady et al., 1999). However, the dystrophic phenotype is comparatively a mild one, which is one of the reasons we chose to study this mouse model, as described above, and no human muscular dystrophy due to mutations in *Dtna* have been identified. To determine if upregulation of NPC1 alters the phenotype in a more severe model of muscular dystrophy, we performed studies of the *mdx* mouse. This mouse model has been studied extensively and is considered a good model of DMD in humans (Bulfield et al., 1984). Each transgenic NPC1 founder line was crossed onto the *mdx* background (Figure 3.4). Muscular dystrophy was assessed in eight-week-old wild-type, *mdx*, and *mdx*-Tg(*Npc1*) by quantifying the percentage of centrally-nucleated myofibers in soleus, TA, and diaphragm muscles (Figure 3.4b) and by examining serum creatine kinase activity (Figure 3.4c) and myofiber size variability (Figure 4d).

In the soleus, TA, and diaphragm muscles, high expression of NPC1 (transgenic lines *mdx*-Tg(*Npc1*)19 and *mdx*-Tg(*Npc1*)58), significantly reduced the percentage of centrally-nucleated fibers, as compared to muscles from *mdx* mice (Figure 3.4b). As observed in the *Dtna*$^{-/-}$-Tg(*Npc1*) mice, transgenic

expression of NPC1 in *mdx* mice also significantly reduced serum creatine kinase levels (Figure 3.4c). Both of the transgenic lines expressing NPC1 at high levels (*mdx*-Tg(*Npc1*)19 and *mdx*-Tg(*Npc1*)58) showed sharply decreased creatine kinase levels (by 52% and 75%), respectively compared to *mdx*. In fact, creatine kinase levels in mdx-Tg(*Npc1*)58 mice were reduced to wild-type levels.

As dystrophic muscles also show variability in muscle fiber diameter due to regeneration and degeneration, we also examined the variability in the soleus muscle of the *mdx*-Tg(*Npc1*)58 mouse as it appeared to be the most improved transgenic line, based on the degree of improvement in central nucleation and creatine kinase levels. Indeed, we found that while fiber sizes varied significantly in the *mdx* soleus compared to wild-type, transgenic expression of NPC1 significantly reduced the variability (Figure 3.4d and 3.4e). These data suggest that transgenic expression of NPC1 in *mdx* skeletal muscle can significantly attenuate the degree of muscular dystrophy in this mouse model of Duchenne muscular dystrophy.

Discussion

Our results suggest a new role for NPC1 in the mechanisms that lead to muscle degeneration in muscular dystrophies. Absence of NPC1 causes severe neuronal degeneration, but this report is the first to implicate NPC1 in diseases of muscle degeneration, specifically the muscular dystrophies. We

used gene expression profiling of α-dystrobrevin-null (*Dtna*$^{-/-}$) mouse muscle to identify downstream cellular and/or molecular alterations that result from the loss of α-dystrobrevin, and that contribute to the onset of the muscular dystrophy observed in *Dtna*$^{-/-}$ mice. Whereas neither dystrophin-deficient (*mdx*) nor *Dtna*$^{-/-}$ muscles exhibit the severe dystrophy observed in patients with Duchenne muscular dystrophy, *Dtna*$^{-/-}$ muscle displays an even milder myopathy than *mdx* muscle (Grady et al., 1999). Previous expression profiling studies of *mdx* muscle have yielded large numbers of changes associated with immune response and regeneration in the dystrophic muscle (Porter et al., 2002; Porter et al., 2004). In an effort to identify alterations in proteins and/or signaling pathways that lead to degeneration, we sought to minimize the influence of transcriptional responses associated with inflammation and muscle repair, by examining the more mildly affected *Dtna*$^{-/-}$ quadriceps muscle at six weeks of age. In addition, we analyzed sufficiently large numbers of samples independently so that the statistical significance of relatively small changes could be assessed. Thus, our selection of important changes was based on statistical significance, rather than an arbitrarily set cut off of the magnitude of the change.

We identified more than 200 differentially expressed transcripts in the *Dtna*$^{-/-}$ quadriceps muscle. As expected based on the dystrophic phenotype of the *Dtna*$^{-/-}$ mouse, a number of the genes with increased expression, such as IGF-II, are likely to be involved in muscle regeneration, as similar trends have

been observed in publicly available datasets (Gene Expression Omnibus (GEO) database, http://www.ncbi.nlm.nih.gov/geo/) from expression analyses of other dystrophy models (Bakay et al., 2002; Haslett et al., 2002; Porter et al., 2002; Tseng et al., 2002). In this study however, we focused on Niemann Pick type C1 (*Npc1*), which showed a highly significant ($p=3.02e^{-7}$) ~50% decrease in transcript levels in *Dtna*$^{-/-}$ muscle. *Npc1* had previously not been studied in the muscular dystrophy field. A search using GEO, however, revealed that *Npc1* levels are decreased in muscles from *mdx* and dysferlin-null mice (Garver et al., 2000; Tseng et al., 2002; Wenzel et al., 2005). However, Npc1 was not selected one of the most significantly altered genes based on the analysis method used.

NPC1 is a multispan membrane protein, residing primarily in late endosomes/lysosomes (Garver et al., 2000; Higgins et al., 1999; Neufeld et al., 1999) as well as the TGN (Higgins et al., 1999) and caveolin-1 containing vesicles (Garver et al., 2000; Higgins et al., 1999). Mutations in NPC1 cause NPC disease, an autosommal recessive, lysosomal storage disease, which results in progressive neurodegeneration and premature death (reviewed in (Patterson et al., 2001). Histologically, the absence of NPC1 results in intracellular accumulations of large amounts of unesterified cholesterol and glycosphingolipids in late endosomes/lysosomes. Non-neuronal *NPC*$^{+/-}$ cells show substantial amounts of accumulation of unesterified cholesterol, too, although at levels intermediate to normal and *NPC*$^{-/-}$ cells (Choi et al., 2003;

Garver et al., 2002; Kruth et al., 1986). In normal cells, cholesterol esters from endocytosed low density lipoprotein (LDL) cholesterol are hydrolyzed in the endocytic pathway. The unesterified, or free, cholesterol is then transported from the endosomes to other cellular membranes. In NPC1-deficient cells, however, the free cholesterol does not exit the endosomal pathway, accumulating instead in late endosomes/lysosomes. The precise function of NPC1 is unknown; however, it appears that NPC1, which can bind cholesterol directly (Ohgami et al., 2004), facilitates the transport of LDL-derived, unesterified cholesterol from late endosomes/lysosomes to other cellular sites, including the plasma membrane (Wojtanik and Liscum, 2003). The transporter-like transmembrane structure of NPC1 is consistent with function. Although cholesterol has been shown to accumulate in every tissue of *Npc1*$^{-/-}$ mice, including skeletal muscle (Xie et al., 1999), to our knowledge, neither the function of NPC1 in skeletal muscle, nor the effects of NPC1 deficiency in skeletal muscle have been examined.

In order to determine if the reduction of NPC1 contributes to the muscular dystrophy of the *Dtna*$^{-/-}$ mouse, we generated *Dtna*$^{-/-}$ mice transgenically expressing *Npc1* under the control of the human skeletal α-actin (HSA) promoter to achieve skeletal muscle-specific expression (Brennan and Hardeman, 1993). The dystrophic characteristics normally seen in *Dtna*$^{-/-}$ mice are greatly ameliorated in *Dtna*$^{-/-}$-Tg(*Npc1*) mice. Serum creatine kinase levels and the percentage of centrally-nucleated fibers in *Dtna*$^{-/-}$ soleus and diaphragm

muscles were restored to near normal levels by transgenic expression of NPC1. Perhaps more importantly, expression of NPC1 in *mdx* muscle also dramatically improved the dystrophic phenotype. Thus, our results suggest a new avenue for treatment of Duchenne muscular dystrophy in humans.

The loss or reduction of NPC1 by itself does not cause muscular dystrophy. We have examined several muscle types (TA, soleus, quadriceps, sternomastoid, and diaphragm) from 6-week-old $Npc^{-/-}$, as well as 6- and 16-week-old $Npc^{+/-}$ mice, and have found no evidence of dystrophy in any of these mice (data not shown). However, we report here that, although the transgenic expression of *Npc1* in *mdx* skeletal muscle is insufficient to completely restore *mdx* muscle to normal, it does appear to ameliorate the dystrophic phenotype in both $Dtna^{-/-}$ and *mdx* mice. Such a paradox has also been observed in the case of nNOS. Neither nNOS-null mice (Chao et al., 1998), nor α-syntrophin-null mice (Adams et al., 2000; Kameya et al., 1999), which have reduced nNOS levels, are dystrophic. Yet, *mdx* mice, which also have reduced levels of nNOS (Brenman et al., 1995), are dystrophic, and transgenically expressing nNOS alleviates the dystrophy in *mdx* mice (Wehling et al., 2001). A "two-hit" hypothesis has been suggested as a possible explanation for the discrepancy between the effect of nNOS reduction in the nNOS-null mouse and *mdx* mouse (Rando, 2001). According to this hypothesis, defects of the DPC are likely to have more than one biochemical consequence. Individually, either consequence may result in cell damage but is not enough to cause cell death;

however, together they result in the severe necrosis observed in dystrophic muscle. In the case of nNOS, the reduction of nNOS causes ischemia in muscle as a result of the loss of protection from nitric oxide to contraction-induced vasoconstriction ("first hit"), but the DPC defects increase the vulnerability ("second hit") of the muscle to ischemia, causing injury to the muscle. Perhaps then while the loss of NPC1 alone may not be sufficient to cause muscle fiber degeneration, it may in the presence of DPC defects contribute to the pathophysiology of dystrophic muscle.

Unfortunately, the mechanism by which NPC1 dysfunction causes neuronal degeneration in Niemann-Pick disease is not understood. However, molecular abnormalities in NPC1-null cells suggest possible links to known causes of muscle degeneration. One particularly intriguing connection involves caveolae and a key protein of this membrane structure, the caveolins. Caveolae are vesicular invaginations in the plasma membrane enriched in cholesterol binding proteins called caveolins (Murata et al., 1995) and require free cholesterol for proper formation (Hailstones et al., 1998). The trafficking of LDL-derived free cholesterol to the plasma membrane is dependent upon NPC1 (Wojtanik and Liscum, 2003). Caveolins transport cholesterol to plasma membrane caveolae (Murata et al., 1995; Smart et al., 1996) where they concentrate and organize cholesterol and sphingolipids, function in vesicle trafficking, and participate in signaling as suggested from their interactions with signaling proteins such as nNOS (Garcia-Cardena et al., 1997; Venema et al.,

1997). Caveolin-3, the muscle-specific caveolin, binds directly to the dystrophin complex members, β-dystroglycan (Sotgia et al., 2000) and nNOS (Garcia-Cardena et al., 1997; Venema et al., 1997), at the sarcolemma (Song et al., 1996), and is required for the correct targeting of the dystrophin complex to cholesterol-sphingolipid rafts/caveolae (Galbiati et al., 2001).

A link between muscular dystrophy and caveolin-3 regulation has been established as has a link between caveolin levels and NPC1 expression. Muscles from Duchenne muscular dystrophy patients have elevated caveolin-3 levels, increased numbers of membrane caveolae, and greater variability of caveolae size and shape, compared to normal muscle (Repetto et al., 1999). Similarly, *mdx* mouse muscles have elevated caveolin-3 levels in both membrane and soluble fractions (Vaghy et al., 1998) and a Duchenne-like muscular dystrophy results from transgenic overexpression of caveolin-3 in mouse muscle (Galbiati et al., 2000). Finally, mutations in caveolin-3 are the genetic basis for limb-girdle muscular dystrophy 1C (LGMD 1C) (Minetti et al., 1998).

Interestingly, elevated caveolin levels are also associated with NPC1 deficiency (Garver et al., 1999; Garver et al., 2002). In *Npc1*-heterozygous fibroblasts, caveolin levels are increased in plasma membrane caveolae (Garver et al., 2002). Associated with this increase is a decrease in the content of free cholesterol in caveolae. This relationship between NPC1 levels, caveolin levels, and cholesterol content suggests that *mdx* muscles and *Dtna*$^{-/-}$

muscles, which have NPC1 levels approximating those of the NPC-heterozygous cells, may also have decreased cholesterol levels in caveolae.

We have identified a significant reduction of NPC1, a cholesterol and sphingolipid trafficking protein, in α-dystrobrevin-null skeletal muscle. Furthermore, we show that transgenically expressing *Npc1* in skeletal muscle alleviates the dystrophic phenotype of both *Dtna*$^{-/-}$ and *mdx* mice, two models of muscular dystrophy. Because cholesterol is known to affect plasma membrane rigidity and lipid-protein interactions, and because caveolae are involved in intracellular signalling, alterations in the cholesterol content of sarcolemmae or caveolae could adversely affect the structural integrity of the sarcolemmae, the ability of the membranes to repair themselves, and/or the binding of signaling proteins, thus contributing to the phenotype of dystrophic muscle. Transgenically expressing *Npc1* in muscle, therefore, may correct abnormalities of the plasma membrane and/or caveolae in *Dtna*$^{-/-}$ and *mdx* muscle. These findings offer new therapeutic targets for muscular dystrophies resulting from abnormalities of the dystrophin complex.

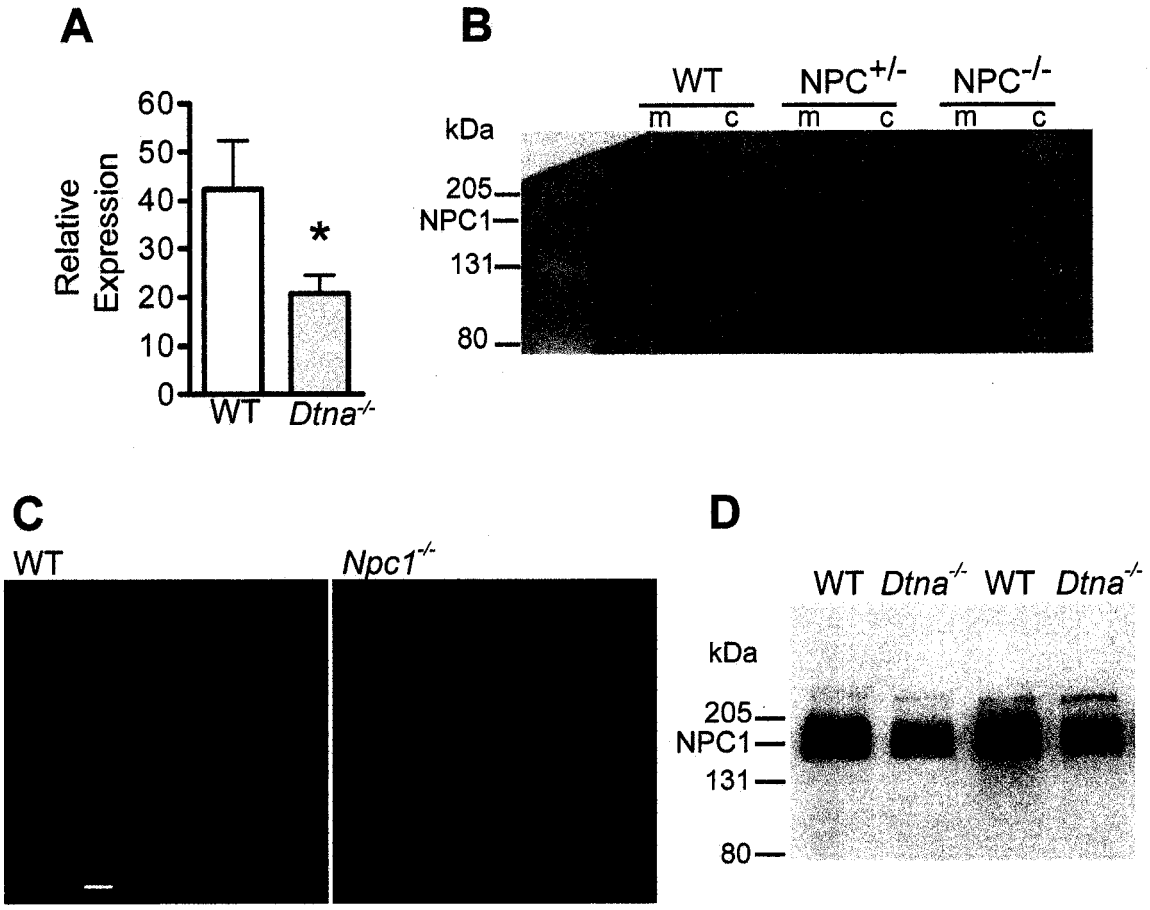

Figure 3.1: Reduction of *Npc1* mRNA and NPC1 protein in *Dtna*$^{-/-}$ quadriceps. (A) *Npc1* transcript levels from *Dtna*$^{-/-}$ and wild-type quadriceps muscles. Data is shown as mean ± standard deviation. *$p<0.05$, vs. wild-type, using Student's paired *t* test. (B,C) Characterization of a rabbit polyclonal NPC1 anti-peptide antibody by (B) immunoblot and (C) immunofluorescence analyses. (B) Immunoblot analysis of membrane-enriched (m) and cytosolic (c) fractions prepared from wild-type, *Npc*-heterozygous (+/-), and *Npc*-null (-/-) mouse quadriceps muscles. (C) Immunofluorescence of individually teased fibers from wild-type and *Npc*$^{-/-}$ quadriceps muscles. (D) Immunoblot analysis of membrane-enriched fractions prepared from wild-type and *Dtna*$^{-/-}$ mouse quadriceps muscles.

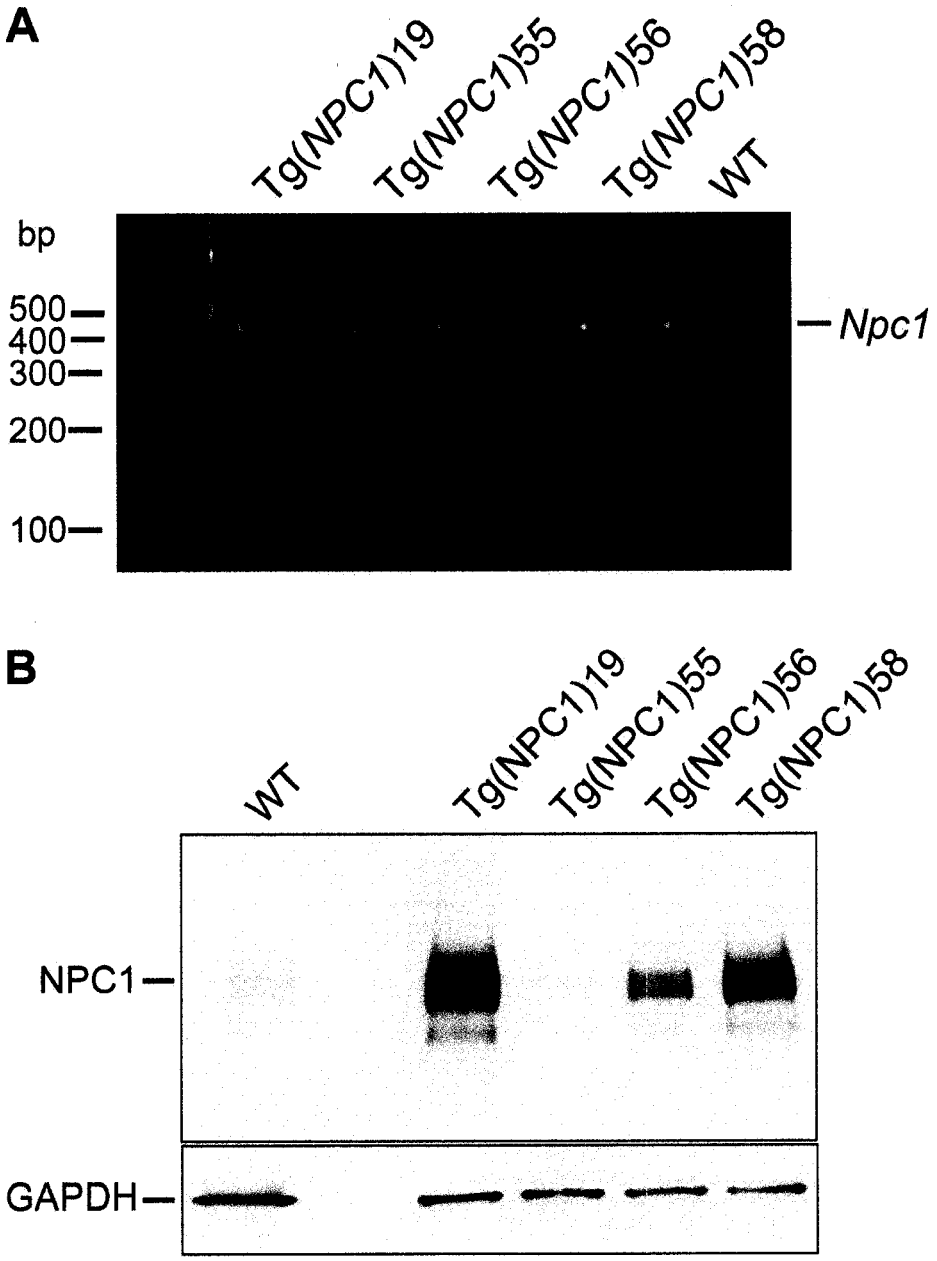

Figure 3.2. Expression of transgenic *Npc1* under human skeletal α-actin promoter. (A) PCR genotyping, identifying four founder lines (19,55,56,58) carrying the *Npc1* transgene. (B) Western analysis of NPC1 expression in diaphragm muscle homogenates from wild-type and four lines (19,55,56,58) of *Dtna*$^{-/-}$-Tg(*Npc1*) mice. Twenty μg of wild-type whole muscle homogenate was loaded versus 5μg for the *Dtna*$^{-/-}$-Tg(*Npc1*) mice. As a loading control, GAPDH was examined on the same blot. WT, wild-type.

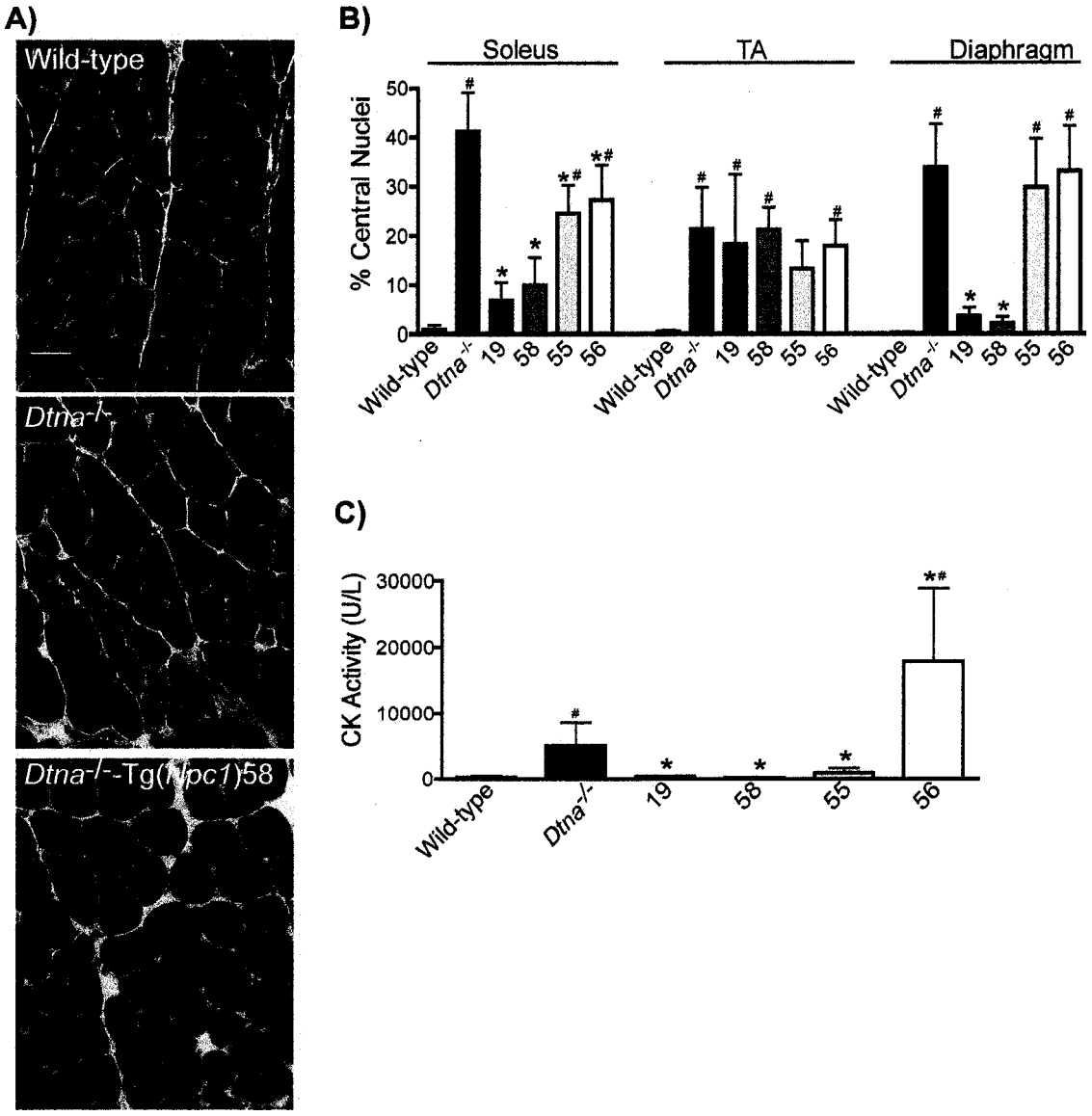

Figure 3.3. Amelioration of dystrophic phenotype by transgenic expression of *Npc1* in *Dtna*$^{-/-}$ mice. (A) H&E staining of solei cross-sections from wild-type, *Dtna*$^{-/-}$, and *Dtna*$^{-/-}$-Tg(*Npc1*) mice (19,58,55,56). Scale bar, 40μm (B) The percentage of soleus, diaphragm, and TA myofibers with central nuclei. n ≥ 5 mice per genotype analyzed. # $p<0.05$ vs. wild-type. * $p<0.05$ vs. *Dtna*$^{-/-}$. (C) Serum creatine kinase levels. n=5, wild-type; n=7, *Dtna*$^{-/-}$; n=5, each transgenic line. # $p<0.05$ vs. wild-type. * $p<0.05$ vs. *Dtna*$^{-/-}$. (A,B,C) Mice were examined at 3 months of age. Data shown are mean ± standard deviation.

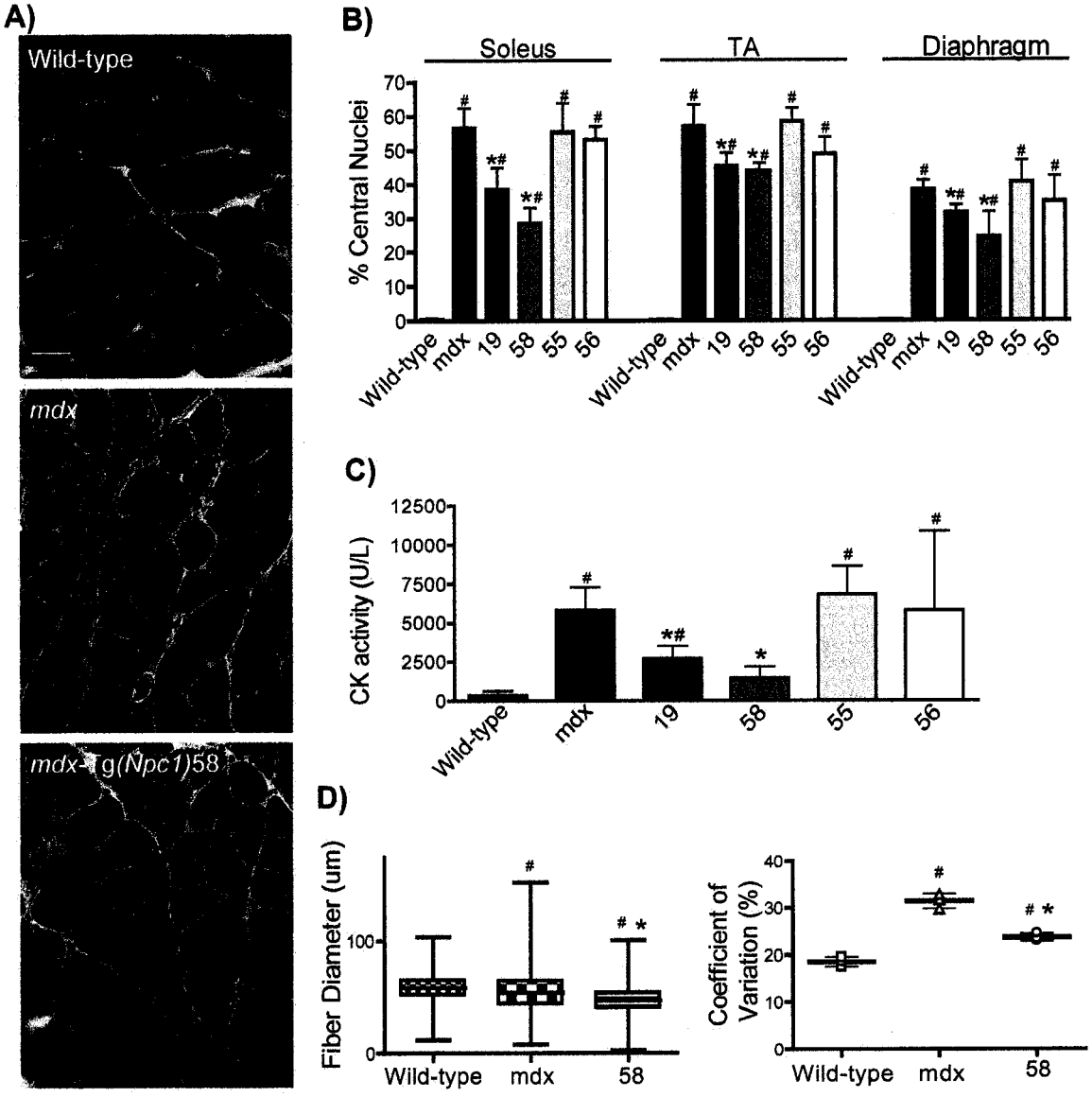

Figure 3.4. Transgenic expression of *Npc1* improves dystrophic phenotype of *mdx* mice. (A) H&E-stained cross-sections of solei from wild-type, *mdx*, and *mdx*-Tg(*Npc1*)58 mice. Scale bar, 40μm. (B) The percentage of soleus, diaphragm, and TA myofibers with central nuclei. n ≥ 5 mice per genotype analyzed. (C) Serum creatine kinase levels. n=5, wild-type, *mdx*-Tg(*Npc1*)19 and *mdx*-Tg(*Npc1*)56; n=6, *mdx* and *mdx*-Tg(*Npc1*)55; n=11, *mdx*-Tg(*Npc1*)58. (D,E) Quantitative analyses of fiber diameter in soleus muscles of wild-type, *mdx*, and *mdx*-Tg(*Npc1*)58 mice, determined using 'Feret's diameter' method. n=3 mice per genotype. (D) Fiber diameters, in which boxes represent the 25th to 75th percentiles and lines represent high and low values. Data was pooled from approximately 500 fibers from each of 3 mice per genotype. (E) Coefficients of variation of soleus fiber diameters. Each data point represents the variance coefficient calculated from each mouse. Lines represent means (dark bar) ± standard deviations (error bars). (A-E) Data obtained from 8-week-old mice. Data shown are mean ± standard deviation. (B-D) #p<0.05 vs. wild-type. *p<0.05 vs. *mdx*. (E) #p<0.05 vs. wild-type. *p<0.05 vs. *mdx*.

CHAPTER 4:

Insertion of transgene rescues phenotype of NPC-null mice

Introduction

Niemann-Pick disease type C (NPC) is an autosomal recessive, neurodegenerative disorder, affecting approximately 1 in 150,000 live births (Patterson et al., 2001). Typically, patients develop symptoms in early childhood and die by late adolescence/ early adulthood. The "classic" phenotype is characterized by ataxia, dystonia, dementia, vertical supranuclear gaze palsy, and hepato- and/or spleno-megaly. The brains of NPC patients show significant neuronal cell loss, particularly of cerebellar Purkinje cells, and neurofibrillary tangles. Biochemically, the disease is characterized by the intracellular accumulation of unesterified cholesterol and gangliosides in the endosomal/lysosomal pathway (Patterson et al., 2001). Interestingly, like other tissues, cells of the CNS also sequester cholesterol; however, the severe demyelination accompanying the disease results in a net loss of cholesterol in the brain (Patterson et al., 2001; Xie et al., 2000). Mutations in the *Npc1* gene cause 95% of NPC disease cases, with the remaining 5% resulting from mutations in the *Npc2* gene. Currently, no treatment for NPC disease exists.

NPC1 is a 1278 amino acid, heavily glycosylated, cholesterol-binding protein (144-184 kDa) with 13 transmembrane domains, a lumenal N-terminus, a cytosolic C-terminus, and a sterol-sensing domain (SSD) (Davies and

Ioannou, 2000; Infante et al., 2007; Ohgami et al., 2004). NPC1 resides in late endosomes and is also found to a smaller extent in the trans-Golgi network, lysosomes, and in caveolin-containing compartments (Garver et al., 2000; Higgins et al., 1999; Neufeld et al., 2004). The precise function of NPC1 is unknown. However, based on studies of cells deficient in functional NPC1, it appears to be involved in the movement of LDL cholesterol from late endosomes to the plasma membrane and endoplasmic reticulum (ER) (Sokol et al., 1988; Wojtanik and Liscum, 2003).

The Balb/c *Npc1*^{m1N} (*Npc*$^{-/-}$) mouse, a murine model for NPC disease has been an invaluable tool in the identification of the *Npc1* gene, in the understanding of NPC1 function, and in the investigation of potential therapies. The *Npc*$^{-/-}$ mouse arose from a spontaneous mutation in *Npc1*, replacing 44 base pairs (bp) of exonic sequence with 24 bp of retroviral sequence, thereby causing a premature truncation of the open reading frame (Loftus et al., 1997). This deletion results in the loss of approximately two-thirds of the NPC1 protein and 11 of its 13 transmembrane domains. Similar to NPC patient tissues, *Npc*$^{-/-}$ mouse tissues accumulate excessive amounts of unesterified cholesterol and sphingomyelin. Additionally, like NPC patients, *Npc*$^{-/-}$ mice display loss of weight, loss of coordination, loss of Purkinje cells, and an early death (80 to 120 days of age) (Morris et al., 1982).

In a previous study, *Npc1* was expressed using a prion-promoter-driven *Npc1* cDNA transgene in order to limit the expression of *Npc1* primarily to CNS-

derived tissues in an effort to determine the extent to which the storage defects of the viscera, versus CNS, contribute to NPC disease (Loftus et al., 2002). Mice from three different transgenic lines maintained wild-type weight for the nine weeks studied and lived beyond 18 months of age. In addition the ataxic gait of the mice was rescued, which the authors attributed to the lack of cerebellar Purkinje cell death or ganglioside accumulation in Purkinje cells in the transgenic mice. In our study, we examined whether or not the loss of *Npc1* in skeletal muscle contributes to the motor abnormalities, wasting, and shortened lifespan associated with this disease, by examining the effects of transgenic expression of *Npc1* in skeletal muscle of $Npc^{-/-}$ mice. While we were unable to show that muscle expression of the *Npc1* transgene, *per se*, ameliorates the disease phenotype, we have identified a line of transgenic mice whose motor dysfunction and lifespan are significantly improved compared to $Npc^{-/-}$ mice.

Materials and Methods

Tg(Npc1) construct

Generation of the Tg(*Npc1*) construct was described previously (Chapter 3). Briefly, the *Npc1* cDNA was cloned into the pBSX-HSAvpA vector (Crawford et al., 2000). The linearized construct was injected into the pronuclei of C57BL/6 x C3H embryos (University of Washington, Department of Comparative Medicine, Transgenic Resources Program). PCR genotyping (5'-

GAT GAA GCA GAC AGT ATT CAG C-3' and 5'-CAG TTC GGC TCG CGG AGC AC-3') identified four founder lines carrying the *Npc1* transgene (Tg(*Npc1*)18, Tg(*Npc1*)55, Tg(*Npc1*)56, Tg(*Npc1*)58. All animal experiments were performed with the approval of the Institutional Animal Care and Use Committee at the University of Washington.

Growth and lifespan evaluation

We obtained breeding pairs of BALB/c mice heterozygous for the Niemann Pick type C1 mutant allele ($Npc1^{m1N}$) (The Jackson Laboratory). Breeding pairs were maintained and bred to produce wild-type (WT) offspring, *Npc1*-null ($Npc1^{-/-}$), and *Npc1*-heterozygous ($Npc1^{+/-}$) mice. PCR genotyping was performed according to suggested Jackson Laboratory protocols (jaxmice.jax.org). Each of the four transgenic lines was bred with $Npc1^{+/-}$ mice. The resulting $Npc1^{+/-}$-Tg(*Npc1*) progeny were subsequently bred with $Npc1^{+/-}$ mice to produce non-transgenic $Npc^{-/-}$ mice and $Npc^{-/-}$ mice hemizygous for the *Npc1* transgene ($Npc1^{-/-}$-Tg(*Npc1*)) and analyzed. Male and female $Npc1^{-/-}$-Tg(*Npc1*) and $Npc1^{-/-}$ offspring were genotyped and weighed, along with WT mice, weekly from four to eleven weeks of age. Three male and female $Npc1^{-/-}$-Tg(*Npc1*)55 and a minimum of four mice from each of the other genotypes were weighed at all time points. Pellets of food and Napa Nectar™ were placed on the cage bottoms at six weeks of age of all $Npc1^{-/-}$ mice and at any point that $Npc1^{-/-}$-Tg(*Npc1*) or WT mice began to display difficulty eating or walking. All

Npc1$^{-/-}$, *Npc1*$^{-/-}$-Tg(*Npc1*)55, *Npc1*$^{-/-}$-Tg(*Npc1*)56, and *Npc1*$^{-/-}$-Tg(*Npc1*)58 mice displayed difficulty eating and walking and were sacrificed between eight to eleven weeks of age. *Npc1*$^{-/-}$-Tg(*Npc1*)19 mice exhibited no weight loss until approximately five months of age and were viable up to approximately six months of age

Quantitative RT-PCR

Quadriceps muscles and brains were dissected from wild-type, *Npc1*$^{-/-}$-Tg(*Npc1*)19, and *Npc1*$^{-/-}$ mice. Total RNA was isolated as described in Chapter 2. Real-Time quantitative RT-PCR was performed with an ABI Prism 7000 Sequence Detection System (Applied Biosystems), using 5ng of RNA, One-Step RT-PCR Master Mix reagents (Applied Biosystems), and *Npc1* primers (5'-AAT GCG GTC TCC TTG GTC AA-3' and 5'-GCT CTC GTT ATA TGG CTG CAG AA-3', Integrated DNA Technologies) and probe (5' 6-FAM d(CAC AGA AAT GCC ACA GCT CAT CAC CAA) BHQ-1 3', Biosearch Technologies, Inc.), or *18S* primers and probe (Applied Biosystems, P/N 4310893E). The relative expression of *Npc1* mRNA was normalized to the amount of *18S* RNA in the same sample. Each sample was run in triplicate. n=1 for each sample.

Membrane enrichment and immunoblots

Tissues were dissected and quick frozen in liquid nitrogen. Membrane preparations and immunoblotting were performed as described in (Garver et al.,

2000) with the following modifications. Following homogenization in 25 mM MES, pH 6.5, 150 mM NaCl, and protease inhibitors, the tissues were centrifuged for 30 min at 100,000 *g*, generating a cytosolic fraction (supernatant) and membrane-enhanced fraction (pellet). Pellets were subsequently homogenized in 25 mM MES, pH 6.5, 150 mM NaCl, 1.0% Triton X-100, and protease inhibitors and centrifuged at 2,000 *g* for 10 min. Sample protein content was determined using the bicinchoninic acid (BCA) protein assay (Pierce). Gels (4-15% Tris-HCl gradient, BioRad) were loaded with 5-20 µg of protein. The separated proteins were transferred to nitrocellulose membrane (Schleicher and Schuell) at 100V for 1-hour. Immunoblots were blocked for 1-hour at room temperature in 10 mM sodium phosphate, pH 7.4, 150 mM NaCl, 0.05% Tween-20, and 4% non-fat dry milk. Immunoblots were incubated at 4° overnight in 10 mM sodium phosphate, pH 7.4, 150 mM NaCl, 0.05% Tween-20, and 1% non-fat dry milk, containing primary antibodies, followed by three 10-min washes. Primary antibody was detected using HRP-conjugated secondary antibody (Jackson ImmunoResearch Laboratories) in 10 mM sodium phosphate, pH 7.4, 150 mM NaCl, 0.05% Tween-20, and 1% non-fat dry milk. Protein bands were detected using SuperSignal® West Femto Maximum Sensitivity Substrate (Pierce) and a CCD camera (AlphaInnotech).

Results

Generation of the transgenic mice.

To investigate whether transgenically expressing *Npc1* in skeletal muscle of *Npc1*$^{-/-}$ mice could alleviate the NPC phenotype, we generated transgenic mouse lines in which *Npc1* was expressed under the control of the human skeletal α-actin promoter. The generation of the Tg*Npc1* construct was described previously (See chapter 3). We obtained four transgenic founder lines (Tg*Npc1*(19), Tg*Npc1*(55), Tg*Npc1*(56), and Tg*Npc1*(58)) (See Chapter 3, figure 3.2a). Expression of NPC1 protein was lowest in the 55 and 56 lines and high in the 19 and 58 lines. We bred each founder line onto the Npc$^{+/-}$ background. The resulting transgenic Npc$^{+/-}$ F1 progeny were then crossed with non-transgenic Npc$^{+/-}$ mice to generate non-transgenic Npc$^{-/-}$ mice and Npc$^{-/-}$ mice hemizygous for the Npc1 transgene (*Npc*$^{-/-}$-Tg(*Npc1*)), which were compared to BALB/c wild-type (WT) mice.

Phenotype of Npc$^{-/-}$-Tg(Npc1) mice

By approximately seven weeks of age, tremors, abnormal gait, and weight loss became evident in the Npc$^{-/-}$ mouse and worsened until their early deaths at approximately 12 weeks of age, consistent with previous reports (Morris et al., 1982). Of the four transgenic lines we evaluated, three (*Npc*$^{-/-}$-Tg(*Npc1*)55, *Npc*$^{-/-}$-Tg(*Npc1*)56, and *Npc*$^{-/-}$-Tg(*Npc1*)58) exhibited these same phenotypic abnormalities. Male and female mice from each of these three

transgenic lines began to show signs of tremor and staggering gait and began rapidly to lose weight in a time and manner indistinguishable from *Npc*$^{-/-}$ mice (Figures 4.1). Lifespans of the transgenic mice from the 55, 56, and 58 lines were similar to those of *Npc*$^{-/-}$ mice as well (Figure 4.2). Surprisingly, however, mice from the *Npc*$^{-/-}$-Tg(*Npc1*)19 line were phenotypically indistinguishable from wild-type mice until approximately five months of age.

Unlike non-transgenic *Npc*$^{-/-}$ mice and transgenic mice from lines 55, 56, and 58, male and female *Npc*$^{-/-}$-Tg(*Npc1*)19 mice consistently gained weight during the seven weeks of measurements, in a manner similar to wild-type mice (Figures 4.1). We did not observe weight loss in the *Npc*$^{-/-}$-Tg(*Npc1*)19 mice until they reached approximately five months of age. This time point coincided with the onset of slight tremors in these mice. In addition to late-onset tremors and weight loss, *Npc*$^{-/-}$-Tg(*Npc1*)19 mice also did not display inward flexing of the hindlimbs until after 20 weeks of age (Figure 4.3). By ten weeks of age, *Npc*$^{-/-}$mice reflexively contracted their hindlimbs, pulling them in toward their bodies, when they were lifted by the tail. Wild-type mice, on the other hand, extended their hindlimbs backward, away from the body, throughout their lives. We did not observe hindlimb contraction in the *Npc*$^{-/-}$-Tg(*Npc1*)19 mice until after 20 weeks of age. Also unlike *Npc*$^{-/-}$ mice, *Npc*$^{-/-}$-Tg(*Npc1*)19 mice maintained a gait pattern similar to wild-type, throughout their lives (data not shown). Lastly, whereas Npc$^{-/-}$ mice lived approximately 12 weeks, *Npc*$^{-/-}$-Tg(*Npc1*)19 mice lived approximately 27 weeks (Figure 4.2).

Expression of transgene mRNA and protein in Npc$^{-/-}$ mice

Under the human skeletal α-actin promoter (HSA), the *Npc1* transgene should only be expressed in skeletal muscle (Brennan and Hardeman, 1993). To verify this and confirm that the improved phenotype of the *Npc*$^{-/-}$-Tg(*Npc1*)19 mice is not due to transgenic expression of *Npc1* in other tissues, we did a preliminary examination (n=1) of *Npc1* transcript levels in wild-type, *Npc*$^{-/-}$-Tg(*Npc1*)19, and Npc$^{-/-}$ mice. By quantitative RT-PCR, we examined transcript levels in brain and quadriceps muscle (Figure 4.4), and by Western blot, we examined NPC1 protein expression in quadriceps, diaphragm, tibialis anterior, brain, and liver, where NPC1 is highly expressed in wild-type mice (Garver et al., 2005) (Figure 4.5). Whereas NPC1 expression was extremely elevated in skeletal muscles of *Npc*$^{-/-}$-Tg(*Npc1*)19 mice compared to wild-type muscles, we found no detectable NPC1 in either of the other *Npc*$^{-/-}$-Tg(*Npc1*)19 tissues.

Discussion

In the present study, we transgenically expressed *Npc1* specifically in skeletal muscles of *Npc1*$^{-/-}$ mice in order to determine if NPC1 loss in skeletal muscle contributes to the NPC disease phenotype. We paid specific attention to motor function, wasting, and lifespan. Of the four resulting transgenic lines, mice from one (*Npc*$^{-/-}$-Tg(*Npc1*)19) of the lines displayed a noticeably improved phenotype compared to the non-transgenic *Npc*$^{-/-}$ mice and the other three lines of transgenic mice. Typically, *Npc*$^{-/-}$ mice display loss of coordination, which is

evident by a staggering gait, tremors, and weight loss, all of which begin at approximately six to seven weeks of age, progressing until an early death of 10-12 weeks of age (Morris et al., 1982). Unlike the *Npc*$^{-/-}$ mice, though, we have found that both male and female mice from the *Npc*$^{-/-}$-Tg(*Npc1*)19 line appeared healthy until about five months of age, at which point they began to slowly lose weight and show signs of tremor. Until that time, however, mice from the *Npc*$^{-/-}$-Tg(*Npc1*)19 line gained or maintained their weights as the healthy, wild-type mice did through eleven weeks of measurements and showed no signs of tremor. Additionally, at no time did the *Npc*$^{-/-}$-Tg(*Npc1*)19 mice display an abnormal gait. Although the lifespans of *Npc*$^{-/-}$-Tg(*Npc1*)19 mice were not corrected to those of wild-types, *Npc*$^{-/-}$-Tg(*Npc1*)19 mice lived at least to six months of age, more than 100% longer than *Npc*$^{-/-}$ mice.

We could not corroborate the improved phenotype we saw in the *Npc*$^{-/-}$-Tg(*Npc1*)19 line with any of the other three lines that were made. One possible explanation for the discrepancy might be that NPC1 protein is expressed at different levels in the *Npc*$^{-/-}$-Tg(*Npc1*)19 line than in the other lines. Based on Western blot analyses, however, the expression levels of NPC1 appear to be similar between the *Npc*$^{-/-}$-Tg(*Npc1*)19 and *Npc*$^{-/-}$-Tg(*Npc1*)58 mouse muscles (Chapter 3, Figure 3.2b); therefore, we would expect a similar phenotype at least with the *Npc*$^{-/-}$-Tg(*Npc1*)58 line, which we did not observe. Another possibility is that NPC1 expression is not confined to skeletal muscle, contrary to previous reports from studies using the HSA promoter (Brennan and

Hardeman, 1993) A reduction of neurodegeneration as a result of NPC1 expression in the *Npc*$^{-/-}$ brain, for example, could explain the improvement of the disease, as has previously been shown using prion-promoter-driven Npc1 expression (Loftus et al., 2002). However, we have examined Npc1 transcript expression and NPC1 protein expression in various skeletal muscles, brain, and liver of *Npc*$^{-/-}$-Tg(*Npc1*)19 mice and find NPC1 overexpression only in skeletal muscle. Because the *Npc1* transgene randomly integrated into the *Npc*$^{-/-}$ mouse genome, a third possibility is that random integration of the *Npc1* transgene affected the expression of a completely unrelated gene. This gene, which for example could be a longevity gene or even a cholesterol lowering gene, might therefore be responsible for the change in phenotype of the *Npc*$^{-/-}$-Tg(*Npc1*)19 mice.

The random integration of transgenes into genomes has been both intentionally (gene trapping) and unintentionally used for the identification of novel genes and gene function. Large-scale gene trapping studies have been used, for example, in the identification of survival genes (Wempe et al., 2001) and cancer-causing genes (Yamamura and Araki, 2007). Recently, a study investigated the molecular cause of a neuromotor disease identified in mice carrying a transgene encoding the SV40 T antigen (Rodriguez-Santiago et al., 2007). The authors found that the transgene had inserted into the promoter of the *Trpc3* gene. The insertion caused transcription of *Trpc3* to be blocked, which the authors postulated affected the development of the CNS, causing the

neurological phenotype of the mice. The defective gene responsible for the phenotype of the reeler mouse was also discovered by the fortuitous, random insertion of a transgene (Miao et al., 1994). In an attempt to examine the function of the *c-fos* gene, the authors produced transgenic mouse lines, expressing a mutated *c-fos* gene. Of the three homozygous transgenic lines generated that expressed *c-fos*, one displayed a severe locomotor defect similar to that of the *reeler* mouse. Genetic analysis determined that the *c-fos* transgene had inserted into the *reeler* locus, thereby causing the reeler phenotype. The *c-fos* transgene then could be used to identify and isolate the *reeler* gene.

In this study we show that the transgenic expression of *Npc1* exclusively in skeletal muscle of *Npc*$^{-/-}$ mice cannot alleviate the phenotype of the *Npc*$^{-/-}$ mouse. However, we did find improvements in one transgenic mouse line, which appear unrelated to the expression of the transgene. We speculate that these improvements are due to the insertion of the *Npc1* transgene into a locus, e.g. promoter sequence, that alters the expression of the gene(s) that is/are responsible for the improved health of the *Npc*$^{-/-}$-Tg(*Npc1)* mouse. We will therefore be able to use this transgene in future studies as a probe to identify the responsible gene(s).

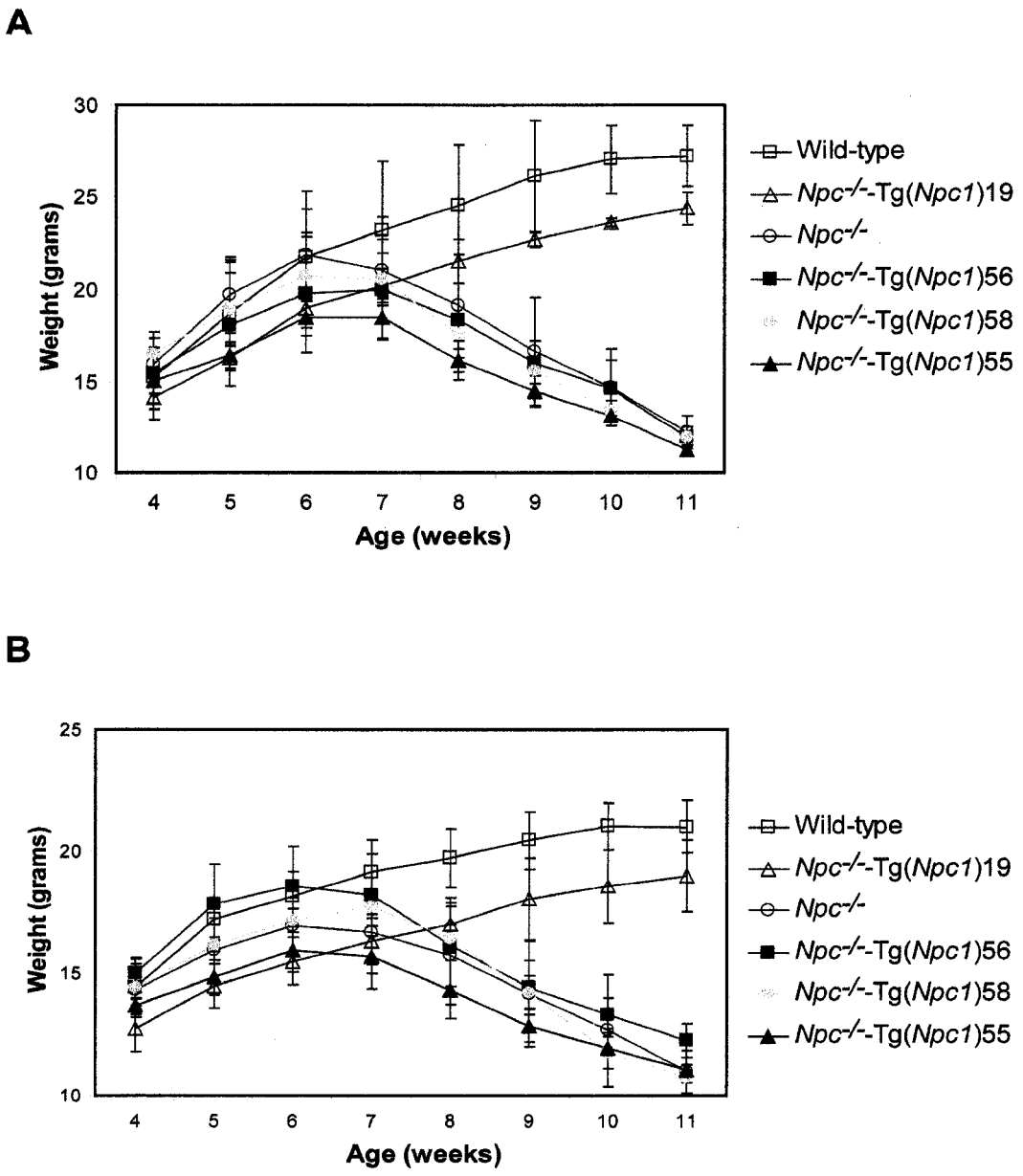

Figure 4.1: *Npc*$^{-/-}$-Tg(*Npc1*)19 mice maintain weight gain similar to wild-type mice. Neither male (A) nor female (B) *Npc*$^{-/-}$-Tg(*Npc1*)19 mice exhibit the severe weight loss that typically occurs in *Npc*$^{-/-}$ mice after seven weeks of age. Each of the other 3 transgenic lines (*Npc*$^{-/-}$-Tg(*Npc1*)55, *Npc*$^{-/-}$-Tg(*Npc1*)56, *Npc*$^{-/-}$-Tg(*Npc1*)58) lost weight in a manner similar to the *Npc*$^{-/-}$ mice. Means ± s.d. are shown.

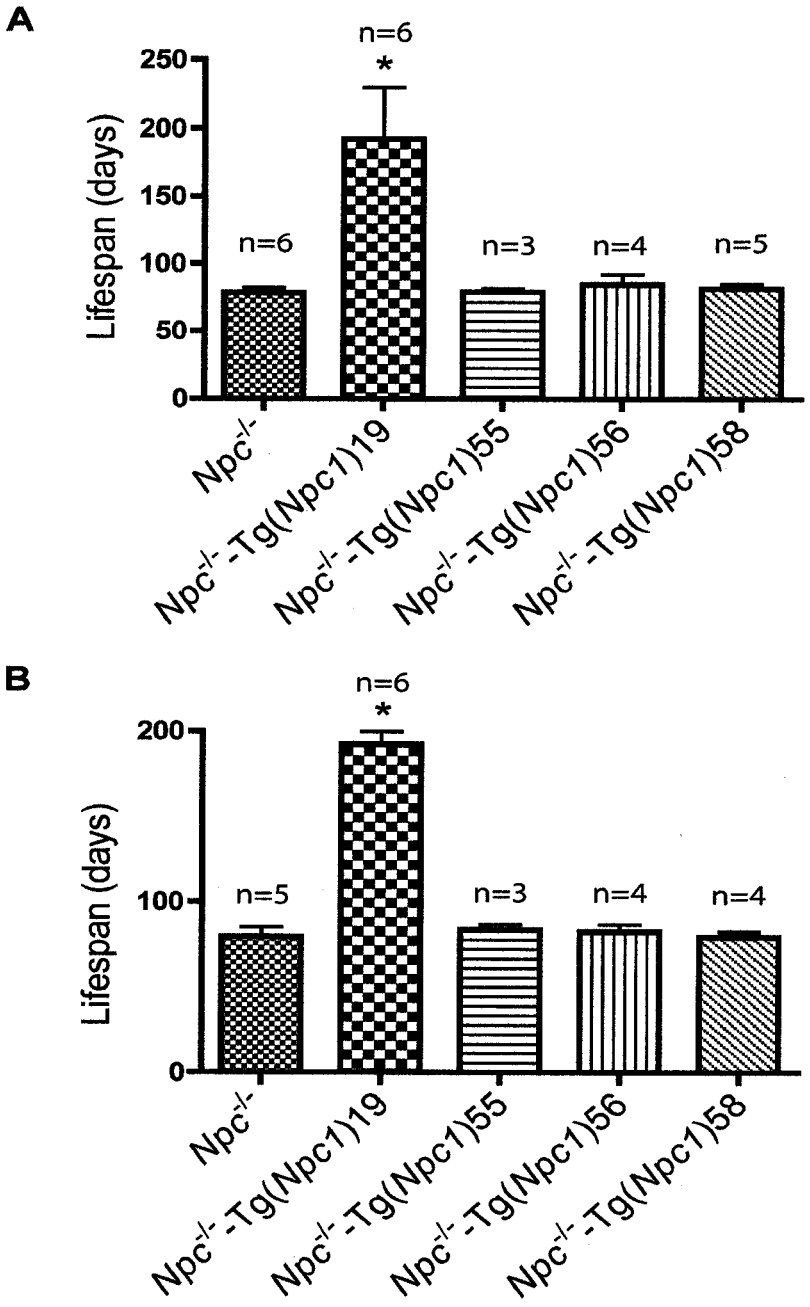

Figure 4.2: Increased lifespans of male (A) and female (B) *Npc*$^{-/-}$-Tg(*Npc1*)19 mice. *Npc*$^{-/-}$-Tg(*Npc1*)19 mice live significantly longer that *Npc*$^{-/-}$ mice and mice from the other 3 transgenic lines. Although *Npc*$^{-/-}$-Tg(*Npc1*)19 mice do not live wild-type lifespans, at no point do they exhibit the severe tremors and ambulatory difficulties of *Npc*$^{-/-}$ mice. Means ± s.d. are shown. *p<0.001, vs. *Npc*$^{-/-}$.

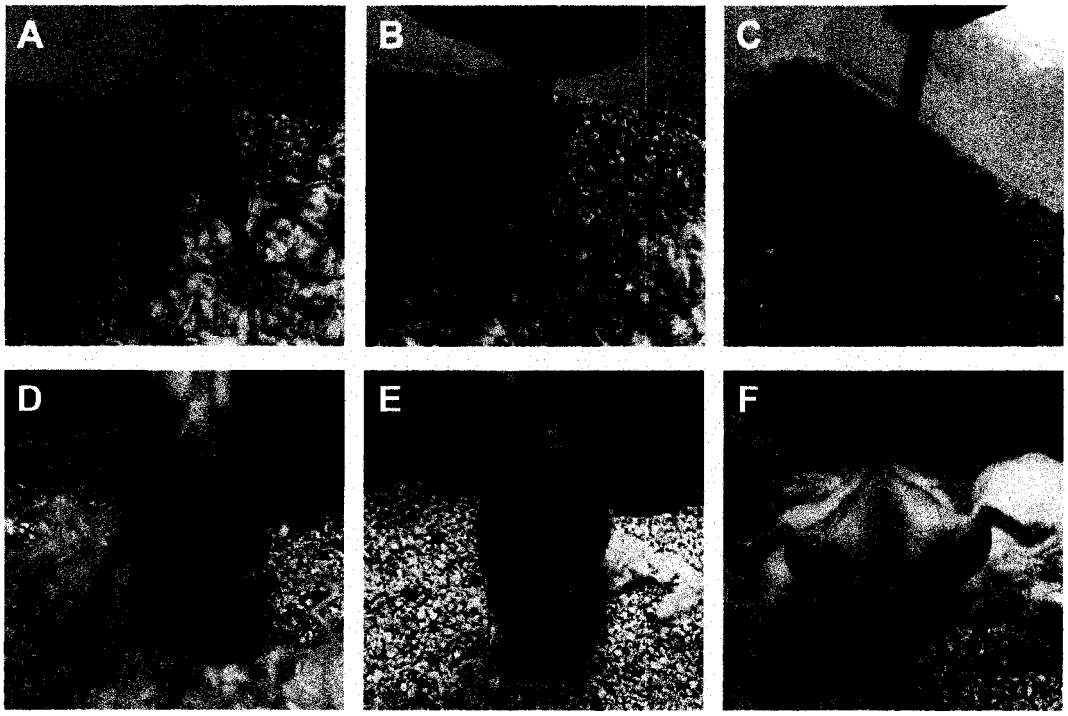

Figure 4.3: Comparison of wild-type, *Npc*$^{-/-}$-Tg(*Npc1*)19, and *Npc*$^{-/-}$ mouse hindlimb responses to being lifted by the tail. (A) 10-week old wild-type showing extension of hind-limbs. (B) 10-week old *Npc*$^{-/-}$ showing contractures of hindlimbs when lifted by the tail. *Npc*$^{-/-}$-Tg(*Npc1*)19 do not demonstrate joint contractures, but are instead able to extend hindlimbs at (C) 10-weeks of age and still at (D) 20 weeks of age. (E) By 29 weeks of age, *Npc*$^{-/-}$-Tg(*Npc1*)19 mice demonstrate severe contractions of the hindlimbs in response to tail-lifting. (F) Demonstration of hindlimb extension in 29-week old wild-type mouse.

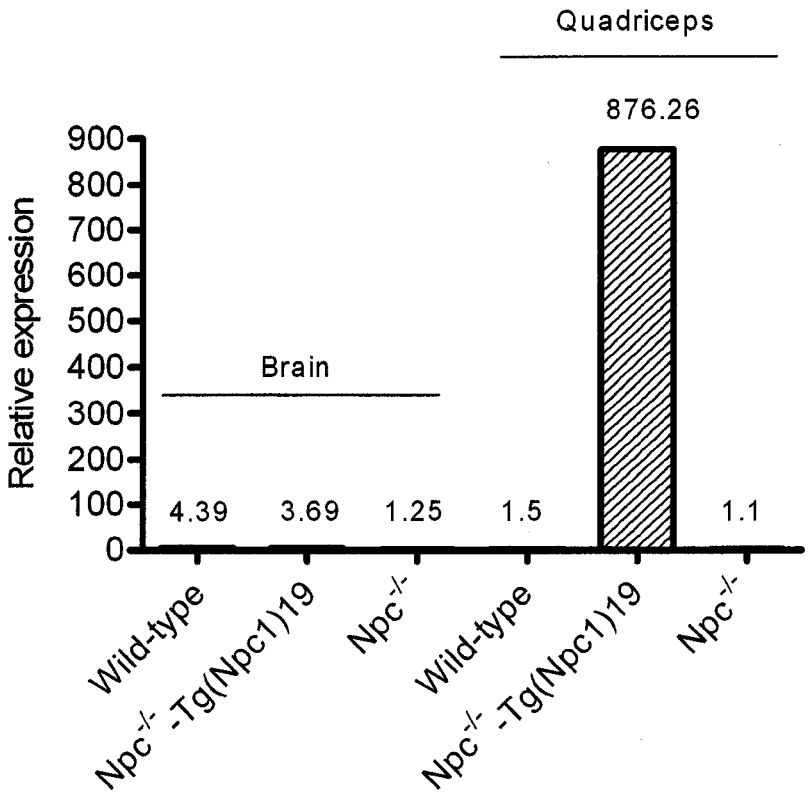

Figure 4.4: Transcript levels in quadriceps muscles and brains from wild-type, *Npc*$^{-/-}$-Tg(*Npc1*)19, and *Npc*$^{-/-}$ mice. Expression levels were examined using real-time quantitative RT-PCR. The relative expression of *Npc1* mRNA was normalized to the amount of *18S* RNA in the same sample. Each sample was run in triplicate. n=1 for each sample.

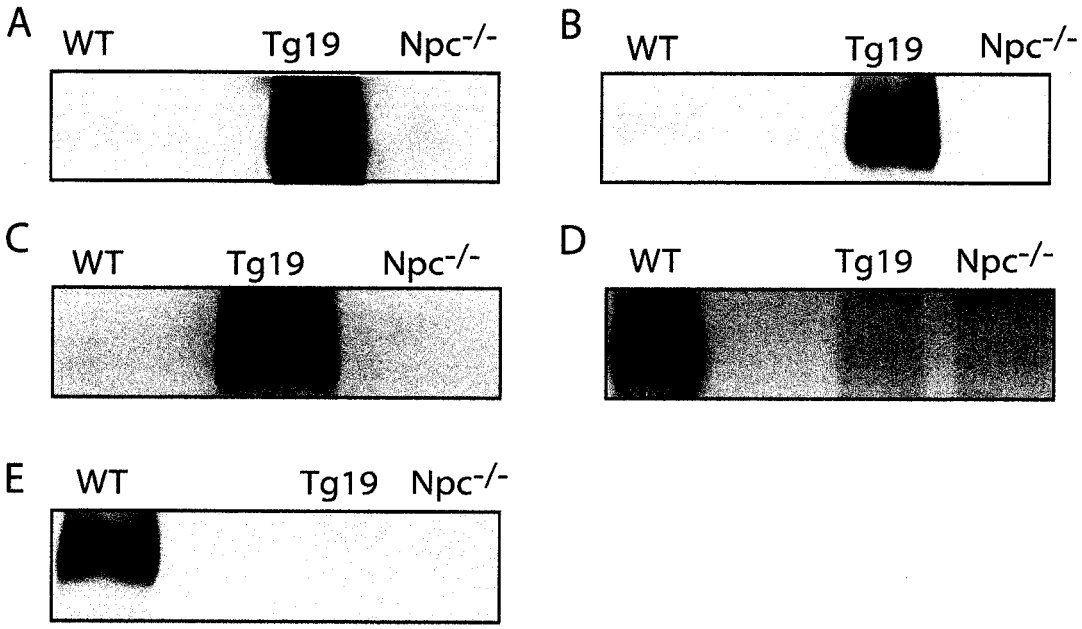

Figure 4.5: Expression of transgenic NPC1 is limited to skeletal muscle. NPC1 was highly expressed in A) quadriceps, B) diaphragm, and C) tibialis anterior muscles of *Npc*$^{-/-}$-Tg(*Npc1*)19 mice. Neither the D) brain nor E) liver had detectable levels of NPC1 in *Npc*$^{-/-}$-Tg(*Npc1*)19 mice. WT, wild-type; Tg19, *Npc*$^{-/-}$-Tg(*Npc1*)19 mice. n=1 for each sample. 25μg protein was loaded for each quadriceps, diaphragm, and tibialis anterior muscle; 50μg protein was loaded for each liver sample; and 100μg protein was loaded for each brain sample.

CHAPTER 5:

Conclusions and future directions

Development of a therapy to treat muscular dystrophy is clearly the ultimate goal of muscular dystrophy research, and in the last several years, significant advances have been made particularly in the field of gene therapy. These studies have largely focused on restoring functional dystrophin to the sarcolemma. However, because of difficulties associated with delivering full-length dystrophin to muscle, owing to the large size of dystrophin, research has been aimed largely at introducing a functional short form of dystrophin to muscle. The use of recombinant adeno-associated viral (AAV) vectors and antisense oligonucleotides (AO) have proven successful in this vein, but several issues associated with these methods must still be addressed, including their long-term efficacy and safety, how to avoid an immune response, and how to effectively reach all the muscles. While these approaches may soon prove beneficial in alleviating the severity of Duchenne muscular dystrophy by converting the patient to a Becker muscular dystrophy patient, ideally one would ultimately hope to completely restore skeletal muscle to normal. Because restoring full-length dystrophin does not appear feasible, a more comprehensive understanding of the pathogenic mechanisms resulting in the degenerative process of muscular dystrophy may yield alternate therapeutic strategies and may even aid in treatments of dystrophies associated with losses of other DPC

or DPC-associated proteins, such as the sarcoglycans or caveolin-3, respectively.

In Chapter 2, I examined gene expression changes of quadriceps muscles from α-dystrobrevin-null mice, compared to wild-type, in order to identify genes whose misregulation results in muscular dystrophy. Gene expression studies have previously been performed on more severely dystrophic muscle, such as from DMD patients and *mdx* mice. Those studies have yielded hundreds of transcripts whose expression levels were altered; however, a large number of those transcripts encode proteins involved in regeneration and inflammation. We therefore chose to examine the less severely affected α-dystrobrevin-null muscle at six weeks of age in order to minimize the influence of transcriptional responses associated with inflammation and muscle repair.

In addition to the α–dystrobrevin-null mouse, we also examined expression changes in the α–syntrophin-null mouse. This was done for two reasons. First, like α–dystrobrevin-null mice, α–syntrophin-null mice have neuromuscular junction defects. Therefore, a comparison of transcriptional changes in these two mice may identify molecular changes occurring downstream of the loss of α–dystrobrevin and α–syntrophin, culminating in the abnormalities of the NMJ. Second, because α–dystrobrevin-null mice have NMJ defects in addition to muscular dystrophy, I hypothesized that the expression changes that the two mice had in common were responsible for the

NMJ defects. Therefore, I could narrow the list of candidate genes involved in muscular dystrophy by eliminating those α–dystrobrevin-null expression changes that are in common with the α–syntrophin-null changes. Unfortunately a comparison of α–syntrophin-null and α–dystrobrevin-null transcriptional alterations yielded only a small list of changes in common. An explanation for this small list likely resides in the fact that we examined transcriptional changes from the whole muscle despite our interest only in the changes at the NMJ, which makes up just a small percentage of muscle. Transcriptional changes at the NMJ may have been obscured by expression of those same transcripts in other parts of the muscle. Enriching for synaptic RNA by microdissecting NMJs, as recently described by Kishi et al. (Kishi et al., 2005), would eliminate the influence of non-synaptic transcripts and likely yield a greater number of changes and more focused changes than we identified here.

An obvious complication of large-scale gene expression analyses is determining which transcriptional change(s) to explore in greater detail. Although other gene expression analyses often focus on the magnitude of the fold-change, we instead chose to base our selection on the level of statistical significance. Our attention was therefore directed to Niemann Pick C1 (NPC1), which was the most statistically significant change in the α–dystrobrevin-null quadriceps. We did not observe a significant change of *Npc1* in the more severely dystrophic diaphragm, and previous studies on *mdx* and DMD muscle also have not reported significant changes in *Npc1*. However, as *Npc1* is

found in skeletal muscle as well as non-skeletal muscle cells, including fibroblasts and macrophages, we speculate that decreases in *Npc1* in more dystrophic muscle may be eclipsed by the influx of cells involved in inflammation and regeneration. In fact, as shown in Chapter 3, not only were the α–dystrobrevin-null quadriceps and diaphragm muscles significantly improved by transgenic overexpression of NPC1, but so were all three muscle examined in the transgenic mdx mice, suggesting that NPC1 deficiency may contribute to the dystrophy in all these muscles.

Our generation of dystrophic mice expressing transgenic NPC1 yielded four important observations. First, introducing *Npc1* into dystrophic mice can ameliorate the phenotype as observed not only from examination of a few individual muscles but also from measurements of creatine kinase levels, which is a body-wide assessment of muscle degeneration. Second, we generated four transgenic lines and found that the two lines that greatly overexpressed NPC1 had the most beneficial effect at ameliorating the dystrophy of the α–dystrobrevin-null and *mdx* mice, indicating that the response to transgenic NPC1 is dose-dependent. Third, the response by muscle appears to be fiber-type specific, as we observed either mild improvements (*mdx* mouse) or no improvements (α-dystrobrevin-null) of the tibialis anterior (TA), a predominantly fast-twitch muscle. Fourth, we observed significant improvement to the *mdx* diaphragm, which most closely mimics DMD muscle. Therapies that attenuate

the degeneration of respiratory muscles are critical as respiratory failure is a leading cause of death in DMD patients.

Our results clearly suggest that transgenic expression of NPC1 has beneficial effects on dystrophic muscle and are suggestive of a mechanistic role for NPC1 in causing muscular dystrophy. Future studies will need to address several unanswered questions, however. First, why does the loss of α-dystrobrevin cause decreased expression of NPC1? Second, does the reduction of NPC1 actually contribute to muscle degeneration, and if so, how? Third, how does the overexpression of NPC1 ameliorate muscular dystrophy? Answering these questions will necessitate more information regarding NPC1-interacting proteins, NPC1 function, and regulators of *Npc1* expression. Current knowledge already provides intriguing connections between NPC1 and DMD. Elevated caveolin levels are associated with *mdx* and DMD muscle, overexpression of caveolin induces a DMD-like dystrophy in mice, and reduced caveolin levels cause limb-girdle muscular dystrophy 1C (Galbiati et al., 2000; Minetti et al., 1998; Repetto et al., 1999; Vaghy et al., 1998). The tight regulation of caveolin thus appears necessary to prevent muscle degeneration. Interestingly, NPC1- heterozygous cells, which have NPC1 levels approximating those that we found in α-dystrobrevin-null muscle, contain elevated levels of caveolin in caveolae (Garver et al., 2002). An intriguing explanation for NPC1's role in muscular dystrophy may then be tied to its relationship with caveolin. Perhaps the loss of α-dystrobrevin and/or dystrophin

causes the reduction of NPC1, which would result in the upregulation of caveolin, thereby contributing to muscle degeneration. By overexpressing NPC1, we may be reducing caveolin levels toward wild-type levels, thus decreasing the phenotypic consequence of elevated caveolin levels. Future experiments should examine caveolin levels in α-dystrobrevin-null muscle and the transgenic α-dystrobrevin-null and mdx muscles.

Reports have also shown that cholesterol, which is an important component of caveolae and plasma membranes is reduced in caveolae of NPC1- heterozygous cells (Garver et al., 2002), suggesting that it may also be reduced in dystrophic muscle. Decreased cholesterol in caveolae could have significant detrimental effects on the signaling function of caveolae or could compromise the ability of the plasma membrane to repair itself, either of which could have implications in muscle degeneration. If cholesterol is indeed reduced at the plasma membrane and/or caveolae of dystrophic muscle, then overexpressing NPC1, which traffics cholesterol to the plasma membrane, may effectively restore cholesterol at these sites. In this case, sarcolemmae would still incur damage due to the disruption of the DPC, however, the cell would maintain its ability to repair itself. Cholesterol levels should thus be examined in caveolae of both the α-dystrobrevin-null and *mdx* mice as well as the transgenic mice.

In our studies we found that transgenic overexpression of NPC1 appears to improve central nucleation, serum creatine kinase levels, and fiber size

variability. We do not yet know, however, if muscle function is improved. Thus, before examining the mechanism of NPC1 action, future studies should first determine if physiological aspects of *mdx* muscle, such as decreased force producing capacity and increased susceptibility to contraction-induced injury, are improved. Additionally, as transgenically expressing NPC1 in humans is obviously not feasible, future studies will also need to examine alternative modes of NPC1 delivery to dystrophic muscle, e.g. AAV-mediated delivery. As opposed to using transgenic mice, using AAV-mediated delivery will also allow for quicker analyses of the effects of NPC1 overexpression on other forms of muscular dystrophy, like the limb-girdle muscular dystrophies. Alternatively, further investigation into the connection between NPC1 and DMD could yield alternative targets suitable for more conventional pharmaceutical intervention.

Mice lacking NPC1 do not display a dystrophic phenotype; however, they are a model for Niemann-Pick disease, a severe neurodegenerative disease in humans, which results in premature death. In Chapter 4, we examined whether transgenically expressing NPC1 in skeletal muscle could alleviate the NPC phenotype in the NPC-null mouse. Indeed, we did observe that transgenic NPC-null mice not only maintained weight better, but also lived significantly longer than NPC-null mice. However, as these improvements only occurred in one of the four transgenic lines, we speculate that overexpression of NPC1 in muscle is not the basis for the improvements. One possible explanation instead could be that expression of *Npc1* under control of the human skeletal α-actin

promoter is occurring in tissues other than just skeletal muscle. Preliminary data from brain and liver, however, indicate that this is not the case. As we looked at tissues from only one mouse, a greater sample size will, of course, need to be examined as will different tissues. An intriguing and more likely explanation for the improved phenotype is that the integration of the transgene fortuitously altered the expression of an unrelated gene(s), thereby improving the phenotype. The identification of the insertion site could therefore provide a target for treatment of the NPC disease.

I have provided data in this thesis suggesting a mechanistic role for NPC1 in the pathogenesis of muscular dystrophy. Mutations in NPC1 are known to cause the neurodegenerative disease, NPC, but to my knowledge, the function of NPC1 has not previously been studied in skeletal muscle. The results presented herein are therefore the first to link a neurological disease, characterized by impaired cholesterol trafficking, to muscular dystrophy and may identify a new therapeutic target for muscular dystrophy. Future studies based on our investigations with our transgenic NPC-null mouse may also be able to isolate a gene that can ameliorate NPC disease.

REFERENCES:

Aartsma-Rus, A., M. Bremmer-Bout, A.A. Janson, J.T. den Dunnen, G.J. van Ommen, and J.C. van Deutekom. 2002. Targeted exon skipping as a potential gene correction therapy for Duchenne muscular dystrophy. *Neuromuscul Disord.* 12 Suppl 1:S71-7.

Aartsma-Rus, A., A.A. Janson, G.J. van Ommen, and J.C. van Deutekom. 2007. Antisense-induced exon skipping for duplications in Duchenne muscular dystrophy. *BMC Med Genet.* 8:43.

Adams, M.E., M.H. Butler, T.M. Dwyer, M.F. Peters, A.A. Murnane, and S.C. Froehner. 1993. Two forms of mouse syntrophin, a 58 kd dystrophin-associated protein, differ in primary structure and tissue distribution. *Neuron.* 11:531-40.

Adams, M.E., N. Kramarcy, T. Fukuda, A.G. Engel, R. Sealock, and S.C. Froehner. 2004. Structural abnormalities at neuromuscular synapses lacking multiple syntrophin isoforms. *J Neurosci.* 24:10302-9.

Adams, M.E., N. Kramarcy, S.P. Krall, S.G. Rossi, R.L. Rotundo, R. Sealock, and S.C. Froehner. 2000. Absence of alpha-syntrophin leads to structurally aberrant neuromuscular synapses deficient in utrophin. *J Cell Biol.* 150:1385-98.

Adams, S.H., C. Chui, S.L. Schilbach, X.X. Yu, A.D. Goddard, J.C. Grimaldi, J. Lee, P. Dowd, S. Colman, and D.A. Lewin. 2001. BFIT, a unique acyl-CoA thioesterase induced in thermogenic brown adipose tissue: cloning, organization of the human gene and assessment of a potential link to obesity. *Biochem J.* 360:135-42.

Ahn, A.H., C.A. Freener, E. Gussoni, M. Yoshida, E. Ozawa, and L.M. Kunkel. 1996. The three human syntrophin genes are expressed in diverse tissues, have distinct chromosomal locations, and each bind to dystrophin and its relatives. *J. Biol. Chem.* 271:2724-30.

Ahn, A.H., and L.M. Kunkel. 1995. Syntrophin binds to an alternatively spliced exon of dystrophin. *J. Cell Biol.* 128:363-371.

Albrecht, D.E., and S.C. Froehner. 2002. Syntrophins and dystrobrevins: defining the dystrophin scaffold at synapses. *Neurosignals.* 11:123-9.

Alessi, A., A.D. Bragg, J.M. Percival, J. Yoo, D.E. Albrecht, S.C. Froehner, and M.E. Adams. 2006. gamma-Syntrophin scaffolding is spatially and functionally distinct from that of the alpha/beta syntrophins. *Exp Cell Res.* 312:3084-95.

Ambrose, H.E., D.J. Blake, R.A. Nawrotzki, and K.E. Davies. 1997. Genomic organization of the mouse dystrobrevin gene: comparative analysis fo the dystrophin gene. *Genomics*. 39:359-369.

Bakay, M., P. Zhao, J. Chen, and E.P. Hoffman. 2002. A web-accessible complete transcriptome of normal human and DMD muscle. *Neuromuscul Disord*. 12 Suppl 1:S125-41.

Bar, S., E. Barnea, Z. Levy, S. Neuman, D. Yaffe, and U. Nudel. 1990. A novel product of the Duchenne muscular dystrophy gene which greatly differs from the known isoforms in its structure and tissue distribution. *Biochem J*. 272:557-60.

Beggs, A.H., M. Koenig, F.M. Boyce, and L.M. Kunkel. 1990. Detection of 98% of DMD/BMD gene deletions by polymerase chain reaction. *Hum Genet*. 86:45-8.

Bewick, G.S., L.V.B. Nicholson, C. Young, E. O'Donnell, and C.R. Slater. 1992. Different distributions of dystrophin and related proteins at nerve-muscle junctions. *NeuroReport*. 3:857-860.

Blake, D.J., R. Nawrotzki, M.F. Peters, S.C. Froehner, and K.E. Davies. 1996. Isoform diversity of dystrobrevin, the murine 87-kDa postsynaptic protein. *J. Biol. Chem.* 271:7802-10.

Blake, D.J., A. Weir, S.E. Newey, and K.E. Davies. 2002. Function and genetics of dystrophin and dystrophin-related proteins in muscle. *Physiol Rev*. 82:291-329.

Bloch, R.J., and H. Gonzalez-Serratos. 2003. Lateral force transmission across costameres in skeletal muscle. *Exerc Sport Sci Rev*. 31:73-8.

Bowe, M.A., D.B. Mendis, and J.R. Fallon. 2000. The small leucine-rich repeat proteoglycan biglycan binds to alpha-dystroglycan and is upregulated in dystrophic muscle. *J Cell Biol*. 148:801-10.

Brenman, J.E., D.S. Chao, S.H. Gee, A.W. McGee, S.E. Craven, D.R. Santillano, Z. Wu, F. Huang, H. Xia, M.F. Peters, S.C. Froehner, and D.S. Bredt. 1996. Interaction of nitric oxide synthase with the postsynaptic density protein PSD-95 and alpha1-syntrophin mediated by PDZ domains. *Cell.* 84:757-67.

Brenman, J.E., D.S. Chao, H. Xia, K. Aldape, and D.S. Bredt. 1995. Nitric oxide synthase complexed with dystrophin and absent from skeletal muscle sarcolemma in Duchenne muscular dystrophy. *Cell.* 82:743-52.

Brennan, K.J., and E.C. Hardeman. 1993. Quantitative analysis of the human alpha-skeletal actin gene in transgenic mice. *J Biol Chem.* 268:719-25.

Briguet, A., I. Courdier-Fruh, M. Foster, T. Meier, and J.P. Magyar. 2004. Histological parameters for the quantitative assessment of muscular dystrophy in the mdx-mouse. *Neuromuscul Disord.* 14:675-82.

Brown, R.H., Jr. 1997. Dystrophin-associated proteins and the muscular dystrophies. *Annu Rev Med.* 48:457-66.

Buechler, C., A. Boettcher, S.M. Bared, M.C. Probst, and G. Schmitz. 2002. The carboxyterminus of the ATP-binding cassette transporter A1 interacts with a beta2-syntrophin/utrophin complex. *Biochem Biophys Res Commun.* 293:759-65.

Bulfield, G., W.G. Siller, P.A. Wight, and K.J. Moore. 1984. X chromosome-linked muscular dystrophy (mdx) in the mouse. *Proc Natl Acad Sci U S A.* 81:1189-92.

Bushby, K.M. 1999. The limb-girdle muscular dystrophies-multiple genes, multiple mechanisms. *Hum Mol Genet.* 8:1875-82.

Butler, M.H., K. Douville, A.A. Murnane, N.R. Kramarcy, J.B. Cohen, R. Sealock, and S.C. Froehner. 1992. Association of the M_r 58,000 postsynaptic protein of electric tissue with Torpedo dystrophin and the M_r 87,000 postsynaptic protein. *J. Biol. Chem.* 267:6213-6218.

Byers, T.J., L.M. Kunkel, and S.C. Watkins. 1991. The subcellular distribution of dystrophin in mouse skeletal, cardiac, and smooth-muscle. *J. Cell Biol.* 115:411-421.

Byers, T.J., H.G. Lidov, and L.M. Kunkel. 1993. An alternative dystrophin transcript specific to peripheral nerve. *Nat Genet.* 4:77-81.

Campbell, K.P., and S.D. Kahl. 1989. Association of dystrophin and an integral membrane glycoprotein. *Nature*. 338:259-62.

Carr, C., G.D. Fischbach, and J.B. Cohen. 1989. A novel Mr 87,000 protein associated with acetylcholine receptors in Torpedo electric organ and vertebrate skeletal muscle. *J. Cell Biol.* 109:1753-1764.

Ceccarini, M., M. Grasso, C. Veroni, G. Gambara, B. Artegiani, G. Macchia, C. Ramoni, P. Torreri, C. Mallozzi, T.C. Petrucci, and P. Macioce. 2007. Association of dystrobrevin and regulatory subunit of protein kinase A: a new role for dystrobrevin as a scaffold for signaling proteins. *J Mol Biol.* 371:1174-87.

Chamberlain, J.S., R.A. Gibbs, J.E. Ranier, P.N. Nguyen, and C.T. Caskey. 1988. Deletion screening of the Duchenne muscular dystrophy locus via multiplex DNA amplification. *Nucleic Acids Res.* 16:11141-56.

Chao, D.S., F. Silvagno, and D.S. Bredt. 1998. Muscular dystrophy in mdx mice despite lack of neuronal nitric oxide synthase. *J Neurochem.* 71:784-9.

Chen, Z., C. Hague, R.A. Hall, and K.P. Minneman. 2006. Syntrophins regulate alpha1D-adrenergic receptors through a PDZ domain-mediated interaction. *J Biol Chem.* 281:12414-20.

Choi, H.Y., B. Karten, T. Chan, J.E. Vance, W.L. Greer, R.A. Heidenreich, W.S. Garver, and G.A. Francis. 2003. Impaired ABCA1-dependent lipid efflux and hypoalphalipoproteinemia in human Niemann-Pick type C disease. *J Biol Chem.* 278:32569-77.

Chung, W., and J.T. Campanelli. 1999. WW and EF hand domains of dystrophin-family proteins mediate dystroglycan binding. *Mol Cell Biol Res Commun.* 2:162-71.

Coffey, A.J., R.G. Roberts, E.D. Green, C.G. Cole, R. Butler, R. Anand, F. Giannelli, and D.R. Bentley. 1992. Construction of a 2.6-Mb contig in yeast artificial chromosomes spanning the human dystrophin gene using an STS-based approach. *Genomics.* 12:474-84.

Collet, C., B. Allard, Y. Tourneur, and V. Jacquemond. 1999. Intracellular calcium signals measured with indo-1 in isolated skeletal muscle fibres from control and mdx mice. *J Physiol.* 520 Pt 2:417-29.

Connors, N.C., M.E. Adams, S.C. Froehner, and P. Kofuji. 2004. The potassium channel Kir4.1 associates with the dystrophin glycoprotein complex via alpha-syntrophin in glia. *J Biol Chem.* 279:28387-28392.

Cox, G.A., N.M. Cole, K. Matsumura, S.F. Phelps, S.D. Hauschka, K.P. Campbell, J.A. Faulkner, and J.S. Chamberlain. 1993. Overexpression of dystrophin in transgenic mdx mice eliminates dystrophic symptoms without toxicity. *Nature.* 364:725-729.

Crawford, G.E., J.A. Faulkner, R.H. Crosbie, K.P. Campbell, S.C. Froehner, and J.S. Chamberlain. 2000. Assembly of the dystrophin-associated protein complex does not require the dystrophin COOH-terminal domain. *J Cell Biol.* 150:1399-410.

Crosbie, R.H. 2001. NO vascular control in Duchenne muscular dystrophy. *Nat Med.* 7:27-9.

Crosbie, R.H., J. Heighway, D.P. Venzke, J.C. Lee, and K.P. Campbell. 1997. Sarcospan, the 25-kDa transmembrane component of the dystrophin-glycoprotein complex. *J. Biol. Chem.* 272:31221-31224.

D'Souza, V.N., T.M. Nguyen, G.E. Morris, W. Karges, D.A. Pillers, and P.N. Ray. 1995. A novel dystrophin isoform is required for normal retinal electrophysiology. *Hum Mol Genet.* 4:837-42.

Davies, J.P., and Y.A. Ioannou. 2000. Topological analysis of Niemann-Pick C1 protein reveals that the membrane orientation of the putative sterol-sensing domain is identical to those of 3-hydroxy-3-methylglutaryl-CoA reductase and sterol regulatory element binding protein cleavage-activating protein. *J Biol Chem.* 275:24367-74.

Deconinck, A.E., A.C. Potter, J.M. Tinsley, S.J. Wood, R. Vater, C. Young, L. Metzinger, A. Vincent, C.R. Slater, and K.E. Davies. 1997. Postsynaptic abnormalities at the neuromuscular junctions of utrophin-deficient mice. *J. Cell Biol.* 136:883-894.

Deconinck, N., M. Scaillon, V. Segers, J.J. Groswasser, and B. Dan. 2006. Opsoclonus-myoclonus associated with celiac disease. *Pediatr Neurol.* 34:312-4.

Durbeej, M., D. Jung, T. Hjalt, K.P. Campbell, and P. Ekblom. 1997. Transient expression of Dp140, a product of the Duchenne muscular dystrophy locus, during kidney tubulogenesis. *Dev Biol.* 181:156-67.

Dwyer, T.M., and S.C. Froehner. 1995. Direct binding of Torpedo syntrophin to dystrophin and the 87 kDa dystrophin homologue. *FEBS Letters.* 375:91-4.

Enigk, R.E., and M.M. Maimone. 1999. Differential expression and developmental regulation of a novel alpha-dystrobrevin isoform in muscle. *Gene.* 238:479-88.

Ervasti, J.M. 2007. Dystrophin, its interactions with other proteins, and implications for muscular dystrophy. *Biochim Biophys Acta.* 1772:108-17.

Ervasti, J.M., K. Ohlendieck, S.D. Kahl, M.G. Gaver, and K.P. Campbell. 1990. Deficiency of a glycoprotein component of the dystrophin complex in dystrophic muscle. *Nature.* 345:315-319.

Florini, J.R., D.Z. Ewton, and S.A. Coolican. 1996. Growth hormone and the insulin-like growth factor system in myogenesis. *Endocr Rev.* 17:481-517.

Flucher, B.E., and M.P. Daniels. 1989. Distribution of sodium channels and ankyrin in the neuromuscular junction is complementary to that of acetylcholine receptors and the 43kD protein. *Neuron.* 3:163-175.

Foster, K., H. Foster, and J.G. Dickson. 2006. Gene therapy progress and prospects: Duchenne muscular dystrophy. *Gene Ther.* 13:1677-85.

Gailly, P., B. Boland, B. Himpens, R. Casteels, and J.M. Gillis. 1993. Critical evaluation of cytosolic calcium determination in resting muscle fibres from normal and dystrophic (mdx) mice. *Cell Calcium.* 14:473-83.

Galbiati, F., J.A. Engelman, D. Volonte, X.L. Zhang, C. Minetti, M. Li, H. Hou, Jr., B. Kneitz, W. Edelmann, and M.P. Lisanti. 2001. Caveolin-3 null mice show a loss of caveolae, changes in the microdomain distribution of the dystrophin-glycoprotein complex, and t-tubule abnormalities. *J Biol Chem.* 276:21425-33.

Galbiati, F., D. Volonte, J.B. Chu, M. Li, S.W. Fine, M. Fu, J. Bermudez, M. Pedemonte, K.M. Weidenheim, R.G. Pestell, C. Minetti, and M.P. Lisanti. 2000. Transgenic overexpression of caveolin-3 in skeletal muscle fibers induces a Duchenne-like muscular dystrophy phenotype. *Proc Natl Acad Sci U S A.* 97:9689-94.

Garcia-Cardena, G., P. Martasek, B.S. Masters, P.M. Skidd, J. Couet, S. Li, M.P. Lisanti, and W.C. Sessa. 1997. Dissecting the interaction between nitric oxide synthase (NOS) and caveolin. Functional significance of the nos caveolin binding domain in vivo. *J Biol Chem.* 272:25437-40.

Garver, W.S., R.A. Heidenreich, R.P. Erickson, M.A. Thomas, and J.M. Wilson. 2000. Localization of the murine Niemann-Pick C1 protein to two distinct intracellular compartments. *J Lipid Res.* 41:673-87.

Garver, W.S., G.S. Hossain, M.M. Winscott, and R.A. Heidenreich. 1999. The Npc1 mutation causes an altered expression of caveolin-1, annexin II and protein kinases and phosphorylation of caveolin-1 and annexin II in murine livers. *Biochim Biophys Acta.* 1453:193-206.

Garver, W.S., K. Krishnan, J.R. Gallagos, M. Michikawa, G.A. Francis, and R.A. Heidenreich. 2002. Niemann-Pick C1 protein regulates cholesterol transport to the trans-Golgi network and plasma membrane caveolae. *J Lipid Res.* 43:579-89.

Garver, W.S., C. Xie, J.J. Repa, S.D. Turley, and J.M. Dietschy. 2005. Niemann-Pick C1 expression is not regulated by the amount of cholesterol flowing through cells in the mouse. *J Lipid Res.* 46:1745-54.

Gautum, M., P.G. Noakes, L. Moscoso, F. Rupp, R.H. Scheller, J.P. Merlie, and J. Sanes. 1996. Defective neuromuscular synaptogenesis in agrin-deficient mutant mice. *Cell.* 85:525-535.

Gee, S.H., R. Madhavan, S.R. Levinson, J.H. Caldwell, R. Sealock, and S.C. Froehner. 1998. Interaction of muscle and brain sodium channels with multiple members of the syntrophin family of dystrophin-associated proteins. *J. Neurosci.* 18:128-137.

Grady, R.M., M. Akaaboune, A.L. Cohen, M.M. Maimone, J.W. Lichtman, and J.R. Sanes. 2003. Tyrosine-phosphorylated and nonphosphorylated isoforms of alpha-dystrobrevin: roles in skeletal muscle and its neuromuscular and myotendinous junctions. *J Cell Biol.* 160:741-52.

Grady, R.M., R.W. Grange, K.S. Lau, M.M. Maimone, M.C. Nichol, J.T. Stull, and J.R. Sanes. 1999. Role for alpha-dystrobrevin in the pathogenesis of dystrophin-dependent muscular dystrophies. *Nature Cell Biol.* 1:215-220.

Grady, R.M., J.P. Merlie, and J.R. Sanes. 1997a. Subtle neuromuscular defects in utrophin-deficient mice. *J. Cell Biol.* 136:871-882.

Grady, R.M., H. Teng, M.C. Nichol, J.C. Cunningham, R.S. Wilkinson, and J.R. Sanes. 1997b. Skeletal and cardiac myopathies in mice lacking utrophin and dystrophin: a model for Duchenne muscular dystrophy. *Cell.* 90:729-738.

Grady, R.M., H. Zhou, J.M. Cunningham, M.D. Henry, K.P. Campbell, and J.R. Sanes. 2000. Maturation and maintenance of the neuromuscular synapse: genetic evidence for roles of the dystrophin-glycoprotein complex. *Neuron.* 25:275-293.

Gregorevic, P., J.M. Allen, E. Minami, M.J. Blankinship, M. Haraguchi, L. Meuse, E. Finn, M.E. Adams, S.C. Froehner, C.E. Murry, and J.S. Chamberlain. 2006. rAAV6-microdystrophin preserves muscle function and extends lifespan in severely dystrophic mice. *Nat Med.* 12:787-9.

Hailstones, D., L.S. Sleer, R.G. Parton, and K.K. Stanley. 1998. Regulation of caveolin and caveolae by cholesterol in MDCK cells. *J Lipid Res.* 39:369-79.

Hasegawa, M., A. Cuenda, M.G. Spillantini, G.M. Thomas, V. Buee-Scherrer, P. Cohen, and M. Goedert. 1999. Stress-activated protein kinase-3 interacts with the PDZ domain of alpha1-syntrophin. A mechanism for specific substrate recognition. *J. Biol. Chem.* 274:12626-12631.

Haslett, J.N., P.B. Kang, M. Han, A.T. Kho, D. Sanoudou, J.M. Volinski, A.H. Beggs, I.S. Kohane, and L.M. Kunkel. 2005. The influence of muscle type and dystrophin deficiency on murine expression profiles. *Mamm Genome*. 16:739-48.

Haslett, J.N., D. Sanoudou, A.T. Kho, R.R. Bennett, S.A. Greenberg, I.S. Kohane, A.H. Beggs, and L.M. Kunkel. 2002. Gene expression comparison of biopsies from Duchenne muscular dystrophy (DMD) and normal skeletal muscle. *Proc Natl Acad Sci U S A*. 99:15000-5.

Haslett, J.N., D. Sanoudou, A.T. Kho, M. Han, R.R. Bennett, I.S. Kohane, A.H. Beggs, and L.M. Kunkel. 2003. Gene expression profiling of Duchenne muscular dystrophy skeletal muscle. *Neurogenetics*. 4:163-71.

Head, S., D. Williams, and G. Stephenson. 1994. Increased susceptibility of EDL muscles from mdx mice to damage induced by contraction with stretch. *J Muscle Res Cell Motil*. 15:490-2.

Hermonat, P.L., J.G. Quirk, B.M. Bishop, and L. Han. 1997. The packaging capacity of adeno-associated virus (AAV) and the potential for wild-type-plus AAV gene therapy vectors. *FEBS Lett*. 407:78-84.

Higgins, M.E., J.P. Davies, F.W. Chen, and Y.A. Ioannou. 1999. Niemann-Pick C1 is a late endosome-resident protein that transiently associates with lysosomes and the trans-Golgi network. *Mol Genet Metab*. 68:1-13.

Hoffman, E.P., R.H. Brown, and L.M. Kunkel. 1987. Dystrophin: The protein product of the Duchenne muscular dystrophy locus. *Cell*. 51:919-928.

Hosaka, Y., T. Yokota, Y. Miyagoe-Suzuki, K. Yuasa, M. Imamura, R. Matsuda, T. Ikemoto, S. Kameya, and S. Takeda. 2002. Alpha1-syntrophin-deficient skeletal muscle exhibits hypertrophy and aberrant formation of neuromuscular junctions during regeneration. *J Cell Biol*. 158:1097-107.

Huang, P.L., T.M. Dawson, D.S. Bredt, S.H. Snyder, and M.C. Fishman. 1993. Targeted disruption of the neuronal nitric oxide synthase gene. *Cell*. 75:1273-1286.

Ibraghimov-Beskrovnaya, O., J.M. Ervasti, C.J. Leveille, C.A. Slaughter, S.W. Sernett, and K.P. Campbell. 1992. Primary structure of dystrophin-associated glycoproteins linking dystrophin to the extracellular matrix. *Nature*. 355:696-702.

Infante, R.E., L. Abi-Mosleh, A. Radhakrishnan, J.D. Dale, M.S. Brown, and J.L. Goldstein. 2007. Purified NPC1 protein: I. Binding of cholesterol and oxysterols to a 1278-amino acid membrane protein. *J Biol Chem*.

Kameya, S., Y. Miyagoe, I. Nonaka, T. Ikemoto, M. Endo, K. Hanaoka, Y. Nabeshima, and S. Takeda. 1999. Alpha-syntrophin gene disruption results in the absence of neuronal-type nitric oxide synthase at the sarcolemma but does not induce muscle degeneration. *J. Biol. Chem.* 274:2193-2200.

Karpati, G., S. Carpenter, G.E. Morris, K.E. Davies, C. Guerin, and P. Holland. 1993. Localization and quantitation of the chromosome 6-encoded dystrophin-related protein in normal and pathological human muscle. *J Neuropathol Exp Neurol*. 52:119-28.

Kingston, H.M., P.S. Harper, P.L. Pearson, K.E. Davies, R. Williamson, and D. Page. 1983. Localisation of gene for Becker muscular dystrophy. *Lancet*. 2:1200.

Kishi, M., T.T. Kummer, S.J. Eglen, and J.R. Sanes. 2005. LL5beta: a regulator of postsynaptic differentiation identified in a screen for synaptically enriched transcripts at the neuromuscular junction. *J Cell Biol*. 169:355-66.

Koenig, M., A.P. Monaco, and L.M. Kunkel. 1988. The complete sequence of dystrophin predicts a rod-shaped cytoskeletal protein. *Cell*. 53:219-228.

Kramarcy, N.R., and R. Sealock. 2000. Syntrophin isoforms at the neuromuscular junction: Developmental time course and differential localization. *Mol. Cell. Neuroscience*. 15:262-274.

Kramarcy, N.R., A. Vidal, S.C. Froehner, and R. Sealock. 1994. Association of utrophin and multiple dystrophin short forms with the mammalian Mr 58,000 dystrophin-associated protein (syntrophin). *J. Biol. Chem.* 269:2870-2876.

Kruth, H.S., M.E. Comly, J.D. Butler, M.T. Vanier, J.K. Fink, D.A. Wenger, S. Patel, and P.G. Pentchev. 1986. Type C Niemann-Pick disease. Abnormal metabolism of low density lipoprotein in homozygous and heterozygous fibroblasts. *J Biol Chem.* 261:16769-74.

Lederfein, D., Z. Levy, N. Augier, D. Mornet, G. Morris, O. Fuchs, D. Yaffe, and U. Nudel. 1992. A 71 kd protein is a major product of the Duchenne muscular dystrophy gene in brain and other non-muscle tissues. *Proc. Natl. Acad. Sci. USA.* 89:5346-5350.

Leonoudakis, D., L.R. Conti, S. Anderson, C.M. Radeke, L.M. McGuire, M.E. Adams, S.C. Froehner, J.R. Yates, 3rd, and C.A. Vandenberg. 2004. Protein trafficking and anchoring complexes revealed by proteomic analysis of inward rectifier potassium channel (Kir2.x)-associated proteins. *J Biol Chem.* 279:22331-46.

Lidov, H.G., S. Selig, and L.M. Kunkel. 1995. Dp140: a novel 140 kDa CNS transcript from the dystrophin locus. *Hum Mol Genet.* 4:329-35.

Liscum, L., R.M. Ruggiero, and J.R. Faust. 1989. The intracellular transport of low density lipoprotein-derived cholesterol is defective in Niemann-Pick type C fibroblasts. *J Cell Biol.* 108:1625-36.

Liu, M., Y. Yue, S.Q. Harper, R.W. Grange, J.S. Chamberlain, and D. Duan. 2005. Adeno-associated virus-mediated microdystrophin expression protects young mdx muscle from contraction-induced injury. *Mol Ther.* 11:245-56.

Loftus, S.K., R.P. Erickson, S.U. Walkley, M.A. Bryant, A. Incao, R.A. Heidenreich, and W.J. Pavan. 2002. Rescue of neurodegeneration in Niemann-Pick C mice by a prion-promoter-driven Npc1 cDNA transgene. *Hum Mol Genet.* 11:3107-14.

Loftus, S.K., J.A. Morris, E.D. Carstea, J.Z. Gu, C. Cummings, A. Brown, J. Ellison, K. Ohno, M.A. Rosenfeld, D.A. Tagle, P.G. Pentchev, and W.J. Pavan. 1997. Murine model of Niemann-Pick C disease: mutation in a cholesterol homeostasis gene. *Science.* 277:232-5.

Love, D.R., D.F. Hill, G. Dickson, N.K. Spurr, B.C. Byth, R.F. Marsden, F.S. Walsh, Y.H. Edwards, and K.E. Davies. 1989. An autosomal transcript in skeletal muscle with homology to dystrophin. *Nature.* 339:55-58.

Love, D.R., G.E. Morris, J.M. Ellis, U. Fairbrother, R.F. Marsden, J.F. Bloomfield, Y.H. Edwards, C.P. Slater, D.J. Parry, and K.E. Davies. 1991. Tissue distribution of the dystrophin-related gene product and expression in mdx and dy mouse. *Proc. Natl. Acad. Sci. USA*. 88:3243-3247.

Lumeng, C., S. Phelps, G.E. Crawford, P.D. Walden, K. Barald, and J.S. Chamberlain. 1999. Interactions between beta2-syntrophin and a family of microtubule-associated serine/threonine kinases. *Nature Neurosci.* 2:611-617.

Lyons, P.R., and C.R. Slater. 1991. Structure and function of the neuromuscular junction in young adult mdx mice. *J Neurocytol.* 20:969-81.

Mann, C.J., K. Honeyman, A.J. Cheng, T. Ly, F. Lloyd, S. Fletcher, J.E. Morgan, T.A. Partridge, and S.D. Wilton. 2001. Antisense-induced exon skipping and synthesis of dystrophin in the mdx mouse. *Proc Natl Acad Sci U S A*. 98:42-7.

Matsuda, R., A. Nishikawa, and H. Tanaka. 1995. Visualization of dystrophic muscle fibers in mdx mouse by vital staining with Evans blue: evidence of apoptosis in dystrophin-deficient muscle. *J Biochem (Tokyo)*. 118:959-64.

Matsumura, K., J.M. Ervasti, K. Ohlendieck, S.D. Kahl, and K.P. Campbell. 1992. Association of dystrophin-related protein with dystrophin-associated proteins in *mdx* mouse muscle. *Nature*. 360:588-591.

Matsumura, K., D.M. Shasby, and K.P. Campbell. 1993. Purification of dystrophin-related protein (utrophin) from lung and its identification in pulmonary artery endothelial cells. *FEBS Lett.* 326:289-93.

McDouall, R.M., M.J. Dunn, and V. Dubowitz. 1990. Nature of the mononuclear infiltrate and the mechanism of muscle damage in juvenile dermatomyositis and Duchenne muscular dystrophy. *J Neurol Sci.* 99:199-217.

Miao, G.G., R.J. Smeyne, G. D'Arcangelo, N.G. Copeland, N.A. Jenkins, J.I. Morgan, and T. Curran. 1994. Isolation of an allele of reeler by insertional mutagenesis. *Proc Natl Acad Sci U S A*. 91:11050-4.

Minetti, C., F. Sotgia, C. Bruno, P. Scartezzini, P. Broda, M. Bado, E. Masetti, M. Mazzocco, A. Egeo, M.A. Donati, D. Volonte, F. Galbiati, G. Cordone, F.D. Bricarelli, M.P. Lisanti, and F. Zara. 1998. Mutations in the caveolin-3 gene cause autosomal dominant limb-girdle muscular dystrophy. *Nat Genet.* 18:365-8.

Mizuno, Y., S. Noguchi, H. Yamamoto, M. Yoshida, I. Nonaka, S. Hirai, and E. Ozawa. 1995. Sarcoglycan complex is selectively lost in dystrophic hamster muscle. *American Journal of Pathology.* 146:530-6.

Mizuno, Y., S. Noguchi, H. Yamamoto, M. Yoshida, A. Suzuki, Y. Hagiwara, Y.K. Hayashi, K. Arahata, I. Nonaka, S. Hirai, and et al. 1994a. Selective defect of sarcoglycan complex in severe childhood autosomal recessive muscular dystrophy muscle. *Biochem Biophys Res Commun.* 203:979-83.

Mizuno, Y., M. Yoshida, I. Nonaka, S. Hirai, and E. Ozawa. 1994b. Expression of utrophin (dystrophin-related protein) and dystrophin-associated glycoproteins in muscles from patients with Duchenne muscular dystrophy. *Muscle & Nerve.* 17:206-16.

Moens, P., P.H. Baatsen, and G. Marechal. 1993. Increased susceptibility of EDL muscles from mdx mice to damage induced by contractions with stretch. *J Muscle Res Cell Motil.* 14:446-51.

Monaco, A.P., C.J. Bertelson, S. Liechti-Gallati, H. Moser, and L.M. Kunkel. 1988. An explanation for the phenotypic differences between patients bearing partial deletions of the DMD locus. *Genomics.* 2:90-5.

Monaco, A.P., A.P. Walker, I. Millwood, Z. Larin, and H. Lehrach. 1992. A yeast artificial chromosome contig containing the complete Duchenne muscular dystrophy gene. *Genomics.* 12:465-73.

Morris, M.D., C. Bhuvaneswaran, H. Shio, and S. Fowler. 1982. Lysosome lipid storage disorder in NCTR-BALB/c mice. I. Description of the disease and genetics. *Am J Pathol.* 108:140-9.

Munehira, Y., T. Ohnishi, S. Kawamoto, A. Furuya, K. Shitara, M. Imamura, T. Yokota, S. Takeda, T. Amachi, M. Matsuo, N. Kioka, and K. Ueda. 2004. Alpha1-syntrophin modulates turnover of ABCA1. *J Biol Chem.* 279:15091-5.

Murata, M., J. Peranen, R. Schreiner, F. Wieland, T.V. Kurzchalia, and K. Simons. 1995. VIP21/caveolin is a cholesterol-binding protein. *Proc Natl Acad Sci U S A*. 92:10339-43.

Neufeld, E.B., J.A. Stonik, S.J. Demosky, Jr., C.L. Knapper, C.A. Combs, A. Cooney, M. Comly, N. Dwyer, J. Blanchette-Mackie, A.T. Remaley, S. Santamarina-Fojo, and H.B. Brewer, Jr. 2004. The ABCA1 transporter modulates late endocytic trafficking: insights from the correction of the genetic defect in Tangier disease. *J Biol Chem*. 279:15571-8.

Neufeld, E.B., M. Wastney, S. Patel, S. Suresh, A.M. Cooney, N.K. Dwyer, C.F. Roff, K. Ohno, J.A. Morris, E.D. Carstea, J.P. Incardona, J.F. Strauss, 3rd, M.T. Vanier, M.C. Patterson, R.O. Brady, P.G. Pentchev, and E.J. Blanchette-Mackie. 1999. The Niemann-Pick C1 protein resides in a vesicular compartment linked to retrograde transport of multiple lysosomal cargo. *J Biol Chem*. 274:9627-35.

Newey, S.E., M.A. Benson, C.P. Ponting, K.E. Davies, and D.J. Blake. 2000. Alternative splicing of dystrobrevin regulates the stoichiometry of syntrophin binding to the dystrophin protein complex. *Curr Biol*. 10:1295-8.

Nguyen, T.M., J.M. Ellis, D.R. Love, K.E. Davies, K.C. Gatter, G. Dickson, and G.E. Morris. 1991. Localization of the DMDL gene-encoded dystrophin-related protein using a panel of nineteen monoclonal antibodies: presence at neuromuscular junctions, in the sarcolemma of dystrophic skeletal muscle, in vascular and other smooth muscles, and in proliferating brain cell lines. *J. Cell Biol.* 115:1695-700.

Oak, S.A., K. Russo, T.C. Petrucci, and H.W. Jarrett. 2001. Mouse alpha1-syntrophin binding to Grb2: further evidence of a role for syntrophin in cell signaling. *Biochemistry*. 40:11270-8.

Ohgami, N., D.C. Ko, M. Thomas, M.P. Scott, C.C. Chang, and T.Y. Chang. 2004. Binding between the Niemann-Pick C1 protein and a photoactivatable cholesterol analog requires a functional sterol-sensing domain. *Proc Natl Acad Sci U S A*. 101:12473-8.

Ort, T., E. Maksimova, R. Dirkx, A.M. Kachinsky, S. Berghs, S.C. Froehner, and M. Solimena. 2000. The receptor tyrosine phosphatase-like protein ICA512 binds the PDZ domains of beta2-syntrophin and nNOS in pancreatic beta-cells. *Eur J Cell Biol*. 79:621-30.

Ozawa, E., Y. Mizuno, Y. Hagiwara, T. Sasaoka, and M. Yoshida. 2005. Molecular and cell biology of the sarcoglycan complex. *Muscle Nerve.* 32:563-76.

Patterson, M.C., M.T. Vanier, K. Suzuki, J.A. Morris, E. Carstea, E.B. Neufeld, E.J. Blanchette-Mackie, and P.G. Pentchev. 2001. Niemann-Pick disease type C: a lipid trafficking disorder. *In* The Metabolic and Molecular Bases of Inherited Disease. Vol. 3. C.R. Scriver, A.L. Beaudet, W.S. Sly, and D. Valle, editors. McGraw-Hill, New York. 3611-3633.

Percival, J.M., P. Gregorevic, G.L. Odom, G.B. Banks, J.S. Chamberlain, and S.C. Froehner. 2007. rAAV6-microdystrophin rescues aberrant Golgi complex organization in mdx skeletal muscles. *Traffic.* 8:1424-39.

Peters, M.F., M.E. Adams, and S.C. Froehner. 1997a. Differential association of syntrophin pairs with the dystrophin complex. *J. Cell Biol.* 138:81-93.

Peters, M.F., N.R. Kramarcy, R. Sealock, and S.C. Froehner. 1994. β2-Syntrophin: Localization at the neuromuscular junction in skeletal muscle. *NeuroReport.* 5:1577-1580.

Peters, M.F., K.F. O'Brien, H.M. Sadoulet-Puccio, L.M. Kunkel, M.E. Adams, and S.C. Froehner. 1997b. β-dystrobrevin, a new member of the dystrophin family: identification, cloning, and protein associations. *J. Biol. Chem.* 272:31561-31569.

Peters, M.F., H. Sadoulet-Puccio, R.M. Grady, N.R. Kramarcy, L.M. Kunkel, J.R. Sanes, R. Sealock, and S.C. Froehner. 1998. Differential membrane localization and intermolecular associations of alpha-dystrobrevin isoforms in skeletal muscle. *J. Cell Biol.* 142:1269-1278.

Petrof, B.J., J.B. Shrager, H.H. Stedman, A.M. Kelly, and H.L. Sweeney. 1993. Dystrophin protects the sarcolemma from stresses developed during muscle contraction. *Proc. Natl. Acad. Sci. USA.* 90:3710-3714.

Porter, J.D., S. Khanna, H.J. Kaminski, J.S. Rao, A.P. Merriam, C.R. Richmonds, P. Leahy, J. Li, W. Guo, and F.H. Andrade. 2002. A chronic inflammatory response dominates the skeletal muscle molecular signature in dystrophin-deficient mdx mice. *Hum Mol Genet.* 11:263-72.

Porter, J.D., A.P. Merriam, P. Leahy, B. Gong, J. Feuerman, G. Cheng, and S. Khanna. 2004. Temporal gene expression profiling of dystrophin-deficient (mdx) mouse diaphragm identifies conserved and muscle group-specific mechanisms in the pathogenesis of muscular dystrophy. *Hum Mol Genet.* 13:257-69.

Rafii, M.S., H. Hagiwara, M.L. Mercado, N.S. Seo, T. Xu, T. Dugan, R.T. Owens, M. Hook, D.J. McQuillan, M.F. Young, and J.R. Fallon. 2006. Biglycan binds to alpha- and gamma-sarcoglycan and regulates their expression during development. *J Cell Physiol.* 209:439-47.

Ragot, T., N. Vincent, P. Chafey, E. Vigne, H. Gilgenkrantz, D. Couton, J. Cartaud, P. Briand, J.C. Kaplan, M. Perricaudet, and et al. 1993. Efficient adenovirus-mediated transfer of a human minidystrophin gene to skeletal muscle of mdx mice. *Nature.* 361:647-50.

Rando, T.A. 2001. Role of nitric oxide in the pathogenesis of muscular dystrophies: a "two hit" hypothesis of the cause of muscle necrosis. *Microsc Res Tech.* 55:223-35.

Repetto, S., M. Bado, P. Broda, G. Lucania, E. Masetti, F. Sotgia, I. Carbone, A. Pavan, E. Bonilla, G. Cordone, M.P. Lisanti, and C. Minetti. 1999. Increased number of caveolae and caveolin-3 overexpression in Duchenne muscular dystrophy. *Biochem Biophys Res Commun.* 261:547-50.

Roberts, R.G., A.J. Coffey, M. Bobrow, and D.R. Bentley. 1993. Exon structure of the human dystrophin gene. *Genomics.* 16:536-8.

Rodriguez-Santiago, M., M. Mendoza-Torres, J.F. Jimenez-Bremont, and R. Lopez-Revilla. 2007. Knockout of the trcp3 gene causes a recessive neuromotor disease in mice. *Biochem Biophys Res Commun.* 360:874-9.

Sadoulet-Puccio, H.M., T.S. Khurana, J.B. Cohen, and L.M. Kunkel. 1996. Cloning and characterization of the human homologue of a dystrophin related phosphoprotein found at the Torpedo electric organ post-synaptic membrane. *Hum. Mol. Gen.* 5:489-496.

Sander, M., B. Chavoshan, S.A. Harris, S.T. Iannaccone, J.T. Stull, G.D. Thomas, and R.G. Victor. 2000. Functional muscle ischemia in neuronal nitric oxide synthase-deficient skeletal muscle of children with Duchenne muscular dystrophy. *Proc Natl Acad Sci U S A.* 97:13818-23.

Schultz, J., U. Hoffmuller, G. Krause, J. Ashurst, M.J. Macias, P. Schmieder, J. Schneider-Mergener, and H. Oschkinat. 1998. Specific interactions between the syntrophin PDZ domain and voltage-gated sodium channels. *Nature Struct. Biol.* 5:19-24.

Sealock, R., M.H. Butler, N.R. Kramarcy, K.X. Gao, A.A. Murnane, K. Douville, and S.C. Froehner. 1991. Localization of dystrophin relative to acetylcholine receptor domains in electric tissue and adult and cultured skeletal muscle. *J. Cell Biol.* 113:1133-44.

Sicinski, P., Y. Geng, A.S. Ryder-Cook, E.A. Barnard, M.G. Darlison, and P.J. Barnard. 1989. The molecular basis of muscular dystrophy in the mdx mouse: a point mutation. *Science.* 244:1578-80.

Smart, E.J., Y. Ying, W.C. Donzell, and R.G. Anderson. 1996. A role for caveolin in transport of cholesterol from endoplasmic reticulum to plasma membrane. *J Biol Chem.* 271:29427-35.

Smith, J., C. Goldsmith, A. Ward, and R. LeDieu. 2000. IGF-II ameliorates the dystrophic phenotype and coordinately down-regulates programmed cell death. *Cell Death Differ.* 7:1109-18.

Sokol, J., J. Blanchette-Mackie, H.S. Kruth, N.K. Dwyer, L.M. Amende, J.D. Butler, E. Robinson, S. Patel, R.O. Brady, M.E. Comly, and et al. 1988. Type C Niemann-Pick disease. Lysosomal accumulation and defective intracellular mobilization of low density lipoprotein cholesterol. *J Biol Chem.* 263:3411-7.

Song, K.S., P.E. Scherer, Z. Tang, T. Okamoto, S. Li, M. Chafel, C. Chu, D.S. Kohtz, and M.P. Lisanti. 1996. Expression of caveolin-3 in skeletal, cardiac, and smooth muscle cells. Caveolin-3 is a component of the sarcolemma and co-fractionates with dystrophin and dystrophin-associated glycoproteins. *J Biol Chem.* 271:15160-5.

Sotgia, F., J.K. Lee, K. Das, M. Bedford, T.C. Petrucci, P. Macioce, M. Sargiacomo, F.D. Bricarelli, C. Minetti, M. Sudol, and M.P. Lisanti. 2000. Caveolin-3 directly interacts with the C-terminal tail of beta -dystroglycan. Identification of a central WW-like domain within caveolin family members. *J Biol Chem*. 275:38048-58.

Suzuki, A., M. Yoshida, K. Hayashi, Y. Mizuno, Y. Hagiwara, and E. Ozawa. 1994. Molecular organization at the glycoprotein-complex binding site of dystrophin. *Eur. J. Biochem.* 220:283-292.

Takemitsu, M., S. Ishiura, R. Koga, K. Kamakura, K. Arahata, I. Nonaka, and H. Sugita. 1991. Dystrophin-related protein in the fetal and denervated skeletal muscles of normal and mdx mice. *Biochem Biophys Res Commun*. 180:1179-86.

Tinsley, J., N. Deconinck, R. Fisher, D. Kahn, S. Phelps, J. Gillis, and K. Davies. 1998. Expression of full-length utrophin prevents muscular dystrophy in mdx mice. *Nat Med*. 4:1441-1444.

Tkatchenko, A.V., G. Le Cam, J.J. Leger, and C.A. Dechesne. 2000. Large-scale analysis of differential gene expression in the hindlimb muscles and diaphragm of mdx mouse. *Biochim Biophys Acta*. 1500:17-30.

Tkatchenko, A.V., G. Pietu, N. Cros, L. Gannoun-Zaki, C. Auffray, J.J. Leger, and C.A. Dechesne. 2001. Identification of altered gene expression in skeletal muscles from Duchenne muscular dystrophy patients. *Neuromuscul Disord*. 11:269-77.

Tseng, B.S., P. Zhao, J.S. Pattison, S.E. Gordon, J.A. Granchelli, R.W. Madsen, L.C. Folk, E.P. Hoffman, and F.W. Booth. 2002. Regenerated mdx mouse skeletal muscle shows differential mRNA expression. *J Appl Physiol*. 93:537-45.

Turner, P.R., P.Y. Fong, W.F. Denetclaw, and R.A. Steinhardt. 1991. Increased calcium influx in dystrophic muscle. *J. Cell Biol.* 115:1701-1712.

Vaghy, P.L., J. Fang, W. Wu, and L.P. Vaghy. 1998. Increased caveolin-3 levels in mdx mouse muscles. *FEBS Lett*. 431:125-7.

van Deutekom, J.C., M. Bremmer-Bout, A.A. Janson, I.B. Ginjaar, F. Baas, J.T. den Dunnen, and G.J. van Ommen. 2001. Antisense-induced exon skipping restores dystrophin expression in DMD patient derived muscle cells. *Hum Mol Genet.* 10:1547-54.

Venema, V.J., H. Ju, R. Zou, and R.C. Venema. 1997. Interaction of neuronal nitric-oxide synthase with caveolin-3 in skeletal muscle. Identification of a novel caveolin scaffolding/inhibitory domain. *J Biol Chem.* 272:28187-90.

Wang, B., J. Li, and X. Xiao. 2000. Adeno-associated virus vector carrying human minidystrophin genes effectively ameliorates muscular dystrophy in mdx mouse model. *Proc Natl Acad Sci U S A.* 97:13714-9.

Wang, Z., C.S. Kuhr, J.M. Allen, M. Blankinship, P. Gregorevic, J.S. Chamberlain, S.J. Tapscott, and R. Storb. 2007. Sustained AAV-mediated dystrophin expression in a canine model of Duchenne muscular dystrophy with a brief course of immunosuppression. *Mol Ther.* 15:1160-6.

Washabaugh, C.H., M.P. Ontell, Z. Shan, E.P. Hoffman, and M. Ontell. 1998. Role of the nerve in determining fetal skeletal muscle phenotype. *Dev Dyn.* 211:177-90.

Wehling, M., M.J. Spencer, and J.G. Tidball. 2001. A nitric oxide synthase transgene ameliorates muscular dystrophy in mdx mice. *J Cell Biol.* 155:123-31.

Wempe, F., J.Y. Yang, J. Hammann, and H. von Melchner. 2001. Gene trapping identifies transiently induced survival genes during programmed cell death. *Genome Biol.* 2:RESEARCH0023.

Wenzel, K., J. Zabojszcza, M. Carl, S. Taubert, A. Lass, C.L. Harris, M. Ho, H. Schulz, O. Hummel, N. Hubner, K.J. Osterziel, and S. Spuler. 2005. Increased susceptibility to complement attack due to down-regulation of decay-accelerating factor/CD55 in dysferlin-deficient muscular dystrophy. *J Immunol.* 175:6219-25.

Williams, J.H., S.R. Sirsi, D.R. Latta, and G.J. Lutz. 2006. Induction of dystrophin expression by exon skipping in mdx mice following intramuscular injection of antisense oligonucleotides complexed with PEG-PEI copolymers. *Mol Ther.* 14:88-96.

Williams, M.W., and R.J. Bloch. 1999. Extensive but coordinated reorganization of the membrane skeleton in myofibers of dystrophic (mdx) mice. *J Cell Biol.* 144:1259-70.

Williamson, R.A., M.D. Henry, K.J. Daniels, R.F. Hrstka, J.C. Lee, Y. Sunada, O. Ibraghimov-Beskrovnaya, and K.P. Campbell. 1997. Dystroglycan is essential for early embryonic development: disruption of Reichert's membrane in Dag1-null mice. *Hum. Mol. Genet.* 6:831-841.

Wojtanik, K.M., and L. Liscum. 2003. The transport of low density lipoprotein-derived cholesterol to the plasma membrane is defective in NPC1 cells. *J Biol Chem.* 278:14850-6.

Xie, C., D.K. Burns, S.D. Turley, and J.M. Dietschy. 2000. Cholesterol is sequestered in the brains of mice with Niemann-Pick type C disease but turnover is increased. *J Neuropathol Exp Neurol.* 59:1106-17.

Xie, C., S.D. Turley, P.G. Pentchev, and J.M. Dietschy. 1999. Cholesterol balance and metabolism in mice with loss of function of Niemann-Pick C protein. *Am J Physiol.* 276:E336-44.

Yamamura, K.I., and K. Araki. 2007. Gene trap mutagenesis in mice: New perspectives and tools in cancer research. *Cancer Sci*:In Press.

Yang, B., D. Jung, J.A. Rafael, J.S. Chamberlain, and K.P. Campbell. 1995. Identification of alpha-syntrophin binding to syntrophin triplet, dystrophin, and utrophin. *J. Biol. Chem.* 270:4975-8.

Yin, H., Q. Lu, and M. Wood. 2007. Effective Exon Skipping and Restoration of Dystrophin Expression by Peptide Nucleic Acid Antisense Oligonucleotides in mdx Mice. *Mol Ther.*

Yuasa, K., M. Yoshimura, N. Urasawa, S. Ohshima, J.M. Howell, A. Nakamura, T. Hijikata, Y. Miyagoe-Suzuki, and S. Takeda. 2007. Injection of a recombinant AAV serotype 2 into canine skeletal muscles evokes strong immune responses against transgene products. *Gene Ther.* 14:1249-60.

CURRICULUM VITAE

Michelle S. Steen, Ph.D.

EDUCATION

Doctor of Philosophy, Physiology and Biophysics
University of Washington, Seattle, Washington (February 2008)
Advisor: Stanley C. Froehner, Ph.D.

Master of Science, Physiological Sciences
University of Arizona, Tucson, Arizona (August 1997)
Advisor: Erik J. Henriksen, Ph.D.

Bachelor of Arts, Human Biodynamics
University of California, Berkeley, California (December 1994)

PROFESSIONAL EXPERIENCE

University of Washington; Department of Physiology and Biophysics
Graduate Student Research Assistant. **4/01-2/08**
Advisor: Stanley C. Froehner, Ph.D.
Dissertation title: Analyses of alpha-dystrobrevin-null mice implicate Niemann-Pick C1 in muscular dystrophy.

Stanford University, School of Medicine; Department of Genetics
Life Science Research Assistant. **7/99-9/00**
P.I.: Richard M. Myers, Ph.D.

Stanford Human Genome Center, Stanford University, School of Medicine
Life Science Research Assistant. **2/98-7/99**
Directors: Richard M. Myers, Ph.D. and David R. Cox, Ph.D.

University of Arizona, College of Medicine; Department of Physiology
Graduate Research Assistant. **8/96-7/97**
Advisor: Erik J. Henriksen, Ph.D.
Project title for Master of Science degree: Effects of exercise training and ACE inhibition on insulin action in rat skeletal muscle.

University of Arizona, College of Medicine; Department of Physiology
Graduate Student Instructor **8/95-6/97**
Undergraduate Anatomy and Physiology Laboratory.

University of California, Berkeley; Department of Human Biodynamics
Undergraduate Research Apprentice. **8/94-5/95**
P.I.: George A. Brooks, Ph.D.

HONORS / AWARDS

Elsevier Award. Awarded to young scientists based on poster or oral presentation. 12th International Congress of The World Muscle Society. Giardini Naxos – Taormina, Italy. October 2007.

WMS Fellowship. Awarded to young scientists based on quality of abstract. 12th International Congress of The World Muscle Society. Giardini Naxos – Taormina, Italy. October 2007.

Nu Sigma Xi Honor Society, Department of Human Biodynamics, University of California, Berkeley. 1994.

PRESENTATIONS

NPC1 overexpression attenuates muscular dystrophy in *mdx* and alpha-dystrobrevin-null mice. Steen, M., Tesch, Y., Adams, M., and Froehner, S.. 12th International Congress of The World Muscle Society. Giardini Naxos – Taormina, Italy. October 2007. Poster.

Amelioration of the dystrophic phenotype by NPC1. 3rd Seattle Muscular Dystrophy Conference. Seattle, Washington, USA. June 2007. Invited Speaker.

Neuromuscular junction abnormalities in mice with reduced levels of NPC1. Michelle S. Steen and Stanley C. Froehner. 2005 Scientific Conference on Niemann-Pick Type C Disease. Tucson, Arizona, USA. June 2005. Poster.

Gene expression analysis of alpha-syntrophin-null and alpha-dystrobrevin-null skeletal muscle: a relationship between Niemann-Pick C1 and muscular dystrophy? 2nd Seattle Muscular Dystrophy Conference. Seattle, Washington, USA. September 2004. Invited Speaker.

PUBLICATIONS

Steen, M.S., M.E. Adams, Y. Tesch, and S.C. Froehner. Attenuation of muscular dystrophy by transgenic expression of Niemann-Pick C1. *In preparation.*

Steen, M.S. and S.C. Froehner. PerleCan fix your muscle AChEs. *Trends Neurosci.* 26(5):241-242, 2003.

Foianini, K.R., M.S. **Steen**, T.R. Kinnick, M. Schmit, E.B. Youngblood, and E.J. Henriksen. Effects of exercise training and ACE inhibition on insulin action in rat skeletal muscle. *J. Appl. Physiol.* 89(2):687-94, 2000.

Steen, M.S., K.R. Foianini, E.B. Youngblood, T.R. Kinnick, S. Jacob, and E.J. Henriksen. Interactions of exercise training and ACE inhibition on insulin action in obese Zucker rats. *J. Appl. Physiol.* 86(6): 2044-2051, 1999.